Ph.D. Dissertation of Engineering

Impacts and Vulnerability Assessment of Landslides to Climate Change in Various Scales

다양한 규모에서의 기후변화에 따른 산사태 영향 및 취약성 평가

February 2017

Graduate School of Seoul National University

Interdisciplinary Doctoral Program in Landscape Architecture

Ho Gul Kim

Impacts and Vulnerability Assessment of Landslides to Climate Change in Various Scales

Advisor : Dong Kun Lee

Submitting a Ph.D. Dissertation of Public Administration

October 2016

Graduate School of Seoul National University

Interdisciplinary Doctoral Program in Landscape Architecture

Ho Gul Kim

Confirming the Ph.D. Dissertation written by

Ho Gul Kim

January 2017

Chair _____(Seal)

Vice Chair _____(Seal)

Examiner _____(Seal)

Examiner _____(Seal)

Examiner _____(Seal)

Abstract

Impacts and Vulnerability Assessment of Landslides to Climate Change in Various Scales

Ho Gul Kim

Interdisciplinary Program in Landscape Architecture,
Graduate School, Seoul National University
Supervised by Professor Dong Kun Lee

Republic of Korea has increasingly experienced extreme weather events such as typhoons or heavy rainfall because of climate change. Extreme weather events result in damage in different forms, among which damage caused by landslide occurs every year. Landslide not only damages property but also causes human loss and calls for imperative adaptive measures to prevent or reduce damage. Currently, studies that seek to identify landslide-prone regions and high-priority areas that need adaptive measures are becoming important field.

Impact of climate change is found on a variety of scales and in many regions, and yet, adaptive measures have been taken in different forms at the levels of nation, province, and county. Data and evaluation of the impact of climate change can differ to the scales of study target. Thus, proper method also differ to scale when assessing the impact of climate change. The purpose of this study is, in this sense, to develop and apply a methodology for different scales—central government, province, and counties—to evaluate the impact of and vulnerability to climate change on the occurrence of landslides.

The research developed a methodology and framework for finding vulnerable and hazard areas considering different scales and available data. At the national

level, the study evaluated many items including landslide and found key vulnerable regions, which the central government needs to priority for support. At the provincial level, the study analyzed areas prone to landslide in Gangwon-do Province from the present to the future and found out specific regions that need adaptive measures. At the county level, Inje-gun of Gangwon-do Province was assessed by 10 models to investigate high-risk areas with uncertainties of models, and the uncertainties were quantified to assist establishing more effective adaptive measures.

This study seeks to propose a method that can support decision-makers in establishing adaptation measures against climate change, by developing and applying a viable methodology and framework that can tailor to each user's objective and available data for evaluating the impact of climate change. The results would be help for establishing adaptive measures to reduce damage from landslide and evaluating the impact of and vulnerability to climate change by governments of different scales.

▣ *Keywords : Statistical distribution models, RCP climate change scenarios, Landslide susceptibility, Uncertainty*
▣ *Student Number : 2012-30679*

Publications

Please note that Chapters 1-3 of this dissertation proposal were written as stand-alone papers (see below), and therefore there is some repetition in the methods and results.

CHAPTER 1

Kim, H.G. et al., 2016. Finding key vulnerable areas by a climate change vulnerability assessment. Natural Hazards, pp.1–50.

CHAPTER 2

Kim, H.G. et al., 2015. Evaluating landslide hazards using RCP 4.5 and 8.5 scenarios. Environmental Earth Sciences, 73(3), pp.1385–1400.

CHAPTER 3

Kim, H.G. et al., 2016. Estimating Landslide Susceptibility Areas in Consideration of the Uncertainty Inherent in Modeling Results. Environmental Research Letters. (Major revision)

Table of Contents

List of Tables

List of Figures

1. INTRODUCTION

The negative impact of climate change has been increasing. The world has tried to establish climate change adaptive measures. Republic of Korea has a system in place for the local administrations to take measures based on the national measures, and those measures require a big budget. With limited resources, there should be priorities set straight in providing support, which could be done by credible data and provided to policymakers.

The evaluation of the impact of climate change and vulnerability test can be an effective tool in establishing grounds for adaptive measures [1][2]. However, previous studies focused on a single scale [3][4][5][6]. In reality, studies should be done on many different scales at the levels of nation, province, and county. Governments of different scales have different needs for evaluation methods and data to establish adaptive measures.

This study comprises three chapters that represent different sites of different scales, and the chapters present different sub-objectives. Chapter 1 explores vulnerable regions via vulnerability assessment on 232 governments across the nation on 32 items in 7 categories. It focused on finding the current vulnerable regions and those of the future to assist each government estimating the level of urgency.

Chapter 2 investigates high-risk regions by analyzing regions prone to landslide under climate change on the basis of spatial statistical analysis model at the provincial level. This study focused on Gangwon-do to estimate the impact of landslide of the present and the future and find regions that urgently need measures to be taken. Chapter 3 investigates high-risk regions by analyzing regions prone to landslide accounting for uncertainties on the basis of spatial statistical analysis model at the county level. Inje-gun was chosen to be subject to the assessment.

The three studies had different subjects and were conducted on different scales. It is not the purpose of this study to write a single complete article by setting a

methodology of evaluating the impact of climate change and running a vulnerability assessment that can apply to the size of the subject site. Instead, the study seeks to propose a way to solve a variety of issues arising from climate change research on different scales. The ultimate goal would be to predict climate change impact and vulnerability for counties to the central government and provide policymakers scientific grounds for establishing adaptive measures.

2. CHAPTER 1 : Climate Change Vulnerability and Impact Assessment for Republic of Korea

2.1. Introduction

Development activities of humankind have emitted a significant quantity of greenhouse gases to cause climate change [7][8], which in turn causes negative or positive effects in various fields on a global scale [9]. These effects simultaneously encompass short-term effects including extreme weather such as typhoons, heavy rainfall, heat waves, and cold waves and long-term effects such as gradual increases or decreases in the temperature and rainfall (e.g., [10][11][12][13]). Thus, the assessment and solution of problems caused by climate change affecting a large area require the consideration of a variety of human activity sectors and environmental characteristics, expressed by means of very diverse variables.

The Intergovernmental Panel on Climate Change (IPCC), a representative community focusing on research relevant to climate change, separated this research theme to into three working groups [9]. Group I assesses the climate system and climate change; group II assesses the vulnerability of systems and adaptation options to reduce damages; and group III assesses mitigation options related to preventing greenhouse gas emissions. The present study focuses on the work of group II in assessing vulnerabilities, predicting negative effects and supporting adaptation options to reduce damage. Many researchers have attempted to assess the impacts and vulnerability to climate change [14][15][16][17]. Moreover, many studies have determined that diverse events are related to climate change and have demanded proper adaptation plans for counteracting its effects.

Such studies have focused mainly on specific items or fields of certain areas. For example, studies on landslide risk have focused only on the identification of landslide hazard area without interest in other items or fields [18][4][7][5][19][20][21][6]. Although such research can help to improve existing methodologies and supports municipalities within the study area, the government cannot utilize the results to prepare national adaptation plans and options. This is an issue because climate change affects large areas rather than only small or local areas.

Therefore, the entire extent of the Republic of Korea (ROK) and various fields should be assessed to support a national adaptation plan.

The objectives of this study are to determine methods for assessing the vulnerability of various fields and areas by using a single framework and to identify their mechanisms. Moreover, this study identifies municipalities with most urgent areas in which to establish adaptation plans and attempts to develop a framework for assessing various fields in many municipalities. The framework is developed to incorporate a combination of quantitative and qualitative methods for improving the comprehension and availability of data of decision makers and considers limitations of time, cost, and data. The properties of the vulnerability fields are analyzed by checking variables. This study identifies key vulnerable areas to support the establishment of a national adaptation plan. The developed framework and method for finding these such areas can also serve as an effective tool for use by governments of other countries.

2.2. Methods

2.2.1. Scope of study

This study comprises two parts (Figure 1: vulnerability assessment and the identification of key vulnerable areas. The first part focuses on the selection of fields and items, establishment of data, and assessment of vulnerability. The second part concentrates on classifying vulnerability grades, creating first-grade and key vulnerability maps, and analyzing the characteristics of key vulnerable municipalities.

The study area is the ROK, which consists of 232 municipalities. The municipalities are used as spatial units for vulnerability assessment because each spatial unit is appropriate for formulating and implementing policies [4]. Additionally, each municipality of the ROK must establish its own climate adaptation plan according to the basic act on low-carbon green growth. Seven fields are considered, including health, forests, water management, ecosystem, agriculture,

fisheries, and disasters, which consist of 32 specific items. The fields and items were selected on the basis of climate change adaptation strategies of the ROK.

The temporal scope was established to include the present (2001–2010) and future (2046–2055) years. In the national adaptation strategy, the ROK government set 2050 as the long-term target year for adaptation. This study considers only the change of climate conditions to identify its effects, as there are not enough data to estimate the future condition of the ROK. In addition, the government of ROK determined that future data have considerable uncertainty.

The variables for sensitivity and adaptive capacity were selected by reviewing previous studies provided by national institutes of various fields. Climate exposure variables were provided by the Korea Meteorological Administration (KMA). The Representative Concentration Pathways (RCP) 8.5 climate change scenario was applied to establish future climate data. This scenario, known as the Business As Usual (BAU) scenario, is the worst of RCP scenarios and assumes that insufficient effort is put forth in reducing greenhouse-gas emissions. The KMA used the HadGEM3-RA model to produce the RCP 8.5 scenario data. An average of 10 years of climate data pertaining to climatic prediction was used in the assessment for anticipating future conditions.

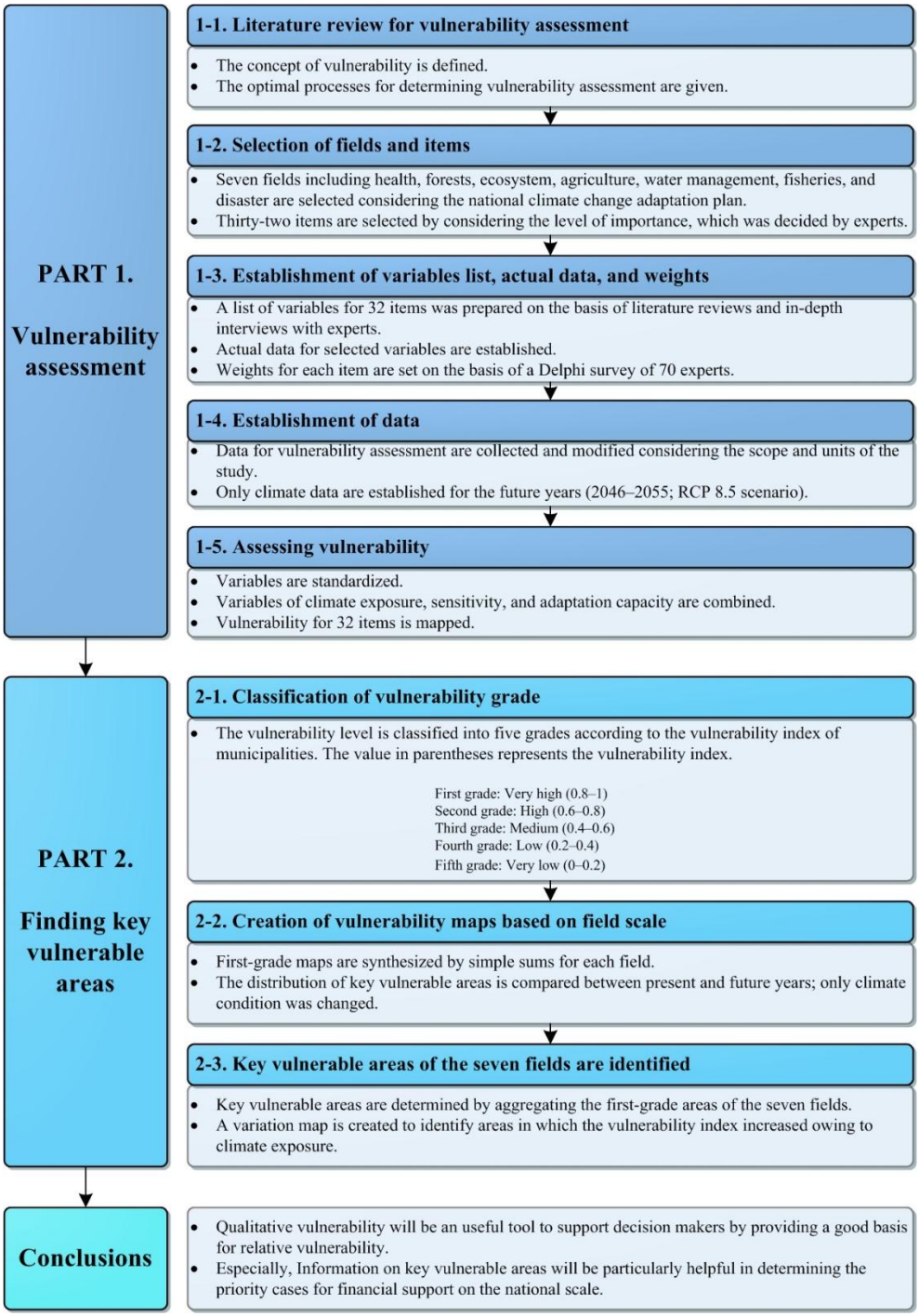

Figure 1. Flow chart of study

Table 1. List of items considered for vulnerability assessment

No.	Field	No.	Item
1	**Health**	1	Health vulnerability due to floods
		2	Health vulnerability due to typhoons
		3	Health vulnerability due to heat waves
		4	Health vulnerability due to cold waves
		5	Health vulnerability due to ozone enhancement
		6	Health vulnerability due to fine dust
		7	Health vulnerability due to air pollutants
		8	Health vulnerability due to infectious diseases
		9	Health vulnerability by waterborne epidemics
2	**Forests**	10	Landslides due to heavy rainfall
		11	Vulnerability of trails due to landslides
		12	Vulnerability to forest fire
		13	Vulnerability of pine trees to disease and pests
		14	Vulnerability of pine trees to pine fungi
		15	Vulnerability of forest productivity
		16	Vulnerability of vegetation due to drought
3	**Ecosystem**	17	Vulnerability of vegetation growth
		18	Vulnerability of insects
		19	Vulnerability of management of protected areas
4	**Agriculture**	20	Vulnerability of farmlands to erosion
		21	Vulnerability of cultivation facility
		22	Vulnerability of productivity of rice crops
		23	Vulnerability of productivity of apple crops
		24	Vulnerability of productivity of livestock
5	**Water management**	25	Vulnerability of flood regulation
		26	Vulnerability of water utilization
		27	Vulnerability of water quality
6	**Fisheries**	28	Vulnerability of fisheries due to change in water temperature
7	**Disaster**	29	Vulnerability of infrastructure to floods
		30	Vulnerability of infrastructure to heat waves
		31	Vulnerability of infrastructure to heavy snow
		32	Vulnerability of infrastructure to sea level increase

2.2.2. Methods of vulnerability assessment

Vulnerability is the degree to which a system is susceptible to negative effects of climate change, such as climate variation and extreme weather [22]. Vulnerability is defined as a function of climate exposure, sensitivity, and adaptive capacity based on the assessment of the magnitude of climate change and variations [23]. Climate exposure is the degree to which a system is exposed to significant climatic variations that can cause damage. Sensitivity is the degree to which a system is affected, either negatively or positively, by climate-related stimulation. The adaptive capacity is the ability of a system to adjust to climate change variability and extreme weather, to reduce potential damage, or to address the results [22][14][4].

The process of this study is detailed in Figure 1. The seven fields selected are the same as those used by the government in the national climate change adaptation strategy. Thirty-two items for the seven fields were selected considering experts' opinions and important issues of the ROK. Representative variables were then selected for the items of each field. Three characteristics were considered for the seven fields, each of which was assessed by using a series of variables.

Variables for the vulnerability assessment were selected on the basis of article reviews and in-depth interviews with experts. The 32 items were assessed by using categories of climate exposure, sensitivity, and adaptation capacity, and each category included four to six variables. Thus, the theoretical number of variables was greater than 360. However, because duplicate variables were applied to various fields and items in some cases, the actual number of variables was approximately 200. The selected variables were improved and verified by consultation with the climate change consulting group of the Korea Environment Institute, which consists of experts in climate change impacts and adaptation in various fields.

After selection of the variables, their weights were developed to determine the contribution of each. Because it was difficult to set weights on the basis of the literature reviews and interviews, the Delphi method was used to reach a consensus value from a large number of experts by synthesizing their subjective value and

using a feedback process.

Seventy experts were selected for application of the Delphi method for the seven fields. The experts consisted of professors and researchers who performed research relevant to climate change. The execution of the Delphi method required three months, from July to September 2011. The weights were surveyed twice to reach agreement. Each expert set weights by comparing his or her own weights with the average weights of the other experts. Two types of weights were identified in the vulnerability assessment (Table 2). The first weights (FW) were set for climate change (FWce), sensitivity (FWs), and adaptation capacity (FWac), and the sum of the first weights was set as one. The second weights (SW) were set for specific variables in the three categories. The sum of the second weights for climate exposure, sensitivity, and adaptation capacity was also set as one.

Table 2. Method of setting weights

Item	Variable	First weights	Sum of weights	Specific variable	Second weights	Sum of weights
Item A	Climate exposure	FWce	1	Variable a	SWa	1
				Variable b	SWb	
				Variable c	SWc	
				Variable d	SWd	
	Sensitivity	FWs		Variable e	SWe	1
				Variable f	SWf	
				Variable g	SWg	
				Variable h	SWh	
	Adaptation capacity	FWac		Variable i	SWi	1
				Variable j	SWj	
				Variable k	SWk	
				Variable l	SWl	

Data were established for assessment after variable selection and weight setting. Climate data for the present years (2001–2010) and future years (2046–2055; RCP

8.5) were obtained from the KMA. The climate data were converted to various types, considering the properties of the field, such that shown in Table 3. For sensitivity, the sources of data varied because the properties differ among fields and items. Data for the forest and ecosystem fields were collected from the Korea Forest Service, the Korea Environment Institute, and the Ministry of Environment. Data on the water management and disaster fields were provided by the Korea Water Resources Corporation and Korea Ministry of Land, Infrastructure, and Transport. Data relevant to the health field were established by using data from the Korea Ministry of Health and Welfare and the National Health Insurance Service. Information on the agriculture field was constructed by using data from the Korea Rural Community Corporation. Fishery field data were obtained from the Korea Ministry of Oceans and Fisheries. Data for adaptation capacity were provided by the National Statistical Office.

The vulnerability assessment processes included several variables, each with different scales. The objective of the vulnerability assessment was to compare relative vulnerabilities. Therefore, this study normalized all of the variables to make the vulnerability indices comparable. The selected variables were standardized by

$$Z_{i,j} = \frac{X_{i,j} - X_i^{MIN}}{X_i^{MAX} - X_i^{MIN}}, \quad (1$$

where Zi, j is the standardized value of the variable i (climate exposure, sensitivity, or adaptation capacity) of item j; Xi, j is the unstandardized value of variable i of item j; XiMAX is the maximum value of the variable for item j; and XiMIN is the minimum value of the variable for item j. The scale of the variables was normalized from 0 to 1 by equation (1). In addition, the vulnerability indices were normalized considering the vulnerability values of present and future years according to climate change scenarios. A similar standardization method was used for the Human Development Index [24][25].

Numerous methods use climate exposure (CE), sensitivity (S), and adaptation

capacity (AC) to assess vulnerability, which may differ according to the scale of analysis, property of field, and availability of data [26][27]. This study used equations (2) and (3) for assessing vulnerability [4][28]. In equation (2), FWce, FWs, and FWac are the first weights for the variables, and $CE_n, S_n,$ and AC_n are the normalized CE, S, and AC. In equation (3), SW is the second weight for each variable, and Variable the variable is normalized from 0 to 1.

$$\mathrm{V} = \mathrm{FWce} \times CE_n + FW_n \times S_n - \mathrm{FWac} \times AC_n \quad (2$$

$$\mathrm{CE} = \Sigma\,(SW_i \times Variable_i)$$
$$\mathrm{S} = \Sigma\,(SW_i \times Variable_i)$$
$$\mathrm{AC} = \Sigma\,(SW_i \times Variable_i) \quad (3)$$

The first and second weights were applied to the equations to reflect the relative importance of the variables. This simple equation has advantages for clarifying the impacts of the weights and facilitating the understanding of decision makers. Additionally, municipalities can easily adjust the equation when more detailed data is needed for vulnerability assessment.

The most vulnerable case has the highest value in the equations and the lowest possible level of adaptation capacity; the least vulnerable cases have the lowest value. The highest and lowest values differed among items. However, because this study focused only on relative levels of vulnerability, such differences did not affect the results. In addition, operators should be aware that although the vulnerability index is expressed as a quantitative value, it has a qualitative meaning according to the properties of the vulnerability assessment.

2.2.3. Methods of identifying key vulnerable areas

The objective of the second part is this study was to create key vulnerability maps for identifying highly vulnerable municipalities and analyzing their properties.

The vulnerability level was classified into five grades according to the vulnerability index of municipalities. The first grade, which represents the highest vulnerability, had a normalized vulnerability value of 0.8–1 (Figure 1).

After classification of the vulnerability grades, the first-grade maps were synthesized on the basis of each field. This was done for two reasons. The first is that the government considers fields and municipalities when allocating financial resources, and the second it that it is difficult to show every map in this study owing to space limitations. Synthesized maps were made for the seven fields. Future maps considered only the changes in climate exposure to determine the effects of climate change. As previously stated, sensitivity and adaptation capacity data were not available for future conditions, and the existing data were not evaluated because of their large uncertainties.

The key vulnerability map was created by synthesizing the seven first-grade maps for each field; thus, the map included the first-grade areas of 32 items. The 232 municipalities were classified into five grades, considering the number of the first grade of each item. The first grade of the key vulnerability map included the most vulnerable areas, and the fifth grade included the least vulnerable areas. The key vulnerability map was created to describe the most vulnerable areas, considering whole fields in the ROK. Therefore, this map could be utilized as an important basis for the allocation of financial resources.

2.3. Results and Discussion

2.3.1. Vulnerability assessment for representative item

The results were too numerous to include comprehensively in this paper. Therefore, a representative item, “landslides due to heavy rainfall,” in the forest field was selected to show a specific result of the vulnerability assessment. Table 3 shows the variables and weights of the landslide item. Information on the variables and weights for the other 31 items is included in the Appendix. Each of the three variables—climate exposure, sensitivity, and adaptation capacity—consists of four

specific variables (Table 3). A map of each of the three main variables was created by multiplying the standardized variables and weights. The vulnerability map was derived from the three maps by using equations (2) and (3).

Table 3. Variables and weights for landslide vulnerability due to heavy rainfall

Item	Variable	First Weight	Specific variable	Second weight
Landslide due to heavy rainfall	Climate exposure	0.40	Number of dates with more than 80 mm of precipitation	0.24
			Daily maximum precipitation (mm)	0.39
			Summer daily precipitation (mm)	0.21
			Five days of maximum precipitation (mm)	0.16
	Sensitivity	0.37	Average slope of regional forest (degrees)	0.35
			Area of coniferous forest (ha)	0.24
			Average height of regional forest (m)	0.12
			Denuded area (ha)	0.29
	Adaptation capacity	0.23	Government officials per population	0.20
			Area of preventing forest destruction (ha)	0.24
			GRDP (trillion won)	0.18
			Financial independence (%)	0.38

Figure 2 shows the result of the vulnerability assessment for landslides due to heavy rainfall in the present years (2000–2010). Four maps, each for climate exposure, sensitivity, adaptation capacity, and vulnerability included approximately 232 municipalities. The map legends are classified into five grades to show the relative levels of vulnerability. The highest grade includes municipalities with values of 0.8–1; the lowest grade includes those with values of 0–0.2. The five grades were categorized as Highest, High, Medium, Low, and Lowest in reference

to a previous study [29].

The climate exposure map was derived by using four specific variables and the weights of each variable (Table 2). Daily maximum precipitation had the highest weight among the variables; therefore, the distribution of the climate exposure map is strongly affected by the daily maximum precipitation. The northwestern and southeastern regions of the ROK showed high climate exposure.

The sensitivity map also considered four specific variables and weights (Table 3); the slope of the forests, area covered by coniferous trees, and denuded area were important standards for assessing the sensitivity. The sensitivity was affected by the area of forests in municipalities because most of the variables are related to forests. In particular, the eastern region of the ROK is steeper and has higher altitudes than the western region. Thus, the western region showed a high sensitivity value on the map.

The adaptation capacity map was calculated by using four specific variables and their weights (Table 3). The variables were focused on the ability of municipalities to address landslides. Financial independence and areas resistant to forest destruction were important variables in reacting to landslides. Moreover, the adaptation capacity was higher in the northwestern and southeastern regions than those in other areas.

The vulnerability map was derived from climate exposure, sensitivity, and adaptation capacity (Equation 2). Vulnerable areas had high climate exposure, high sensitivity, and low adaptation capacity. Therefore, areas with high adaptation capacity could still have low vulnerability [29]. In the vulnerability map, the northwestern and southeastern regions showed low vulnerability because they had a high adaptation capacity.

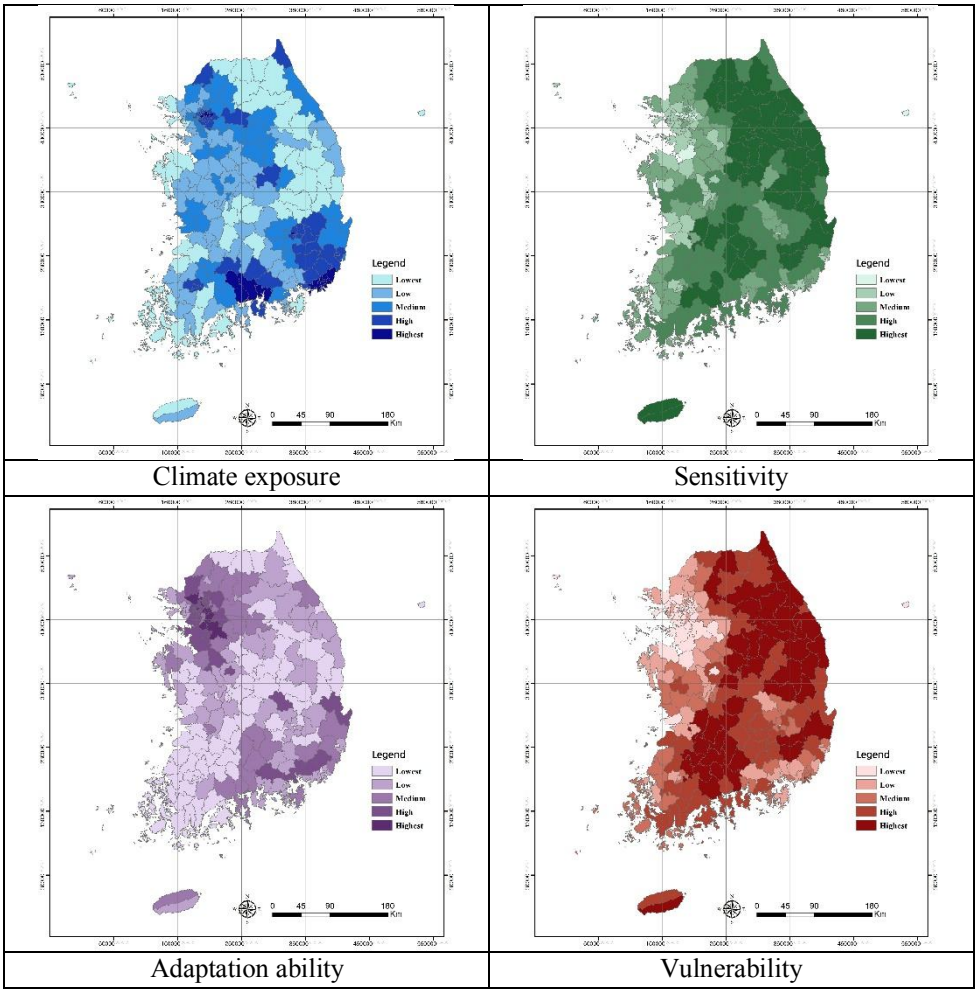

Figure 2. Maps of vulnerability to landslides due to heavy rainfall

2.3.2. Validation for representative item

The validation process was conducted for the vulnerability of landslides due to heavy rainfall by comparing the vulnerability index with records of past landslide occurrences. The records contain landslide occurrence areas and the number of landslide occurrences in the 232 municipalities for the years 2001–2010. Table 4 shows an example of 2006 landslide occurrence data for the representative province, Gangwon-do, which includes 18 municipalities, and 81.7% forestland. These characteristics indicate that Gangwon-do is highly vulnerable to landslides.

The Pearson correlation analysis for the 232 municipalities revealed a correlation coefficient for the vulnerability index and landslide occurrence areas (ha) of 0.594, significant at the 0.01 level according to the two-tailed test. The correlation coefficient of the vulnerability index and landslide number (counts) was 0.457, significant at the 0.05 level also according to the two-tailed test. The vulnerability index for landslides was considered to be reliable based on a high correlation with independent data. Landslide occurrence data for other areas was not available for security reasons.

Table 4. Example of landslide occurrence records and vulnerability index (Source: Gangwon-do, 2006)

Province	Name of municipality	Area of landslide (ha)	Number of occurrences	Vulnerability index
		(Temporal scope: 2006)		
Gangwon-do	Chuncheon-si	9.88	148	0.80
	Wonju-gun	2.60	15	0.72
	Gangneung-gun	7.20	116	0.77
	Donghae-si	0	0	0.72
	Taebaek-si	1.80	12	0.68
	Sokcho-si	0	0	0.63
	Samcheok-si	2.50	11	0.73
	Hongcheon-gun	11.00	137	0.76
	Hoengseong-gun	27.44	205	0.82
	Yeongwol-gun	3.80	57	0.80
	Pyeongchang-gun	279.41	2269	0.83
	Jeongseon-gun	7.3	93	0.74
	Cheorwon-gun	0	0	0.59
	Hwacheon-gun	2.00	50	0.67
	Yanggu-gun	24.66	224	0.81
	Inje-gun	106.20	801	0.81
	Goseong-gun	0	0	0.61
	Yangyang-gun	3.70	79	0.78

This study also conducted Pearson correlation analysis as validation for other items using independent data, including the frequency of events, damage from events, and monitoring information. In addition, correlation of vulnerability indices

and independent data was made by Pearson analysis. The correlation coefficient and significance were checked to assess the reliability of the vulnerability indices. Every item showed reliable results upon conducting a feedback process considering the correlation coefficient with independent data.

The results and data related to validation were too lengthy to include in this paper. Thus, to provide detailed information, Table 5 shows the data type and source for validation. Each field required various data types for validation of the vulnerability index. In many cases, alternative data were used because it was difficult to find optimal data for all items. For example, the water management field compared the vulnerability of the water quality with the budget of purifying the contaminated water in each municipality.

Table 5. Validation data for vulnerability items

Fields	No.	Item	Data type for validation (unit)	Source of data
Health	1	Health vulnerability due to floods	Mortality rates due to floods, morbidity of waterborne epidemics (ratio)	National Emergency Management Agency, Ministry of Health and Welfare
	2	Health vulnerability due to typhoons	Mortality rates due to typhoons (ratio)	National Emergency Management Agency, Ministry of Health and Welfare
	3	Health vulnerability due to heat waves	Mortality rates due to heat waves, records of emergency room visits during heat waves (ratio)	Ministry of Health and Welfare, National Emergency Department Information System
	4	Health vulnerability due to cold waves	Mortality rates due to cold waves, records of emergency room visits during cold waves (ratio)	Ministry of Health and Welfare, National Emergency Department Information System
	5	Health vulnerability due to ozone enhancement	Records of emergency room visits during ozone warning (ratio)	Ministry of Health and Welfare, National Emergency Department Information System
	6	Health vulnerability due to fine dust	Morbidity of lung disease and respiratory disease	Ministry of Health and Welfare

			(ratio)	
	7	Health vulnerability due to air pollutants	Morbidity of lung disease and respiratory disease, records of allergy patients (ratio)	Ministry of Health and Welfare
	8	Health vulnerability due to infectious diseases	Morbidity of infectious diseases (ratio)	Ministry of Health and Welfare, National Health Insurance Corporation
	9	Health vulnerability by waterborne epidemics	Morbidity of waterborne epidemics (ratio)	Ministry of Health and Welfare, National Health Insurance Corporation
Forests	10	Landslides due to heavy rainfall	Landslide occurrence records (area, number)	Korea Forest Service, National Emergency Management Agency
	11	Vulnerability of trails due to landslides	Landslide occurrence records, restoration records for forest trails (area)	Korea Forest Service, Korea National Park Service
	12	Vulnerability to forest fire	Forest fire records (area, number)	Korea Forest Service, National Emergency Management Agency
	13	Vulnerability of pine trees to disease and pests	Records of disease and pests in pine trees (area)	Korea Forest Service, Korea National Park Service
	14	Vulnerability of pine trees to pine fungi	Records of damage due to pine fungi (area)	Korea Forest Service, Korea National Park Service
	15	Vulnerability of forest productivity	Gross primary production, net primary production data (number)	Korea Forest Service, Korea Forest Research Institute
	16	Vulnerability of vegetation due to drought	Records of dead trees due to drought (number)	Korea Forest Service
Ecosystem	17	Vulnerability of vegetation growth	Age class of vegetation, gross primary production, net primary production data (number)	Korea Forest Service, Korea Forest Research Institute
	18	Vulnerability of insects	Records of damage to trees due to insects (area)	Korea Forest Service, Korea Forest Research Institute, Korea National Park Service
	19	Vulnerability of management of protected areas	Damage of protected areas due to extreme weather (cost)	Korea National Park Service, Ministry of Environment
Agriculture	20	Vulnerability of farmlands to erosion	Damage of farmlands due to erosion (area)	Ministry of Agriculture, Food and Rural Affairs
	21	Vulnerability of cultivation facility	Damage of cultivation facility due to extreme	Ministry of Agriculture, Food and Rural Affairs,

			weather (cost)	National Emergency Management Agency
	22	Vulnerability of productivity of rice crop	Decrease in rice productivity due to extreme weather (yield)	Ministry of Agriculture, Food and Rural Affairs
	23	Vulnerability of productivity of apple crop	Decrease in apple productivity due to extreme weather (yield)	Ministry of Agriculture, Food and Rural Affairs
	24	Vulnerability of productivity of livestock	Decrease in livestock productivity due to extreme weather, decrease in dairy productivity due to climate change (yield)	Ministry of Agriculture, Food and Rural Affairs
Water management	25	Vulnerability of flood regulation	Records of flood inundation (area)	Korea Water Resources Corporation, Ministry of Land, Infrastructure and Transport
	26	Vulnerability of water utilization	Records of water supply decrease due to drought (amount)	Korea Water Resources Corporation, Ministry of Land, Infrastructure and Transport
	27	Vulnerability of water quality	Budget for water purification (cost)	Korea Water Resources Corporation, Ministry of Land, Infrastructure and Transport
Fisheries	28	Vulnerability of fisheries due to change in water temperature	Decrease in fishery productivity due to water temperature change (yield)	Ministry of Maritime Affairs and Fisheries, National Fisheries Research & Development Institute
Disaster	29	Vulnerability of infrastructure to floods	Damage of infrastructure due to floods (area)	Ministry of Land, Infrastructure and Transport, National Emergency Management Agency
	30	Vulnerability of infrastructure to heat waves	Damage of infrastructure during heat waves (cost)	Ministry of Land, Infrastructure and Transport, National Emergency Management Agency
	31	Vulnerability of infrastructure to heavy snow	Damage of infrastructure due to heavy snow (cost)	Ministry of Land, Infrastructure and Transport, National Emergency Management Agency
	32	Vulnerability of infrastructure to sea level increase	Damage of infrastructure due to sea level increase (area)	Ministry of Land, Infrastructure and Transport, Korea

				industrial complex corporation

2.3.3. Vulnerability maps based on field scale

The first-grade municipalities of each item were synthesized for each field, and the resultant synthesized vulnerability map provides information about highly vulnerable areas in each field. Each field unit has an important indication for the establishment of adaptation plans and the allocation of financial resources because when establishing the climate change adaptation strategy, the government separated these seven fields considering the characteristics of government ministry. These maps were created for the present years (2001–2010) and future years (2046–2055; RCP 8.5) to compare changes in the first-grade areas resulting from climate change (Figure 3).

The health field consists of various items directly or indirectly related to temperature and rainfall. Most municipalities showed values of 0–2 (first grade) for the present years. However, approximately 10% of the 232 municipalities showed high vulnerability to four–eight items of the health field. These vulnerable municipalities were separated into the following four types according to the property of vulnerability: (a) the climate exposure is higher than that in other municipalities, (b) the sensitivity is higher than that in other municipalities, (c) the adaptation capacity is lower than that in other municipalities, and (d) a combination of (a), (b), and (c). For example, Busan, which is located in the southern area, showed type (d) vulnerability.

Future vulnerability was assessed by using only the change in climate conditions. That is, the results were obtained by simulating future vulnerability using the present conditions of sensitivity and adaptation capacity. Items related to rainfall showed much higher vulnerability than that in the present years. The health vulnerability of Seoul, which is the capital of the ROK, showed a particularly dramatic increase in future climate conditions, which demonstrates that the present condition of the adaptation capacity may not be sufficient in the future. Moreover,

Busan showed a continuously high vulnerability in the present and future years, which shows that improvement in the adaptation capacity is very important for type (d) municipalities for reducing climate impacts.

The forest field includes seven items that are affected by rainfall and temperature, and its vulnerability is strongly affected by areas of forest in the municipality. The eastern and southwestern areas of the ROK have more forestland than the other areas and therefore showed many first-grade vulnerability items in the present years. These highly vulnerable areas of the forest field were classified as type (a) vulnerability; therefore, these areas should extend their adaptation capacities to reduce damage related to forests.

The future vulnerability of the forest was increased for items related to rainfall such as landslide, vulnerability of trails, drought, and forest fire. The reason for the increase in some eastern areas that showed much higher vulnerability than that in the present years was determined to be the increased prevalence of extreme weather such as heavy rainfall and severe drought.

The ecosystem field had three items for vulnerability assessment, all of which were related to long-term changes in rainfall and temperature. The areas with high ecological value were determined to have higher vulnerability than other area and were classified as type (a) vulnerability. The eastern and southwestern areas had many first-grade vulnerable areas, similar to that in the forest field. The vulnerability was more highly affected by sensitivity variables than climate exposure and adaptation capacity. The distribution of first-grade areas did not change significantly in the future because the sensitivity is more important than climate conditions for the ecosystem field.

Five items were included in the agriculture field. Productivity of rice, apples, and livestock were related to gradual changes in rainfall and temperature. The other two items, erosion of farmlands and damage to cultivation facility, were related to extreme weather such as heavy rainfall. The first-grade areas of the agriculture field were classified as type (d) vulnerability. Thus, the items were similarly affected by

all three characteristics of climate exposure, sensitivity, and adaptation capacity.

The water management field included three items. Flood and water utilization were related mainly to rainfall variables, and water quality was related to temperature and rainfall. However, the adaptation capacity is a more important factor than climate exposure for assess vulnerability in this field. The vulnerable municipalities of water management were classified as type (c) vulnerability.

The first-grade areas are concentrated in the capital area and western areas at the present. The capital area vulnerability is due to its high population density, and the western areas are vulnerable to water management because most of the rivers are located in the eastern areas of the ROK. The future vulnerability did not differ significantly from that of the present according to the important role of the adaptation capacity.

The fisheries field focused on assessing the negative effects of the increase in water temperature, and the analysis targets were limited to municipalities near the sea. The western and southern areas showed higher vulnerability than other areas. Climate exposure and sensitivity are important factors for this field; therefore, it was categorized as both (a) and (b) types. The future vulnerability showed a distribution similar to that of the present.

The disaster field focused on damages to infrastructure, and all of the items were strongly affected by climate exposure and sensitivity, and the vulnerable areas were classified as (a) and (b) vulnerability types. The capital area showed many first-grade items because of its greater infrastructure relative to other municipalities. Some municipalities in the southeastern areas showed high vulnerability due to sensitivity variables related to areas of infrastructure, and the future vulnerability was similar to that of the present. These results indicate that sensitivity is a more important factor than climate exposure in the disaster field.

	Present (2001–2010)	Future (2046–2055)
1. Health	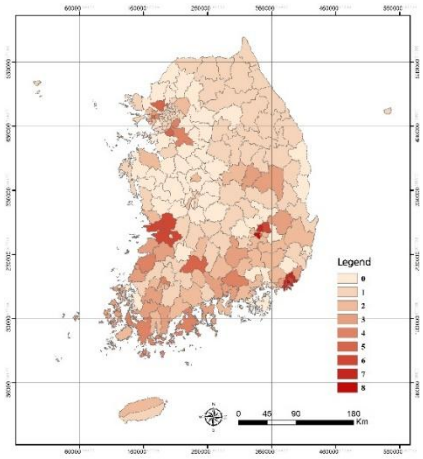	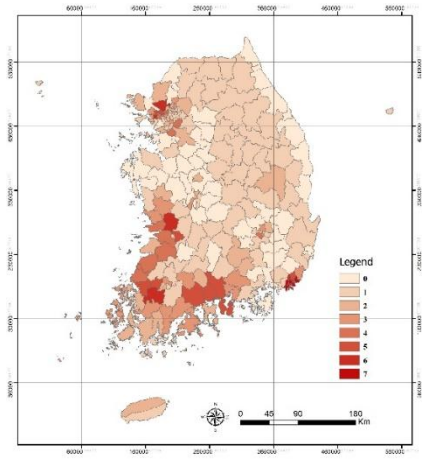
2. Forest	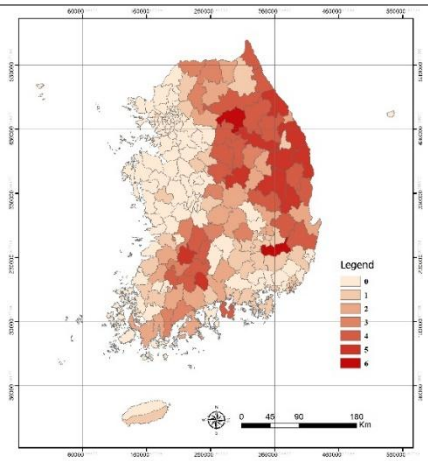	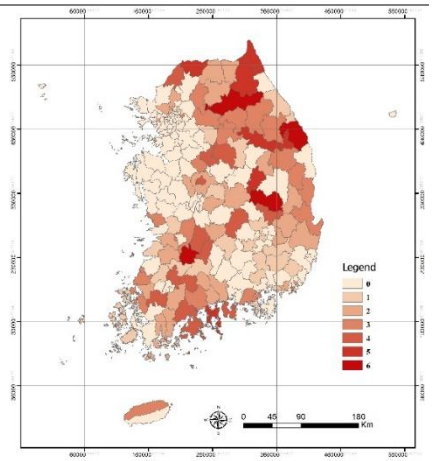
3. Ecosystem	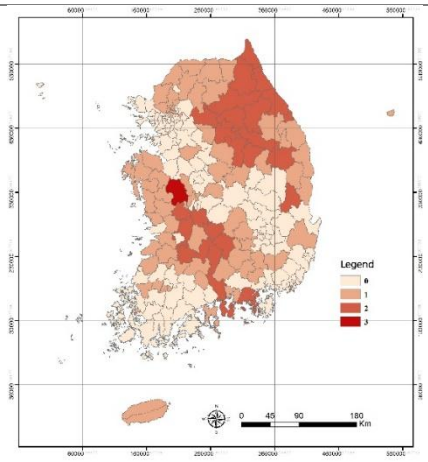	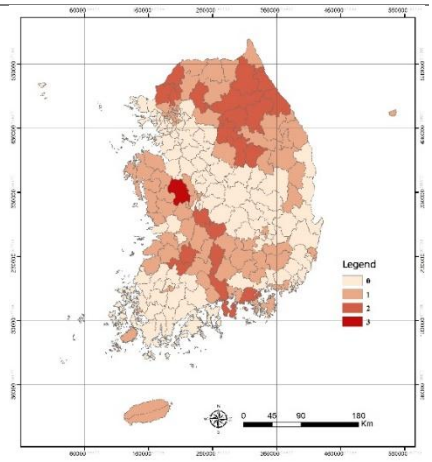

4. Agricul-ture	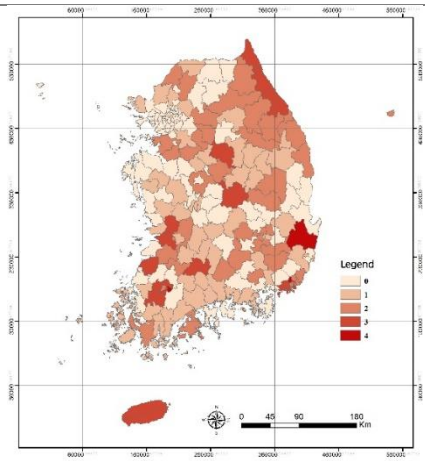	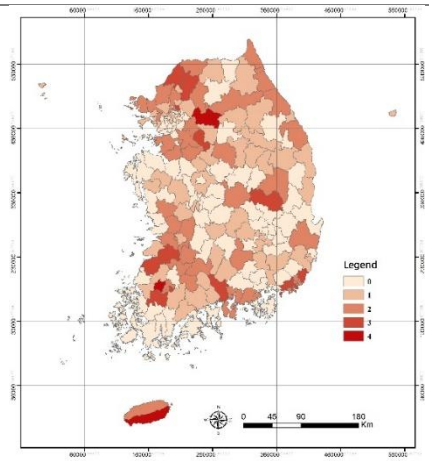
5. Water Manag e-ment	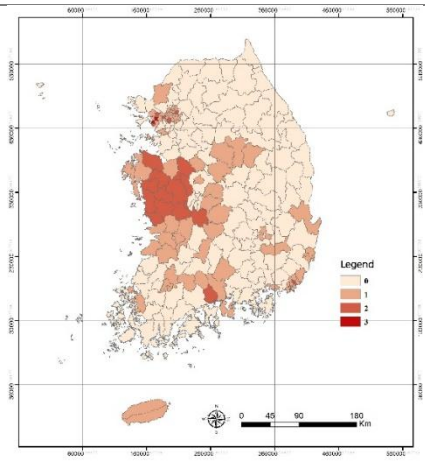	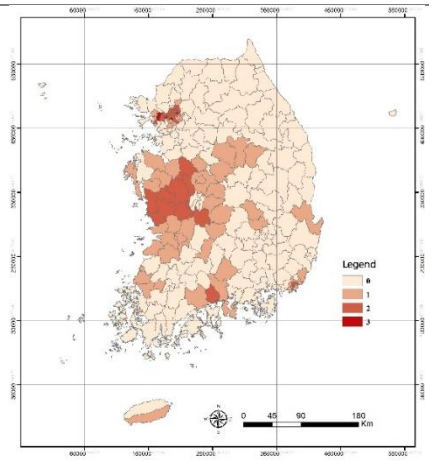
6. Fisheri es	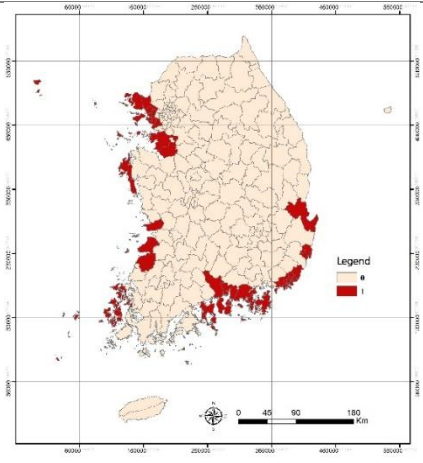	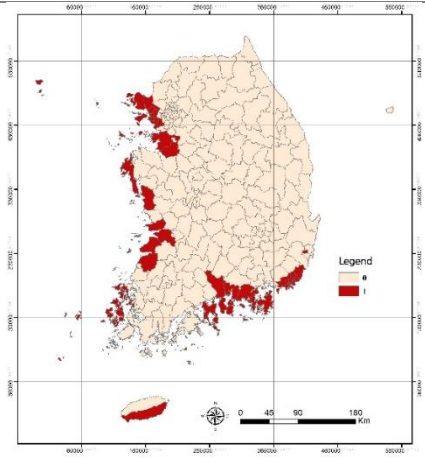

7. Disaster

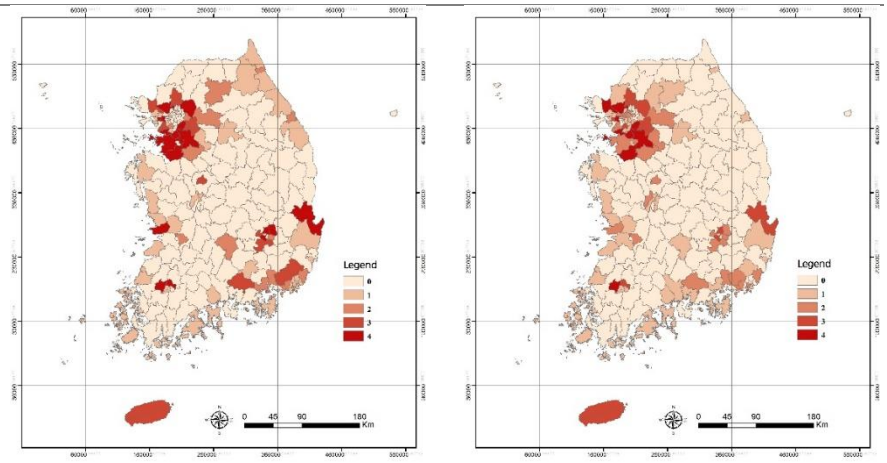

Figure 3. Distribution of the first-grade areas for the seven fields in the present and future

2.3.4. Vulnerability maps based on field scale

The first-grade maps of each field were aggregated as synthesis maps to describe the most vulnerable areas of the present and future years (Figures 4a, 4b) in order to support the government program. The government has the authority to allocate financial resources for establishing adaptation plans. Government decision makers can utilize these synthesis maps to determine the most urgent needs of municipalities in the establishment of adaptation plans.

The classification of the first-grade areas in the synthesis map was used to compare the relative vulnerability among municipalities. The highest grade includes 12 to 17 items assessed as first grade (Figures 4a, 4b). The northeastern, southwestern, and southeastern areas had the highest grade of municipalities at the present including 9–11 items distributed in the northeastern and southwestern areas (Figure 4a).

The main reasons for these high-grade areas are the health, forest, agriculture, and disaster fields, which showed distributions similar to those in the present first-grade map. Highly vulnerable municipalities that were assessed with the highest and high grades showed all vulnerability types, although type (c) was the most common. Moreover, the municipalities of type (c) vulnerability showed the highest grade in

the future synthesis map (Figure 4b). Thus, the municipalities that had a high climate exposure and sensitivity and low adaptation capacity showed the greatest vulnerability to climate change impacts.

The variation map shows different values of a number of first-grade items between the present and future years (Figure 4c). This map helps to easily identify municipalities in which first-grade items are abruptly increased in the future. The highest-grade municipalities appeared in the northwestern and southwestern areas of the ROK, where the climate exposure increased in the future, and the adaptation capacity was relatively low. The lowest grade municipalities showed highest or high grades at the present.

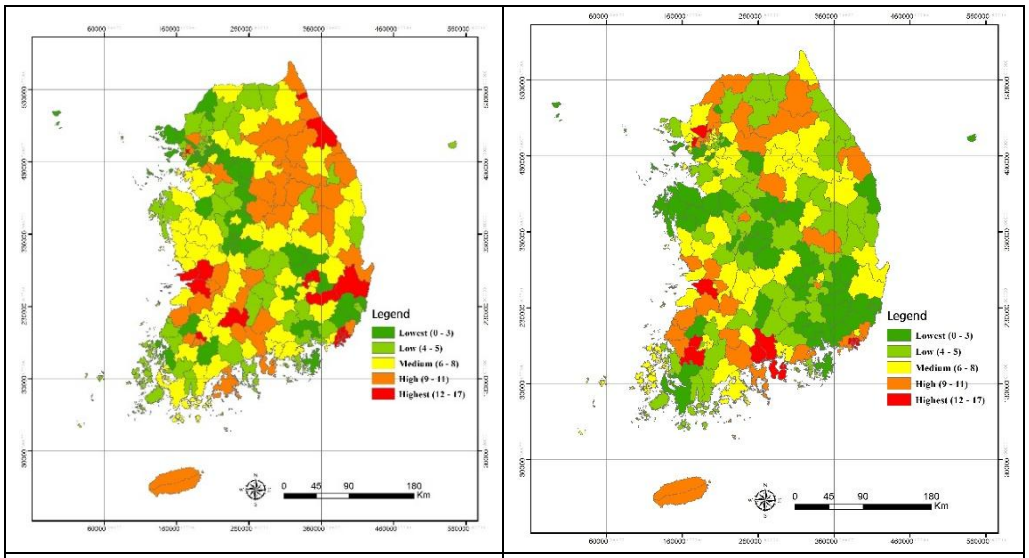

a. Present (2001–2010) | **b. Future (2046–2055, RCP 8.5)**

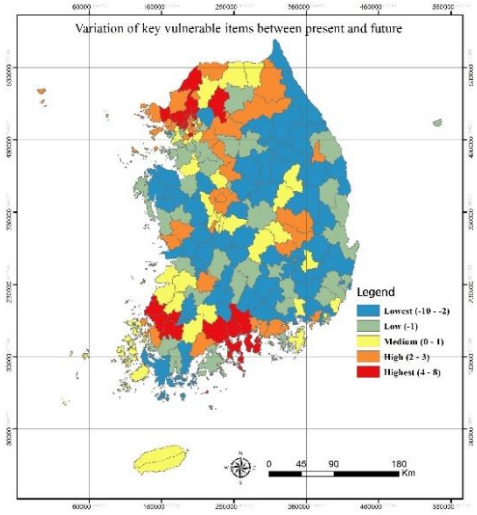

c. Variation maps between present and future

Figure 4. Key vulnerability areas of the seven fields

2.4. Conclusion

This study used a combination of quantitative and qualitative methods for vulnerability assessment of 32 items in 7 fields in 232 municipalities. The suggested framework can reduce the subjectivity and clarify the assessment process because the variables, weights, and integration method are explicit (Appendix). Therefore, all operators can obtain the same results as those reported in this study, and readers can understand the exact results and methods used [30][11]. Equations (2) and (3) reflect the direct impact of weights on variables by following the basic concept of vulnerability [28].

Setting priorities and allocating resources are the most difficult processes for the government in adapting to climate change [4][31][9][32], and identification of the most urgent municipalities poses further challenges. Thus, information about the priority of vulnerability is helpful for allocating financial resources to highly threatened municipalities. In this context, the present study can provide useful knowledge and serve as an important basis in establishing adaptation plans. By using the results of this vulnerability assessment, decision makers can clearly

identify vulnerable areas, vulnerable fields of a particular municipality, and the reason for the vulnerability. Moreover, this study can be utilized as a reference or a basic tool for more specific vulnerability assessments than those on the national scale.

Readers should consider that the vulnerability indices cannot provide objective values or absolute vulnerabilities. The Delphi method, one of the important methods used in this study, is an effective tool for reaching a consensus value; however, it cannot provide objective weights. Additionally, only the climate conditions are changed in the future vulnerability assessment even though damage can have a significantly stronger dependence on other conditions such as land-surface modification [33][34]. This limitation is attributed to the lack of future environmental and socio–economic data. Although several studies have predicted changes in socio–economic information for the ROK, the results have not been validated and have a large amount of uncertainty [35][36][37][38]. Therefore, the government of the ROK analyzed future vulnerability by using only future climate data. This method has merit in identifying negative and positive effects according to changes in climate condition. However, improvement is needed in further studies to obtain more reliable results.

Acknowledgement

This work was supported by the Climate Change Vulnerability Assessment of Local Government for Establishment of Adaptation Plan project (Korea Environment Institute, National Institute Environmental Research), the 2015 BK 21 Plus Project (Seoul National University Interdisciplinary Program in Landscape Architecture, a global leadership program toward innovative green infrastructure), the Development of Economic Assessment Technique for Climate Change Impact and Adaptation Considering Uncertainties (Korea Ministry of Environment, Project No. 2014001310010), the Development of Climate Change Adaptation, Management Techniques, and Supportive System (Korea Ministry of Environment, Project No. 416-111-014), the Development of Climate Change Policy Supporting Model for Impact Assessment and Adaptation Planning (Korea Ministry of Environment, Project No. 2014001310005).

3. CHAPTER 2 : Evaluating Landslide Impact Assessment Considering Climate Change for Gangwon-do

3.1. Introduction

The Witseoreum area of Jeju Island recorded precipitation of 810 mm on May 27, 2013. This event constituted a record for single-day rainfall in May and is the second highest incidence of single-day rainfall on an annual basis, surpassed only by the 978.5 mm of precipitation received on August 18, 2004 (Korea Meteorological Administration, 2013). This heavy rain caused large-scale and small-scale damage, including flooding of farmland and houses, the isolation of people owing to flooded valleys, and blocked roads. The significance of this rainfall event becomes evident when one considers that average annual rainfall in Korea is approximately 1300 mm.

Extreme meteorological events, such as this recent one, have become increasingly severe in recent years. Heavy rain is a major cause of landslides, and the number of landslides triggered by heavy rain is increasing [39][40][41]. According to the Representative Concentration Pathways (RCP) scenario provided by the Korea Meteorological Administration (KMA), average annual rainfall in Korea is expected to increase by 4.5–6% by 2100. However, a significant problem is that torrential rains will most likely be concentrated during a particular period. Figure 1 shows a graph of daily maximum rainfall caused by heavy rain, based on the above-mentioned RCP scenario. The graph shows daily maximum rainfall in Gangwondo from 2011 to 2099 (Figure 5). Daily maximum rainfall is colored blue in the graph, and its frequency and scale increase toward the year 2099.

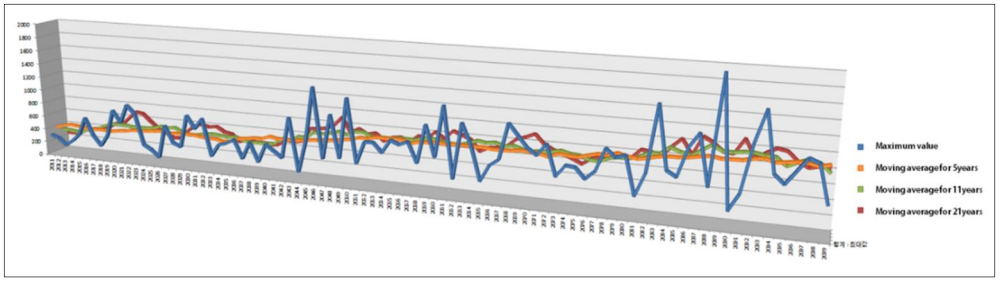

Figure 5. Daily maximum rainfall in Gangwondo. The graph shows the RCP 8.5 scenario from 2011 to 2099

Gangwondo is located in the eastern area of South Korea (Figure 2-2). The area has high elevation and a dynamic topography, with large elevation differences. Gangwondo is thus at high risk of landslides. In 2006, the province suffered large-scale damage caused by torrential rains resulting from typhoon Ewiniar, affecting 44 human lives (25 casualties and 19 missing persons). Furthermore, 5,617 hectares of farmland were flooded or washed away. Most of the damage was presumed to be directly or indirectly related to landslides and flooding. Much larger landslides may occur as a result of enhanced extreme meteorological events due to future climate change. The province is thus in urgent need of hazard evaluation of landslides caused by heavy rain due to climate change.

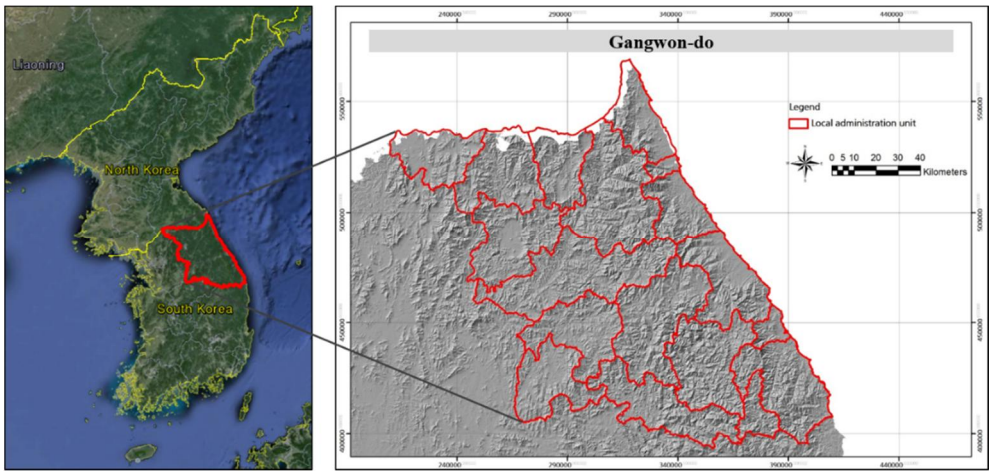

Figure 6. Study site (Gangwondo, South Korea)

The purpose of this study is to evaluate landslide hazards in the Gangwondo area using the RCP 4.5 and 8.5 scenarios for climate change, and to assemble and compare results. The RCP 4.5 scenario predicts climate under the assumption that the present level of carbon dioxide emissions is maintained. The RCP 8.5 scenario predicts climate under the assumption that the present level of carbon dioxide emissions changes drastically. It is possible to estimate potential landslide hazard due to climate change using these scenarios. Meanwhile, given the uncertainties inherent in such climate change scenarios [42], statistical methods were applied in order to evaluate the extent of uncertainty in this study.

The results of this study are significant in that the study adopts RCP scenarios that have not been previously applied to any landslide hazard evaluation. Most development plans only take into account economic and social parameters. As a result, developed areas are vulnerable to natural disasters because they are located in hazard areas [43]. A map of landslide hazard areas is therefore necessary for natural hazard management and for planning development in mountainous areas like Gangwondo [44]. The landslide hazard map produced by this study is expected to be a useful resource for setting priorities in establishing policies for the Gangwondo area.

3.2. Methods

3.2.1. MaxEnt model

There have been several landslide studies that have used Geographic Information Systems (GIS) and spatial distribution models (SDMs). These studies generally assess the probability of landslides and construct hazard maps [45][46][47][48][49]. There are several SDMs that can be applied to the assessment of landslides. SDMs can be divided into two categories (Table 6). One category requires only presence data, while the other category requires both presence and absence data. It is generally very difficult to acquire both presence and absence data. The local government of Gangwondo also has only landslide occurrence data (presence); GARP and MaxEnt were therefore considered to be appropriate models for use in this study.

Table 6. Spatial distribution models

Model	Characteristics	Data requirement
GLM (Generalized Linear Model)	• Linear model • Type of logistic regression model	Presence / Absence data
GAM (Generalized Additive Model)	• Nonlinear model • GRASP 3.0 is representative model	
CART (Classification and Regression Tree)	• Nonlinear model • Using binary tree to recursively part • By moving from the root node through to the terminal node of the tree	
ANN (Artificial Neural Network)	• Nonlinear model (apply to linear and nonlinear data) • Using concept of artificial neural network	
GARP (Genetic Algorithm for Rule-Set Prediction)	• Nonlinear model • Machine-learning algorithm that creates ecological niche models for a species	Only presence data
MaxEnt (Maximum Entropy Model)	• Nonlinear model • Using concept of Maximum Entropy • Validated by ROC curve	

Literature was reviewed to identify the most appropriate model for analysis of landslide hazards. MaxEnt has recently been applied in landslide assessments and

showed better performance than GARP in SDMs [50]. The performance of models was assessed using the area under curve (AUC) value of receiver operating characteristic (ROC) curve analysis. Other studies of landslide susceptibility indicated that MaxEnt had the highest AUC value from among 4 SDMs (logistic regression, multiple adaptive regression splines, classification and regression trees, and MaxEnt) [51]. The MaxEnt model has also been used to identify driving factors of landslides [52] and has been utilized in the latest studies of landslide modeling. Additionally, MaxEnt exhibited the best performance among the models considered; it was therefore selected as the most appropriate.

The MaxEnt SDM was developed by the AT&T Labs research team. It constitutes a general method to predict or estimate data using incomplete information. The origins of maximum entropy lie in statistical mechanics [53]; however, the MaxEnt method has also been applied to various other areas, including statistical physics, astronomy, optimization, and image construction [50]. MaxEnt was first applied in SDMs approximately ten years ago [54].

3.2.2. Research process

Figure 7 is a flowchart explaining the full process followed in this study. Before constructing the landslide model, literature was reviewed in order to identify variables and an appropriate model. The variables that were input into the model are weather, topography, ground material, and vegetation, with these being major factors that influence landslides [55][56][57]. For variables that constitute major factors, variables considered valid in previous studies were selected (Table 7).

Weather variables, such as maximum rainfall and cumulative precipitation, are related to landslides [40]. Various criteria, such as number of days with more than 80 mm, 120 mm, or 160 mm of rainfall, were applied to determine factors affecting landslides. The contributions of other variables were identified through model operation and major variables were selected considering the interrelationships

between variables. Each variable was constructed using a 100 m × 100 m cell size.

Table 7. Variables for landslide model

Category	Variables	References	Data References
Climate factor	Daily maximum rainfall (mm)	(Guzzetti et al. 2008; Choi et al. 2011)	AWS (KMA, 2006), RCP 4.5, 8.5 scenario (KMA, 2013)
	5 days of maximum precipitation (mm)	(Kim and Chae 2009; Choi et al. 2011)	
	Number of days with over 80 mm of rainfall	(Kim and Chae 2009; Yoo et al. 2012)	
	Number of days with over 120 mm of rainfall		
	Number of days with over 160 mm of rainfall		
Topography factor	Slope	(Ayalew and Yamagishi 2005; Ermini et al. 2005; Kim and Chae 2009; Oh 2010; Choi et al. 2011; Yeon 2011)	DEM (KME, 2008)
	Elevation	(Ayalew and Yamagishi 2005; Oh 2010; Choi et al. 2011; Kim et al. 2011)	
	Aspect	(Ayalew and Yamagishi 2005; Oh, 2010; Yeon 2011)	
	Distance from mountain range	(Yeon 2011)	
	Distance from stream flow	(Oh 2010)	Map of stream order (WAMIS, 2008)
Ground material	Soil depth Soil drainage Soil name Soil type	(Pradhan and Lee 2010; Oh 2010; Yeon 2011)	Soil map (WAMIS, 2006)
Vegetation factor	Coniferous, Deciduous, Mixed forest	(Yao et al. 2008; Kim et al. 2011; Yeon 2011)	Map of forest type (KME, 2005)
	Age of forest	(Yeon 2011; Oh 2010)	
	Class of DBH (diameter at breast height)	(Kim et al. 2011; Yeon 2011)	
	Natural forest, Artificial forest	(Kim et al. 2011)	

After inputting relevant data, the MaxEnt model was run using various types of data, in order to extract the optimal combination. The AUC value was considered to be an important factor in selecting the optimum landslide model. Based on this work, an optimal landslide model was designed in order to identify potential future landslide hazard areas. RCP 4.5 and 8.5 climate change scenario data were used to construct future climate variables. The 30-year average value was calculated in order to apply the climate scenarios to the landslide model. The scenario periods were divided into three categories (2011–2040, 2041–2070, and 2071–2099). Probability maps of future landslide occurrence were constructed through modeling.

The potential landslide hazard area was also estimated by applying threshold values of the landslide model.

Potential landslide hazard maps were generated using the aforementioned methods. These potential landslide hazard areas could face threats that may potentially result in negative impacts for people and infrastructure. The relationship between potential landslide hazard areas and current land use (land cover) was therefore analyzed in order to derive insights for decision makers and planners in Gangwondo. Additionally, given that climate change scenarios have inherent high uncertainty [42], this was analyzed using statistical methods. Seven values (minimum value, ±95% confidence level, mean, ±90% confidence level, and maximum value) were derived from each climate variable, also considering the standard distribution.

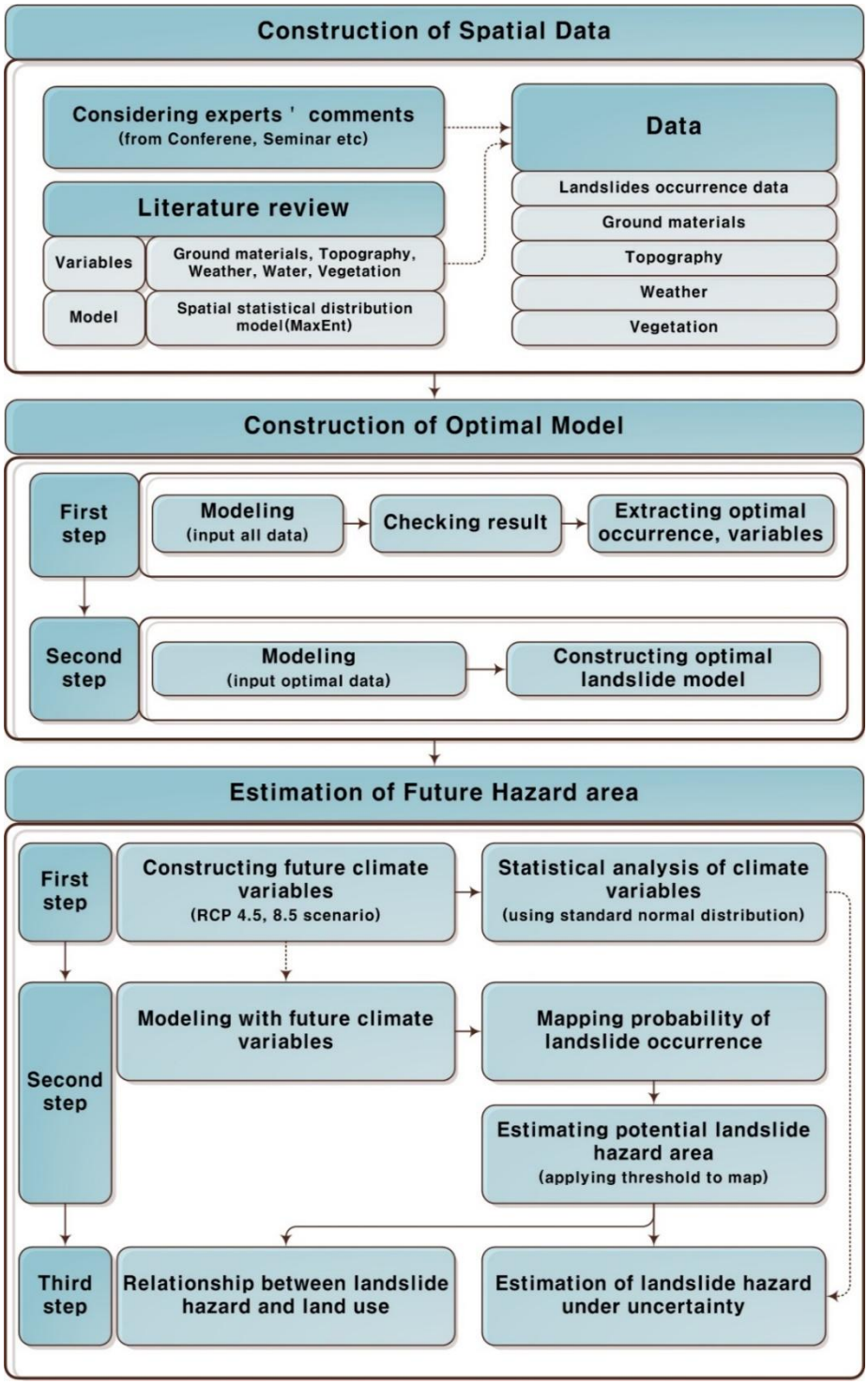

Figure 7. Flowchart of study

3.3. Results

3.3.1. First model run

In the process of inputting landslide location data into the MaxEnt model, location was categorized into three types according to the extraction method, and the most statistically reliable type was selected through the first model run. Three types of locations were extracted: whole landslide locations (type 1), landslide locations within the forest (type 2), and top 1,000 landslide locations within the forest (type 3). A comparison of ROC validation results according to the method of extracting landslide locations revealed the highest AUC value for type 3, followed by type 2, and then type 1 (Figure 8). The landslide model with the statistically highest forecast accuracy could therefore be extracted from type 3. This study thus used the 1,000 largest landslide locations within the forest.

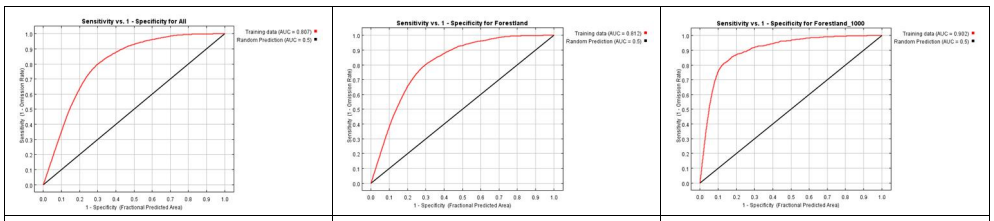

Type 1 (AUC value : 0.807)	Type 2 (AUC value : 0.812)	Type 3 (AUC value : 0.902)

Figure 8. ROC curve and AUC values by extraction type of landslide location

After selecting the appropriate landslide location type, the contribution of each variable was checked through the modeling process with all input-enabled variables. MaxEnt provides information on the importance of variables through various methods. The three most representative information items are percent contribution, permutation importance, and the jackknife of regularized training gain. Percent contribution is extracted in the process of model training. It is obtained by continuously recording the degree of variable contribution to the training process to obtain the optimal model. As for MaxEnt, the coefficients of variables are adjusted to obtain an optimal model that has high training gain and the most frequently used

variables have high contribution. Contribution should be interpreted by considering the intervariable relationship, and a specific variable with high contribution does not necessarily have singular importance [66].

Given the interrelationship between variables, percent contribution is therefore not a sole indicator of variable importance and other important information is provided to complement this aspect. A second information item pertaining to importance is permutation importance. This is different from percent contribution in that it is not obtained in the process of model operation but from the final MaxEnt model. Permutation importance is extracted by measuring AUC with random variable substitution against the training point, such that the permutation importance can be extracted by determining that a variable showing a large decrease in AUC is a variable on which the model is heavily dependent. Importance is provided by a figure converted into a percentage.

A further item of information on importance is extracted through jackknife analysis. Together with the contribution analysis result, this is an additional method that can be used to help determine the importance of a variable. Many additional models are generated when jackknife analysis is used. First, a model is produced by removing each variable one by one. Second, a model is generated with only one variable. Through this process, training gain values are compared, and the relevant variable is evaluated to determine if it is useful for estimating landslide location distribution. Table 8 and Figure 9 show variable importance information that was extracted through the first run.

Table 8. Percent contribution and permutation importance (results of the first model run)

Rank	Variable	Variable code	Percent contribution	Permutation importance
1	5 days of maximum precipitation (mm)	day5	34	49.3
2	Number of days with over 120 mm	over120	25.9	15.2
3	Elevation	elevation	14	13.9
4	Natural forest, Artificial forest	naturalplant2	7.4	3.1
5	Coniferous, Deciduous, Mixed forest	forest	3.4	0.4

6	Soil drainage	soildrain	3.2	0.8
7	Daily maximum rainfall (mm)	maxrn	3	8.3
8	Slope	slope	2.9	3.5
9	Distance from mountain range	rangedis	1.5	2.2
10	Number of days with over 80 mm	over80	1.5	0.9
11	Soil name	soilname	0.9	0.1
12	Soil type	soiltype	0.6	0.3
13	Age of forest	yung	0.5	0.4
14	Aspect	aspect	0.4	0.3
15	Soil depth	soildepth2	0.3	0.2
16	Number of days with over 160 mm	over160	0.3	0.6
17	Class of DBH	kyung	0.1	0.2
18	Distance from stream flow	streamdis	0	0.1

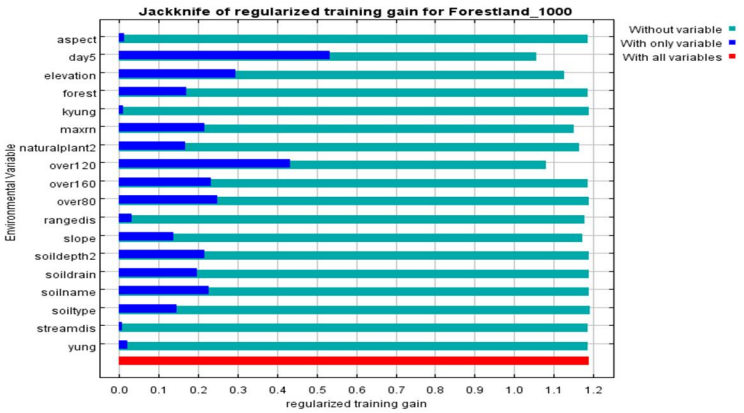

Figure 9. Variable importance through jackknife analysis (results of the first model run)

To eliminate variables with a low contribution rate from those identified as having high importance, a selection was made among the variables for the number of days having more than 80 mm, 120 mm, or 160 mm rainfall (with high correlation). The number of days with more than 120 mm of rainfall was selected as a major variable because it showed the highest contribution rate. Variables with low contribution rates were excluded; as a result, all variables concerning direction, class of DBH, age of forest, distance from a ridge, and distance from a stream were excluded from the model. The selected major variables were daily maximum rainfall, number of days with more than 120 mm of rainfall, the five days of maximum precipitation, altitude, forest type (coniferous, deciduous, or mixed stand

forest), natural/artificial forest, slope, soil depth, soil drainage, soil name, and soil type (Table 9).

Table 9. Final variables input into landslide model

Classification	Variables	References
Climate factor	Daily maximum rainfall (mm) 5 days of maximum precipitation (mm) Number of days with over 120 mm of rainfall	AWS (KMA, 2006), RCP 4.5, 8.5 scenario (KMA, 2013)
Topography factor	Slope Elevation	DEM (KME, 2008)
Ground material	Soil depth Soil drainage Soil name Soil type	Soil map (WAMIS, 2006)
Vegetation factor	Coniferous, Deciduous, Mixed forest Natural forest, Artificial forest	Map of forest type (KME, 2005)

3.3.2. Second model run

The model was run again after inputting the data for optimal landslide locations extracted from the first model run. During the second model run, five-fold cross-validation was carried out to minimize the errors that occurred in the process of extracting training data for landslide locations. This study divided the population of 1,000 landslide locations into five small groups for analysis. The results of the second model run showed an average AUC value of 0.891, obtained with ROC verification through five-fold cross-validation, representing very good1 forecast accuracy (Figure 10).

[1] Standard of AUC value [100] : 0.9 –1.0 : excellent, 0.8–0.9 : very good, 0.7–0.8 : good, 0.6–0.7 : average, 0.5–0.6 : poor.

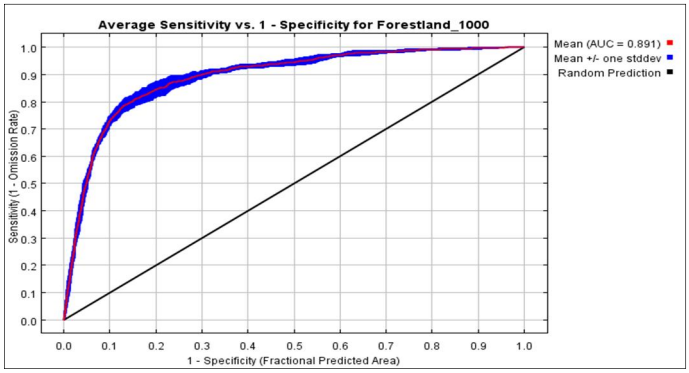

Figure 10. ROC curve and AUC value (second model run)

3.3.2.1. Variable importance

The variable importance extracted from the second run is shown in Table 10 and Figure 2-7. Although there was no significant difference from the results of the first run, the importance of daily maximum rainfall tended to increase and the importance of soil drainage tended to decrease. Jackknife analysis showed that the most influential variables on model training, when not included in the model, were five days of maximum precipitation, number of days with more than 120 mm of rainfall, altitude, daily maximum rainfall, slope, and natural/artificial forest (bluish green color in Figure 11). Soil name, soil depth, soil drainage, and forest type were found to be very influential as individual variables (blue color).

Table 10. Percent contribution and permutation importance (result of second model run)

Rank	Variable	Variable code	Percent contribution	Permutation importance
1	5 days of maximum precipitation (mm)	day5	35.8	51.7
2	Number of days with over 120mm	over120	26.8	15.9
3	Elevation	elevation	13.4	14
4	Natural forest, Artificial forest	naturalplant2	8	2.6
5	Daily maximum rainfall (mm)	maxrn	4.1	9.8
6	Coniferous, Deciduous, Mixed forest	forest	3.5	0.3
7	Slope	slope	3.3	4
8	Soil depth	soildepth2	3.3	0.7

9	Soil drainage	soildrain	1	0.3
10	Soil name	soilname	0.4	0.3
11	Soil type	soiltype	0.3	0.3

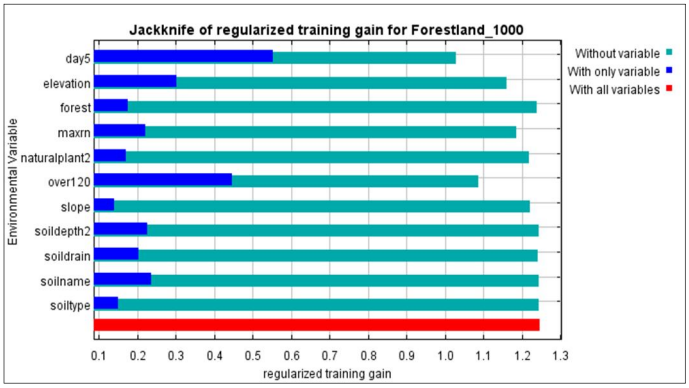

Figure 11. Variable importance through jackknife analysis (results of the second model run)

3.3.2.2. Variable response graph

Figure 12 is a reaction curve that shows the relationship between the input variables and the possibility of landslide occurrence. First, variables related to precipitation were examined. The possibility of landslide occurrence was found to be high when there is daily maximum rainfall of about 200–250 mm, and the possibility was shown to increase when the number of days with more than 120 mm of rainfall is two or more. For the variable measuring the five days of maximum precipitation, the area with rainfall exceeding 500 mm showed an increased possibility of landslide occurrence. There was a section that showed a lower possibility of landslide occurrence irrespective of the value of the rainfall variable (small or large). This is understood to be a phenomenon that may occur because the number of variables belonging to the relevant section is small.

In the case of slope, the possibility of landslide occurrence was high when slope was 15–20°. In the case of soil type, moderately coarse texture showed high possibilities of landslide occurrence, while in the case of soil drainage, well-drained

soil was shown to have similar high landslide susceptibility. Soil with moderately coarse texture is well drained and vulnerable to landslides. This tendency coincides with general landslide locations (National Academy of Agricultural Science, 2008). Artificial forests (of natural/artificial forests) and coniferous forests (among coniferous, deciduous, and mixed-stand forests) exhibited high possibilities for landslide occurrence. Artificial forests are considered to be vulnerable to landslides because they have a single-stratum vegetation structure and have mostly shallow-rooted, rapidly growing trees. Coniferous forests also may have a high possibility of landslides because of shallow-rooted trees (Korea Forest Service, 2009).

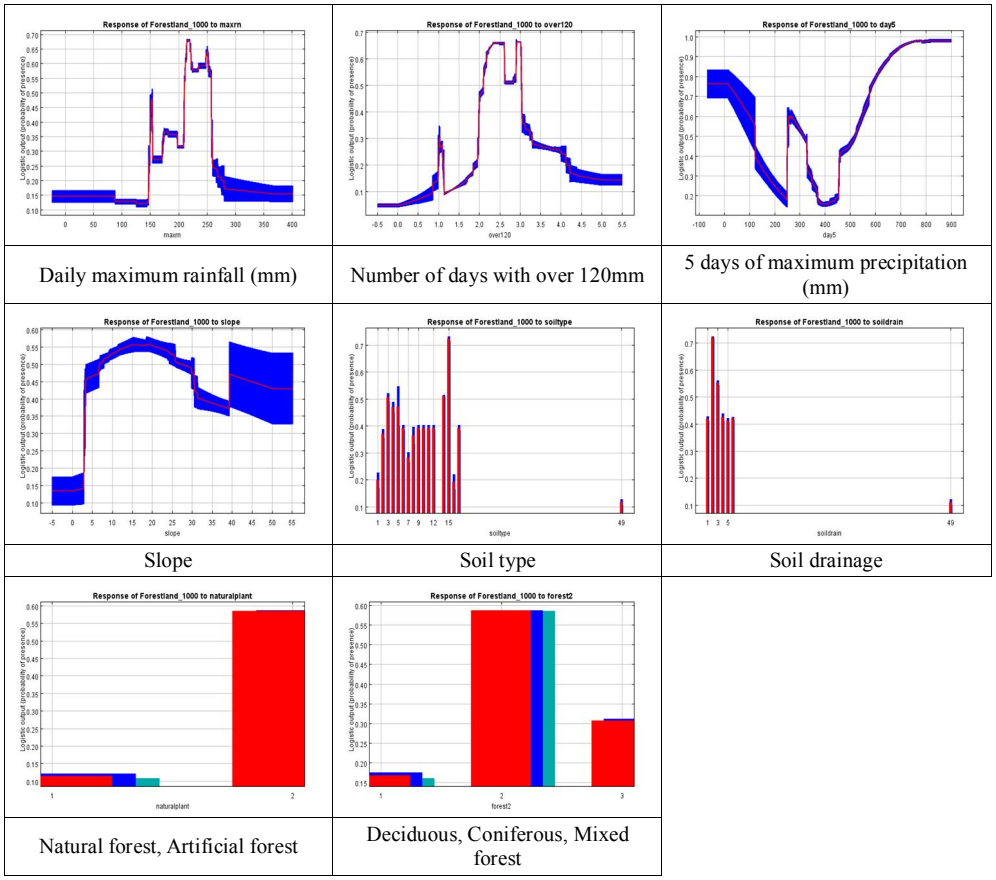

Figure 12. Response graphs for variables, provided by the MaxEnt model

3.3.2.3. Landslide occurrence probability map

Figure 9 shows the operation result of the optimal model, which was extracted using the relationship between landslide occurrence areas in 2006 and variables. Five-fold cross-validation was used for model operation, and Figure 13 shows the average value of five maps of probable landslide occurrence. Landslide probability was high around major landslide areas, including Pyeongchang, Inje, and Chuncheon. The logistic threshold value of 10 percentile training presence, which serves as a basis for identifying major landslide hazard areas, was shown to be 0.200.

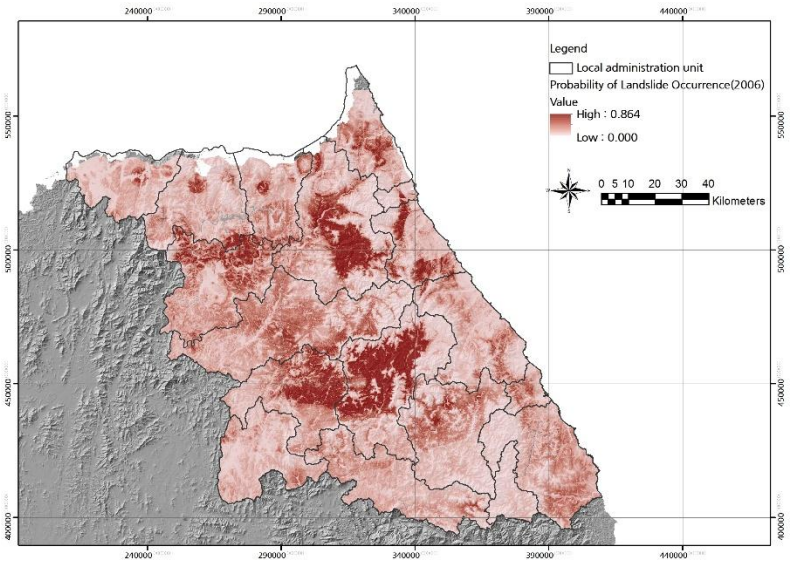

Figure 13. Landslide occurrence probability map for 2006

3.3.3. Probability prediction of landslide occurrence

The probability of landslide occurrence was predicted based on the landslide model derived from 2006 data and on weather variables extracted from the RCP 4.5

and 8.5 scenarios (Figure 14). Climate, as defined by IPCC, is the average value of 30-year meteorological conditions. This study thus extracted weather variables for each year from 2011 to 2099 and used the 30-year average value. In other words, the average value was obtained by extracting the extreme weather variables of each year, not by extracting weather variables of the average value of 30 years. Average 30-year values were obtained for 2011–2040, 2041–2070, and 2070–2099, and three maps of probable landslide occurrence, based on the RCP scenarios, were drawn.

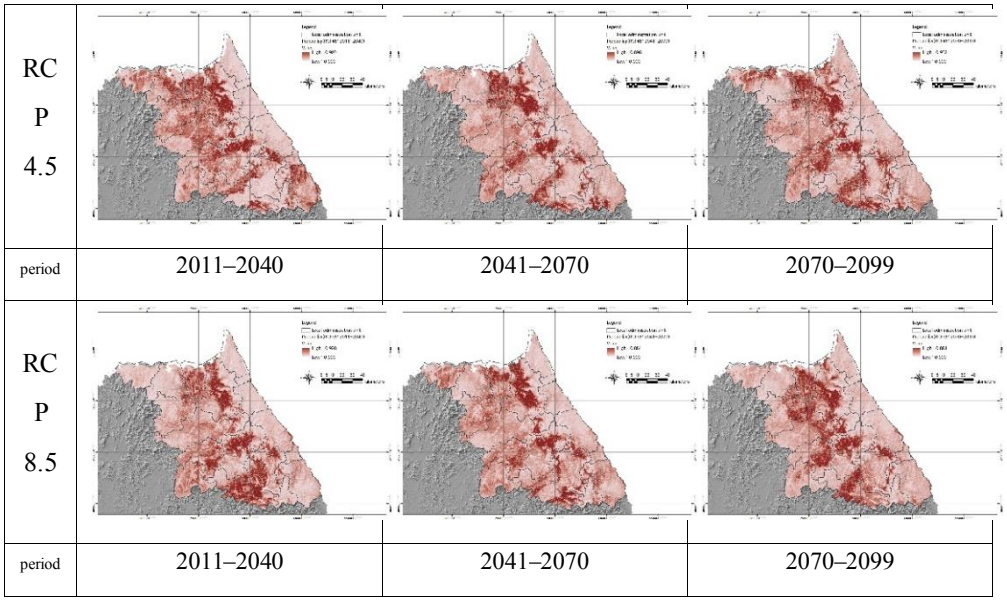

Figure 14. Maps of future probability of landslide occurrence, showing different probability distributions

3.3.4. Result of potential landslide hazard areas

A logistic threshold of ten percentile training presence was applied to the landslide probability occurrence map to identify potential landslide hazard areas. Only areas with a probability of more than 0.200 were extracted from the probability maps (Figure 15). The sizes of the extracted potential hazard areas were analyzed and organized by period (Table 11). Results show that the landslide hazard

area increases to 154 km² in future. The size of the hazard area was about 59 km² larger when the RCP 8.5 scenario was applied than when the RCP 4.5 scenario was applied.

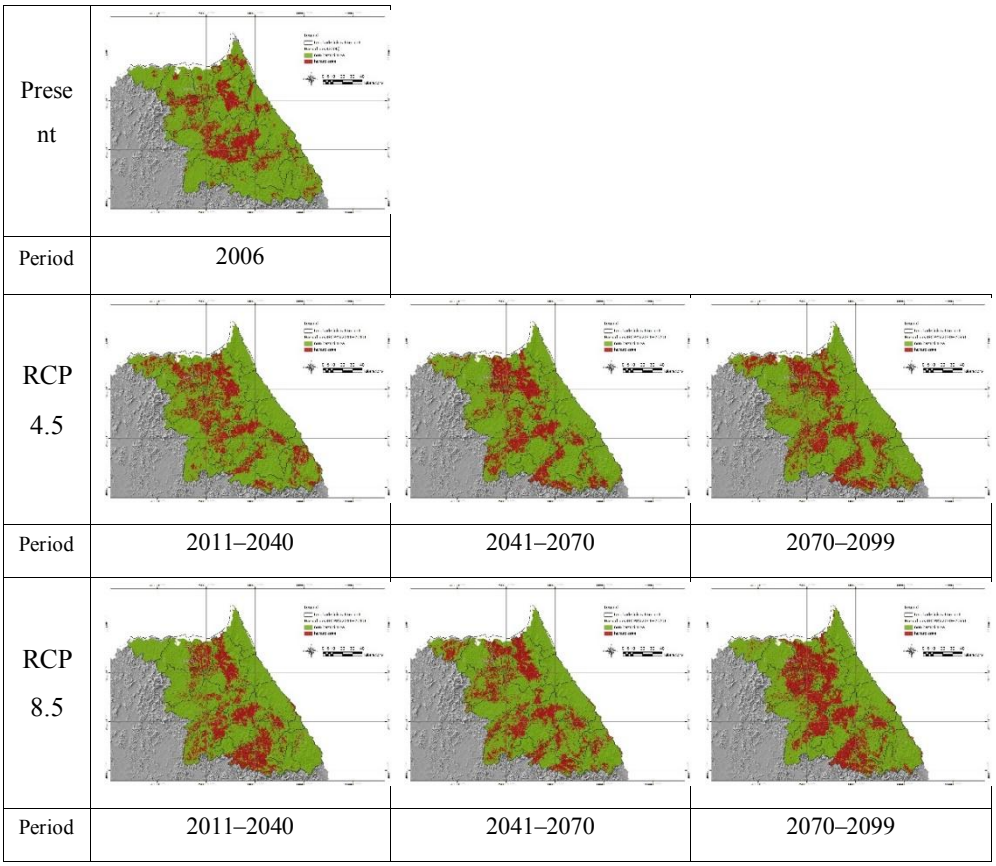

Figure 15. Landslide hazard maps derived using logistic thresholds, showing the main dangerous area

Table 11. The main area of landslide hazard during each period

	2006	**2011–2040**	**2041–2070**	**2070–2099**
Present	309.2 km²			
RCP 4.5		367.95 km²	381.34 km²	404.72 km²
RCP 8.5		365.31 km²	404.33 km²	463.64 km²

The hazard maps were overlaid to identify the main hazard areas for each scenario. RCP 4.5 and 8.5 showed similar distribution of hazard areas (Figure 16). The key hazard areas were the center area, the northern area, and the southern area of Gangwondo. These areas also suffered substantial landslide damage in 2006. However, the distribution of detailed hazard areas was different depending on scenario. RCP 8.5 showed a larger southern area than RCP 4.5.

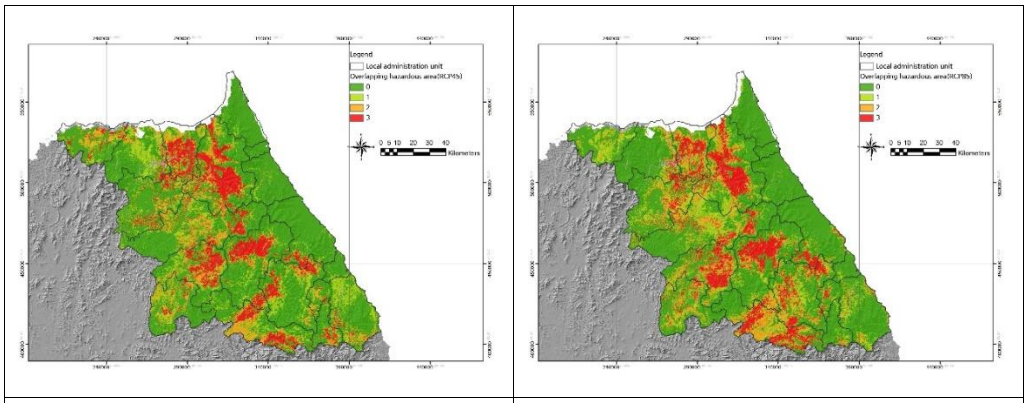

RCP 4.5	RCP 8.5

Figure 16. Overlaid landslide hazard maps; three periods (2011–2040, 2041–2070, 2070–2099) of hazard maps have been overlaid

3.3.5. Estimation of landslide hazard area under uncertainty

The 30-year average value was used to estimate the potential landslide hazard area. However, use of only average values in climate change scenarios results in high uncertainty [42]. Statistical values for the scenarios were therefore calculated using standard normal distribution. The statistical values included minimum, -95% confidence level, -90% confidence level, mean, +90% confidence level, +95% confidence level, and maximum. These values were calculated for each period of the RCP 4.5 and 8.5 scenarios.

The statistical values were input into the optimal landslide model. Potential hazard areas of each period were calculated under uncertainty (Table 12). Figure 17

describes the trend of each hazard area during each period, with the bar graphs effectively showing the difference in areas. Hazard areas differed greatly between minimum and maximum values. The hazard area of the maximum value, in particular, had the highest value. The uncertainty of climate change scenarios can thus be verified by applying these statistical methods.

Table 12. Potential landslide hazard area when considering uncertainty of climate change scenarios. Statistical values for each scenario were used to explore uncertainty

	RCP 4.5			RCP 8.5		
	2011–2040	**2041–2070**	**2071–2099**	**2011–2040**	**2041–2070**	**2071–2099**
Minimum	286.60	290.51	304.33	343.19	366.09	413.03
-95%	348.64	312.55	337.23	353.46	372.23	432.55
-90%	350.49	320.78	358.62	355.06	387.67	437.20
Mean	367.95	381.34	404.72	365.31	404.33	463.64
+90%	473.54	460.61	493.51	394.76	418.69	561.28
+95%	476.69	485.28	526.41	405.88	443.66	581.76
Maximum	523.55	551.08	598.79	433.00	625.57	657.24

(unit: km²)

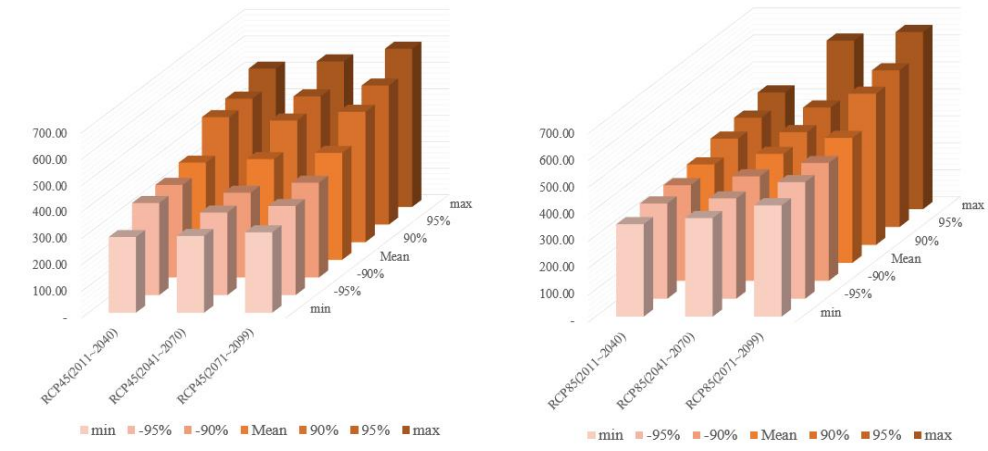

RCP 4.5 RCP 8.5

Figure 17. Bar graphs showing landslide hazard areas when taking into account statistical values of climate change scenarios

3.3.6. Relationship between landslide hazard and land use

Analysis was conducted to evaluate the relationship between the landslide hazard map and the land cover map, in order to identify the land-use properties of areas vulnerable to landslides (Table 13). Urbanization and agricultural areas overlapped with the landslide hazard map for the 2070–2099 period of the RCP 4.5 and 8.5 scenarios. As a result, farming land has the largest hazardous area of all land cover types. It was estimated that 40.60% of farming area would be in danger of landslides in 2070–2099 (RCP 8.5). Under the RCP 8.5 scenario, the land use types occupying more than 20% of areas susceptible to landslide hazards are transportation areas, recreational facilities, and greenhouses for farming.

Table 13. Relationship between landslide hazard area and land cover, showing land use types most vulnerable to landslides in future (2070–2099)

Land cover		Total area of land cover (km²)	Landslide hazard area (km²)			
			RCP 4.5	Proportion	RCP 8.5	Proportion
Urbanization area	Residential area	158.43	19.45	12.28%	26.52	16.74%
	Manufacturing area	21.01	1.87	8.90%	2.82	13.42%
	Commercial area	32.07	4.38	13.66%	4.80	14.97%
	Recreational facilities	**6.04**	**1.25**	**20.70%**	**1.37**	**22.68%**
	Transportation area	**106.00**	**22.76**	**21.47%**	**26.13**	**24.65%**
	Public facilities	66.15	12.84	19.41%	11.60	17.54%
Agricultural area	Rice paddy	715.49	62.84	8.78%	84.33	11.79%
	Farm	**1050.56**	**362.17**	**34.47%**	**426.54**	**40.60%**
	Greenhouses for farming	**6.40**	**1.01**	**15.78%**	**1.42**	**22.19%**
	Orchard	11.67	0.94	8.05%	2.29	19.62%
	Other cultivation area	23.87	3.50	14.66%	4.58	19.19%

3.4. Discussion

Based on landslide locations in Gangwondo in 2006, this study analyzed the probability of landslide occurrence by considering variables directly or indirectly related to landslides. Variables of high importance were selected through the first model run to extract variables of major influence. Data on landslide locations was divided into three types according to location characteristics, and the first run of the model was carried out by applying these three types. Of the latter, landslide locations with the highest AUC values (i.e., top 1,000 landslide locations within the forest) were finally selected for consideration. An optimal landslide model for Gangwondo was extracted through this process.

Weather variables were also extracted from the RCP 4.5 and 8.5 scenarios provided by the KMA to reflect the expected increase in precipitation due to future climate change. Weather variables for each year were extracted from the 2011–2099 scenarios. Based on the definition of climate, average values of 30-year weather variables were obtained and applied to the model. This study therefore provides guidance for landslide hazard assessment using climate change scenarios. In this research, one model was used to assess landslide hazard; however, future study is needed that will compare various models in order to validate their results [67].

The landslide hazard map showed changes in distribution as patterns of weather variables changed. The result of overlaying potential hazard areas would be helpful to identify repetitive hazard areas (Figure 12). The landslide hazard area based on RCP 8.5 is much larger (about 59 km²) than that generated by RCP 4.5 and is concentrated on the eastern and western areas of Gangwondo. The hazard area of RCP 4.5 was also concentrated in this same area but specific locations were a little different to those of RCP 8.5. Pyeongchang, Inje, and Chuncheon had especially large hazard areas in both scenarios. The analysis of uncertainty (Figure 13) could broaden understanding about the uncertainty of climate change scenarios [68].

Areas facing continuous landslide hazards are considered to urgently require a

landslide adaptation plan and related measures. Results showed that urban and agricultural areas were much more susceptible to landslides than other land use types (Table 8). This means that casualties from landslides will likely increase in future. This also signifies the absence of policies to manage development. Policy makers should thus take into account the natural hazard map (Figure 11) when making decisions [67].

Policy makers, planners, and managers conventionally consider social, economic, and geographical factors. However, the potential hazard area should also be considered in order to prevent damage due to natural disasters [43]. Potential hazard areas can be an important consideration for sustainable development [69]. Potential landslide hazard areas require limited development if a proper adaptation plan is not applied. An optimal land use plan, which takes into account natural hazards and protects humans, can be developed by considering natural hazard areas in development plans [43].

Gangwondo is especially famous for alpine agriculture, which capitalizes on geographic characteristics such as high altitude. This special type of agriculture creates large revenues through different production periods. Alpine agriculture areas require high altitude and are therefore generally adjacent to mountains. For this reason, they largely overlap with landslide hazard areas. In conclusion, the local government of Gangwondo must therefore take into account natural hazard maps, such as maps showing landslide hazard areas, when planning for alpine agriculture and people in order to prevent landslide damage.

3.5. Conclusion

According to results obtained by applying future weather variables, the scale of major landslide hazard areas is estimated to increase in future. In particular, the magnitude of landslide hazard areas was found to be larger (about 59 km^2) when applying the RCP 8.5 scenario than when applying the RCP 4.5 scenario. About 40%

of the farming area was shown to overlap with predicted landslide hazard areas in 2070–2099 (RCP 8.5). The uncertainty of climate change scenarios was also considered, by taking into account the statistical values for each scenario period. Gangwondo notably has the largest alpine agriculture area in the Republic of Korea. The local government of Gangwondo must thus take into account natural hazards, especially landslides, in order to reduce damage to alpine agriculture areas resulting from this hazard. The landslide hazard map was also overlaid with maps of recreational facilities, transportation areas, and public facilities. Results indicate that damages from landslides could increase in future. Policy makers, planners, and managers of Gangwondo must therefore consider potential hazard areas in order to prevent the occurrence of damages due to natural hazards.

Acknowledgement

This work was supported by the BK 21 Plus Project in 2014 (Seoul National University Interdisciplinary Program in Landscape Architecture, Global leadership program towards innovative green infrastructure), The Development of Economic Assessment Technique for Climate Change Impact and Adaptation Considering Uncertainties (Korea Ministry of Environment, Project number: 2014001310010), and The Development of climate change adaptation and management technique, and supportive system (Korea Ministry of Environment, Project number: 416-111-014).

4. CHAPTER 3 : Estimating Landslide Susceptibility Areas in Consideration of the Uncertainty Inherent in Modeling Results

4.1. Introduction

Extreme weather events such as heavy rainfall, typhoons, heat waves and cold waves have increased because of climate change, and these events have caused extensive damage in the Republic of Korea (ROK). Landslides are one of the worst types of disasters caused by heavy rainfall, and local governmental decision makers are trying to establish disaster prevention zones to reduce landslide damage; these zones restrict construction activities in landslide susceptible areas and specify safe separation distances for development. Additionally, government officials of the ROK are trying to establish climate adaptation plans that will prevent future losses of lives and properties from landslides.

Inje-gun, Gangwon-do, experienced severe damage due to landslides in 2006 and 2007 [70] [71], and these landslides were associated with many human injuries and losses to public facilities. Inje-gun consists of 91% mountainous terrain, and various residential and agricultural land cover types (i.e., households, farmlands and roads) are located adjacent to the forested land [71]. In this region, alpine agriculture is an important source of income. The local government of Inje-gun is required to develop strategic management plans that will protect lives and properties from landslides.

As a key tool of strategic management plans, landslide susceptibility maps are needed by Inje-gun's local government [72] [73]. These maps can identify the areas of forestland that are vulnerable to landslides triggered by extreme rainfall, and thus, they can be used to restrict potentially risky human activities in susceptible areas, such as the construction of roads and residential facilities and crop plantings. Additional development without consideration of the region's landslide susceptibility will make Inje-gun more vulnerable to future damage. Maps of landslide susceptible areas are also critical for climate adaptation plans that decision makers can use to improve community resilience [51].

Uncertainties in landslide susceptibility information can lead to undesirable social costs such as infringements on private property rights and unnecessary economic investments. With the aim of reducing these uncertainties, this study investigated the amount of uncertainty associated with different types of landslide susceptibility modeling data. Figure 18 shows the general process that can be used to establish a landslide adaptation plan [74]. As noted, a landslide susceptibility assessment involves finding priority areas in STEP 1, and this is typically accomplished with the use of statistical distribution models (SDMs). However, there are problems and challenges in regard to the uncertainty and reliability of SDM data.

Many previous studies have developed SDMs that can be used to analyze a region's landslide susceptibility [75] [46] [72] [48] [76] [77]. However, differences among these SDMs have been the cause of uncertainties in assessing landslide susceptible areas [78] [79] [80]. Uncertainties can occur because of the complex interactions between landslides and environmental variables and also because of the different assumptions used by various SDMs [51]. Ideally, the results of a landslide susceptibility assessment should provide reliable scientific information than can support the identification of priority areas and forecast susceptible areas [81] [82], and consistent data from different models will have a higher level of reliability than inconsistent data. Thus, researchers have proposed a method to minimize uncertainty that relies on the use of multiple models [83] (it can be very difficult to establish only one optimum model for landslide susceptibility mapping). In particular, some researchers have applied ensemble methods to minimize the limitations of each model and decrease the uncertainty associated with the final dataset [84].

In this context, the main objective of this study was to assess the landslide susceptibility in a target region with the use of multiple SDMs and quantify the uncertainty. This study addressed two research questions. First, how to quantify the uncertainty from various SDMs? Second, can an ensemble model help to decrease the uncertainty of SDMs and support decision making effectively? Both of these questions are related to attempts to produce more reliable data on landslide

susceptible areas that can support the decision making process regarding land development.

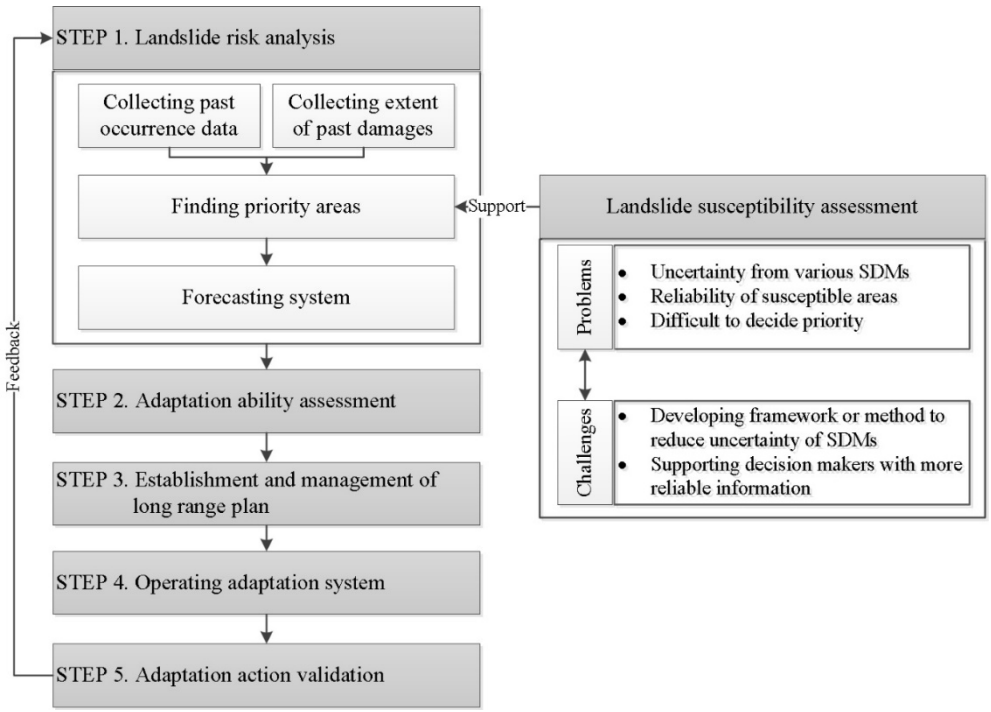

Figure 18. Challenges of landslide susceptibility assessments used for supporting the decision making process

4.2. Methods

4.2.1. Scope of study

The study site was Inje-gun, Gangwon-do, ROK (Figure 19). Inje-gun is located in the northeastern area of the ROK. The study site experienced severe damage due to landslides in 2006 and 2007. Moreover, alpine agricultural resources, which represent an important industrial output in Inje-gun, have been damaged by landslides every year. Thus, Inje-gun was deemed as an appropriate study site to develop landslide susceptibility maps. The spatial resolution of the data for the study area was set to 30 m × 30 m. The temporal scope of the study was set to 2006

in consideration of the reliability of historical landslide occurrence data.

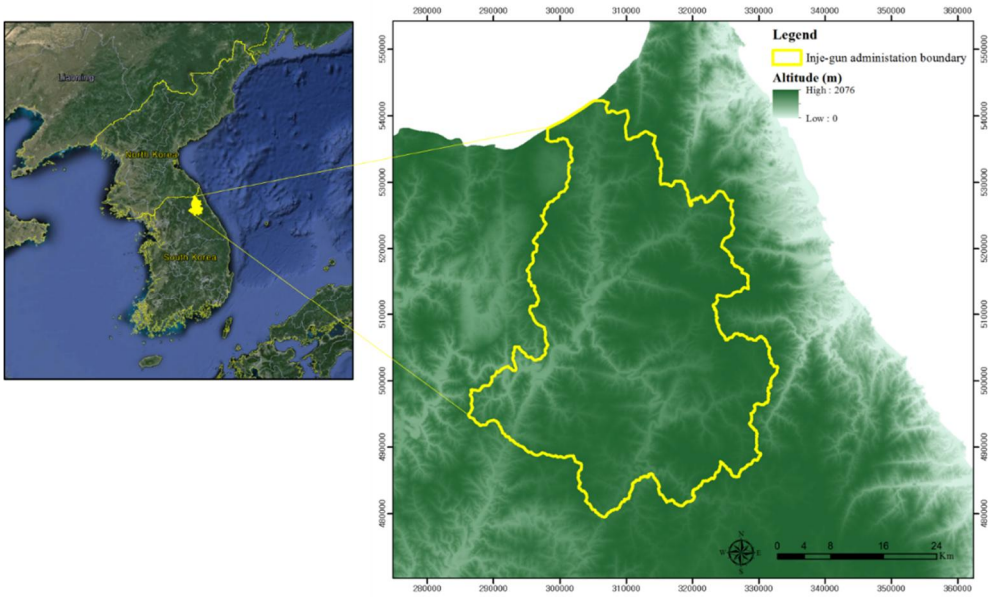

Figure 19. Study site (Inje-gun, Gangwon-do, ROK)

Figure 20 shows the framework used for this study. The first part of this study involved establishing data for the spatial models, and this work included reviewing the literature related to the relevant environmental and geological variables, selecting SDMs for analysis and choosing the ensemble methods. The second part involved landslide susceptibility modeling, which was the main focus of this study. Each SDM was run five times with the selected variables while considering the importance of multicollinearity. The results of each SDM were then aggregated by five types of ensemble methods. The last part involved quantifying the uncertainty among the results of the various SDMs and assessing the uncertainty through the use of an uncertainty map of the study site (i.e., a map showing the coefficient of variation values for the data). A final landslide susceptibility map was produced by employing the best ensemble method, and the uncertainty information was incorporated for decision making purposes.

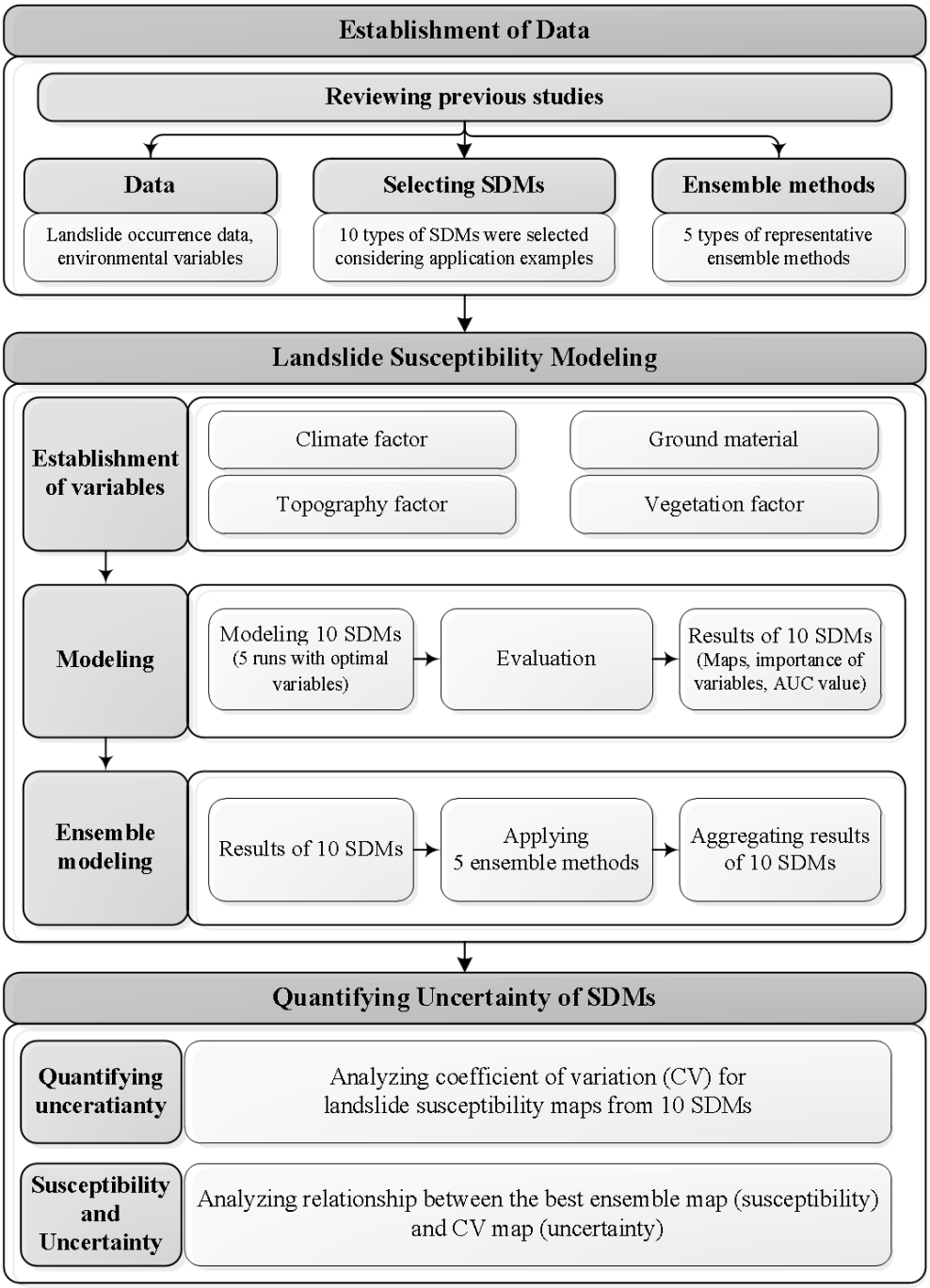

Figure 20. Flowchart for this study[2]

[2] The 10 models are explained in Table 3.

Landslide occurrence data were required for the establishment of SDMs in support of the local government of Gangwon-do (Figure 21). These data were comprised of spatial coordinates, damaged area extents and addresses, all of which were collected during field surveys and aerial photography surveys in 2006. This study focused on landslides areas over 2,000 m2 in accordance with a previous study on landslide susceptibility models [85]. In the previous study, models that employed landslide occurrence areas over 2,000 m2 showed the highest area under the curve (AUC) compared to other models that used different sizes. A total of 341 occurrence points were used here as input data for the landslide susceptibility modeling. For the absence data, 700 pseudo absence points were made by considering a minimum distance of 200 m from the occurrence areas [86].

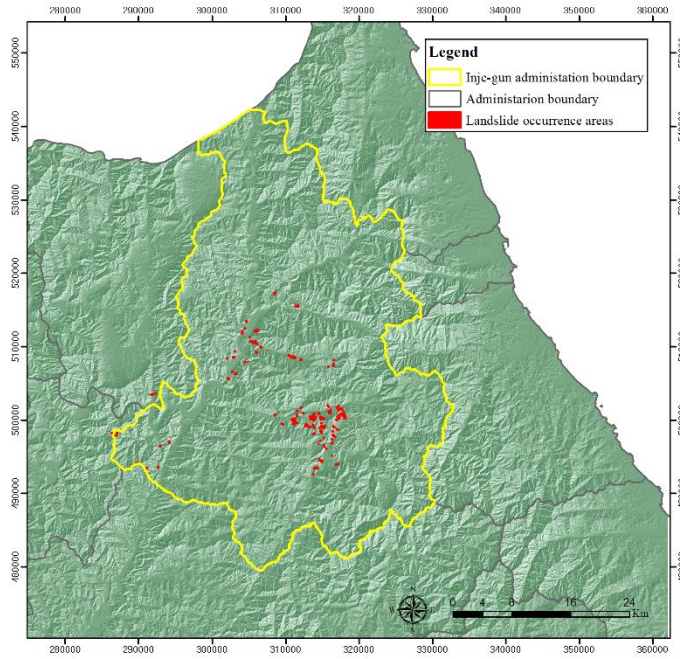

Figure 21. Landslide occurrence areas in Inje-gun (2006)

Variables were collected on the basis of previous studies (Table 14). The major factors used were classified into four categories, namely, climate factors, topography factors, ground material and vegetation factors. To establish the model, subsidiary factors were employed, and these consisted of a total of 13 variables (see the variables listed in the second column of Table 14). Analytical programs used included ArcMap 10.1 and Python 2.7 of ESRI.

Table 14. Variables for establishing the landslide models

Category	Variables	Code name	References	Data references
Climate factor	Number of days with over 100 mm of rainfall	X011_100mm	(Kim and Chae 2009; Choi et al. 2011; Yoo et al. 2012)	Observation data (KMA, 2006)
	Number of days with over 120 mm of rainfall	X012_120mm		
	3 days of maximum rainfall (mm)	X021_3days	(Guzzetti et al. 2008; Kim and Chae 2009; Choi et al. 2011)	
	5 days of maximum rainfall (mm)	X022_5days		
	Number of days with over 150 mm for 3 days of maximum rainfall	X060_3day		
	Daily maximum rainfall (mm)	X070_dailymax	(Kim and Chae 2009; Yoo et al. 2012)	
Topography factor	Slope (degrees)	slope	(Ayalew and Yamagishi 2005; Ermini et al. 2005; Kim and Chae 2009; Oh 2010; Choi et al. 2011; Yeon 2011)	Digital elevation model (DEM) (KME, 2008)
	Altitude (m)	altitude	(Ayalew and Yamagishi 2005; Oh 2010; Choi et al. 2011; Kim et al. 2011)	
Ground material	Soil depth	soildepth_km	(Pradhan and Lee 2010; Oh 2010; Yeon 2011)	Soil map (WAMIS, 2006)
	Soil drainage	soildrain_km		
	Soil type	soiltype_km		
Vegetation factor	Age of forest	ageclass	(Yeon 2011; Oh 2010)	Map of forest type (KME, 2005)
	Class of diameter at	diamclass	(Kim et al. 2011; Yeon	

	breast height (DBH)	2011)	

4.2.2. Spatial distribution models and ensemble methods

Researchers have used various SDMs to identify landslide susceptible areas correctly. There are two categories of SDMs based on the mechanism of the model, namely, statistically based models and machine learning based models. Generalized linear models (GLMs), generalized additive models (GAMs) and multivariate adaptive regression splines (MARS) are all statistically based models. Machine learning based models include the generalized boosted regression model (GBM), classification tree analysis (CTA), artificial neural network (ANN), rectilinear envelope similar to BIOCLIM (SRE), mixture discriminant analysis (MDA), random forest (RF) and maximum entropy algorithm (MAXENT).

The first research question of this study involved quantifying the uncertainty among SDMs. To answer this question, this study used every type of model mentioned above and the uncertainty was quantified by calculating the variations among the results of various SDMs. Specific features each model are explained in Table 16 [87]. Each SDM has different characteristics in terms of categories, data requirements and response functions. Additionally, SDMs do not always produce the same results from the same data because the model can be established differently during every run. Thus, each SDM was run five times so that this study could consider the differences among the results from the same model. The uncertainty of the SDMs was quantified by calculating the coefficient of variation (CV), which represents the ratio of the standard deviation to the mean. The CV values were used to compare the relative dispersion among the SDM data. Large CV values indicate that the data has a high amount of uncertainty.

Meanwhile, the second research question of this study involved determining the reliability of an ensemble model. Researchers are interested in ensemble methods

because they can improve the prediction performance by aggregating data from multiple models. In particular, ensemble methods have been used to forecast future climate conditions [88] [89]. Ensemble methods have also been applied to assess landslide susceptibilities. Bartlett and Shawe-Taylor (1999) reduced the bias error by using the theory of large margin classifiers coupled with ensemble techniques [90]. Bühlmann and Yu (2003) developed an ensemble of two different linear regression models [91]. Rokach (2010) reviewed various ensemble methods to achieve improved prediction performances [92]. Recently, Ghosh and Acharya (2011) used consensus clustering to produce more robust and stable results [93]. Lee and Oh (2012) developed and applied an ensemble method to make a reliable model by using logistic regression, the frequency ratio, weight of evidence information and ANN [94]. Althuwaynee et al. (2014) used the bivariate evidential belief function (EBF) as a bivariate to explore the integration validity with the analytic hierarchy process (AHP) and employed logistic regression as a multivariate method for spatial mapping [95].

There are various ensemble methods than can integrate multiple models. This study reviewed various ensemble methods that are based on the concept of minimizing the average dissimilarity [96]. As a result of the review process, five types of representative ensemble methods were selected (Table 15). Each ensemble method utilized different methods to aggregate probabilities or binary values from various SDMs. Specifically, the ensemble methods tested included the 1) mean of probabilities, 2) confidence interval of the mean of probabilities (upper and lower), 3) median of probabilities, 4) mean of the binary and 5) weighted mean based on model performance.

An R package, Biomod2, was utilized to run the SDMs [97]. For the evaluation of the reliability of the established model, this study selected the receiver operating characteristic (ROC) method. The ROC calculates the area under the ROC curve (i.e., the AUC), which provides the basis for judging the reliability of the model by utilizing true and false occurrence predictions [52]. Meanwhile, the cutoff value (threshold) was also calculated for each model to make binary maps, which were

used to apply the ensemble methods.

Table 15. Ensemble methods to integrate results of SDMs

Abbreviation	Description
PM	Mean of probabilities. The PM ensemble model calculates the mean of probabilities for the selected models.
PCI (upper and lower)	Confidence interval. The ensemble model for PCI is the confidence interval for the probability of the mean. This model is a good complement for the probability of means. Two ensemble models are made by using this model: 1) The upper model (there is less than a 100 × PCI/2% chance to obtain probabilities higher than the ones given). 2) The lower model (there is less than a 100 × PCI/2% chance to obtain probabilities lower than the ones given).
PME	Median of probabilities. The PME ensemble model is the same as the probability of the median for the selected models. The median is better than the mean for assessing the impacts of outliers.
CA	Models committee averaging. The CA ensemble model first transforms the probabilities of selected models into binary values by using the cutoff value of each model. After transformation, the model calculates the average of binary values.
PMW	Weighted mean of probabilities. The PMW calculates the relative importance of the weights by using the proportion of evaluation scores. Therefore, the results of ″good″ models are discriminated from ″bad″ models.

Table 16. Key features of the 10 models [87]

Model	Full name of model	Category	Occurrence data required	Response function	Features of the model
GLM	Generalized linear model	Statistically based model	Occurrence / No occurrence	Parametric linear, polynomial, piecewise, interaction terms	GLMs are a representative model among SDMs. GLMs are a generalization of the multiple regression model that uses the link function to accommodate response variables that are distributed normally, namely, the response distributions.
GAM	Generalized additive model	Statistically based model	Occurrence / No occurrence	Smoothing function, estimated using local regression, splines or other methods	GAMs in SDMs are suggested as a powerful methodology to detect and describe non-linear response functions. The results of GAMs can be used to build a parametric model.
MARS	Multivariate adaptive regression splines	Statistically based model	Occurrence / No occurrence	Adaptive piecewise linear regression combines splines and binary recursive partitioning	MARS can be a type of a generalization of a stepwise linear regression. MARS are suited to analyses with large numbers of variables or a modification of the regression tree method.
GBM	Generalized boosted regression model	Machine learning based model	Occurrence / No occurrence	Weighted and unweighted model averaging applied to decision trees	GBMs are similar with weighting variables that consider higher probabilities of selection, instead of weighting equal probabilities for subsequent variables.
CTA	Classification tree analysis	Machine learning based model	Occurrence / No occurrence	Divisive, monothetic decision rules (thresholds) from binary recursive partitioning	The goal of CTA is to divide data into homogeneous subgroups. The subgroups consist of variables that have similar values or are in the same class in regard to the ranges of values for the variables.
ANN	Artificial neural network	Machine learning based model	Occurrence / No occurrence	Non-linear decision boundaries in covariate space	ANN can be described as a two-stage classification or regression model. A hidden layer of ANN comprises features that are linear combinations of input variables. The output variable is a weighted combination of features in the hidden layer.
SRE	Rectilinear envelope similar to BIOCLIM	Machine learning based model	Occurrence only	Fuzzy classification approach	SRE is a boxcar or parallelepiped classifier that uses BIOCLIM. SRE assesses the potential distribution of the dependent variable by using the multi-dimensional environmental space bounded by the values for all dependent variables.

MDA	Mixture discriminant analysis	Machine learning based model	Occurrence / No occurrence	Linear	MDA is a type of linear discriminant analysis that models the multivariate density of variables by using a mixture of multivariate normal distributions.
RF	Random forest	Machine learning based model	Occurrence / No occurrence	Weighted and unweighted model averaging applied to decision trees	Random forests is a type of bootstrap aggregating method that builds de-correlated trees and averages the trees. Many trees are made with subsets of input data. Furthermore, each division of the tree model is also made with a random subset of input variables.
MAXENT	Maximum entropy algorithm	Machine learning based model	Occurrence only	Non-linear response functions can be described	Maximum entropy is based on statistical mechanics and information theory. MAXENT can analyze the best approximation of an unknown distribution by using the maximum entropy method that considers the most spread out and closest to uniform values.

4.3. Results and Discussion

4.3.1. Landslide susceptibility modeling

Selecting variables is an important step in establishing an optimal landslide model. Multicollinearity was considered here by excluding variables where the correlation coefficient was over 0.6 from the list. As a result of the selection process, 10 variables were selected as optimal variables. They included X012_120mm (number of days with over 120 mm of rainfall), X022_5days (5 days of maximum rainfall), X060_3day (number of days with over 150 mm for 3 days of maximum rainfall), X070_dailymax (daily maximum rainfall), ageclass (age of forest), altitude, slope, soildepth_km (soil depth), soildrain_km (soil drainage) and soiltype_km (soil type). Previous studies suggested the curvature and topographic wetness index as important factors [98] [99]. However, those variables did not shown an important relationship with the landslide occurrence points in this study. The reason for this difference was based on the scale of analysis.

The 10 SDMs were run by using the selected variables. The number of evaluations for each model was set at five times, and the uncertainty of the training process was considered. Of the landslides occurrence data, 80% of the data were used to train the model and 20% of the data were utilized to test the model. Table 4 shows the average importance of the variables for the five evaluations. The average of the 10 models was also calculated to find the relatively important variables. The altitude, X070_dailymax (daily maximum rainfall), X060_3day (number of days with over 150 mm for 3 days of maximum rainfall) and X022_5days (5 days of maximum rainfall) showed higher importances than the other variables according to the average of the 10 models. The soildrain_km (soil drainage), slope and X012_120mm (number of days with over 120 mm of rainfall) showed moderate levels of importance.

Meanwhile, the standard deviation (SD) revealed different aspects of importance among the variables (Table 17). The SD represents the quantification value for the amount of variation among the SDMs. Climate related variables and altitude showed relatively low SD values compared to the average. The averages of other variables were low, but their relative SD values were higher than those for the other variables. Thus, the SD value of each SDM was one of the basic features of uncertainty for the properties of SDMs.

Table 17. Average of the importance of variables for evaluation

Variables	Average of five evaluations										Average of 10 models	Standard deviation
	MAXENT	CTA	SRE	FDA	MARS	RF	GLM	GBM	GAM	ANN		
X012_120mm	0.244	0.182	0.027	0.189	0.267	0.082	0.216	0.083	0.212	0.140	**0.164**	**0.075**
X022_5days	0.166	0.135	0.173	0.139	0.418	0.095	0.185	0.097	0.214	0.645	**0.227**	**0.165**
X060_3day	0.164	0.383	0.173	0.056	0.192	0.199	0.109	0.075	0.126	0.374	**0.185**	**0.107**
X070_dailymax	0.578	0.545	0.269	0.671	0.478	0.414	0.654	0.478	0.641	0.401	**0.513**	**0.123**
ageclass	0.027	0.004	0.036	0.000	0.000	0.009	0.000	0.003	0.003	0.021	**0.010**	**0.012**
altitude	0.358	0.441	0.389	0.321	0.312	0.239	0.369	0.308	0.358	0.342	**0.344**	**0.051**
slope	0.048	0.009	0.065	0.000	0.000	0.009	0.000	0.002	0.000	0.041	**0.017**	**0.023**
soildepth_km	0.034	0.005	0.159	0.013	0.000	0.017	0.170	0.011	0.087	0.035	**0.053**	**0.060**
soildrain_km	0.020	0.000	0.135	0.019	0.000	0.003	0.056	0.001	0.033	0.008	**0.028**	**0.040**
soiltype_km	0.023	0.000	0.160	0.000	0.000	0.003	0.016	0.000	0.002	0.003	**0.021**	**0.047**

Through modeling, the probabilities of landslide occurrence were calculated for every cell (30 m × 30 m). The probabilities were changed to binary values (0 or 1) by using a cutoff value for each model. If the probability of a certain cell was over the cutoff value, the cell was considered a landslide susceptible area. The 10 binary maps were projected by using the result of the 10 SDMs (Figure 22). The red

colored areas were deemed as landslide susceptible areas for every run of each SDM.

The 10 SDMs showed different spatial patterns of landslide susceptible areas (Figure 22). These differences among SDMs were the main reason for the uncertainty in estimating landslide susceptible areas in the study area. The SRE showed the largest susceptible areas, while RF showed the smallest susceptible areas among the 10 SDMs. The center area of Inje-gun was identified as a susceptible area in almost all SDMs. However, the detailed locations of susceptible areas were different according to the SDMs. Therefore, ensemble methods were needed to account for the uncertainty that was derived from the differences among SDMs.

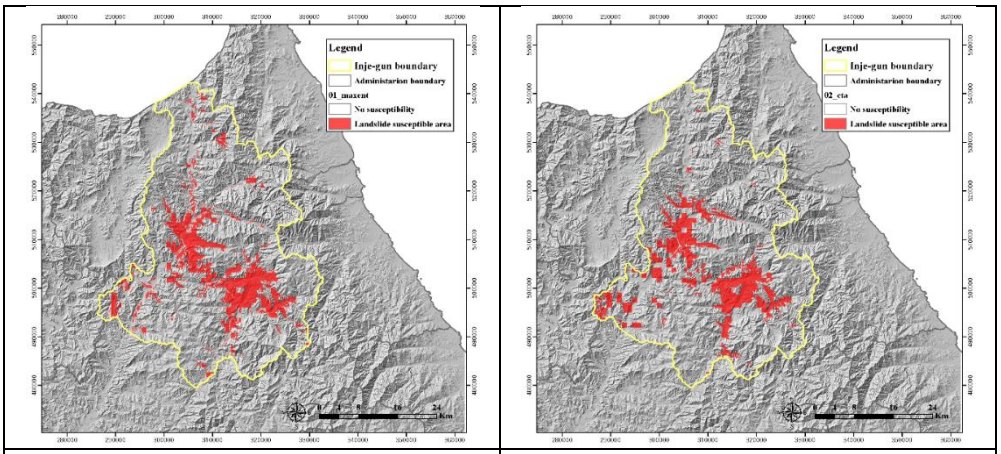

MAXENT **CTA**

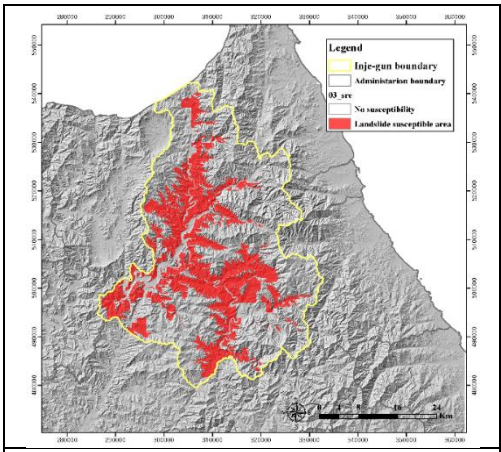

SRE

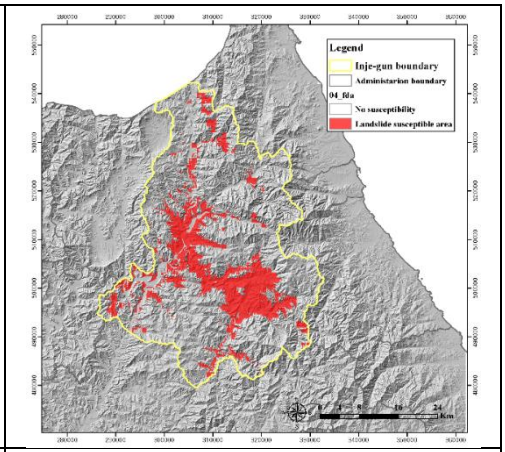

FDA

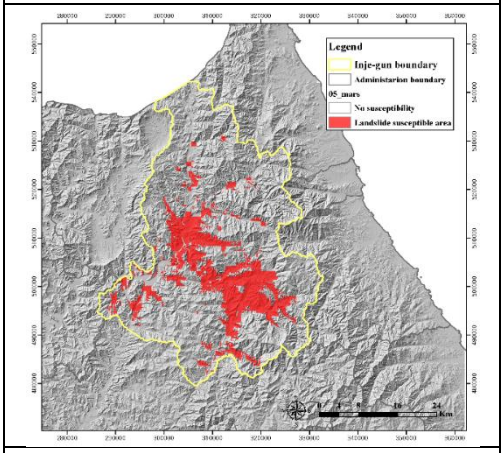

MARS

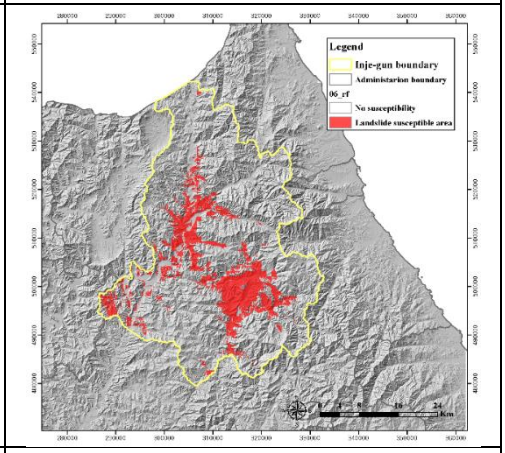

RF

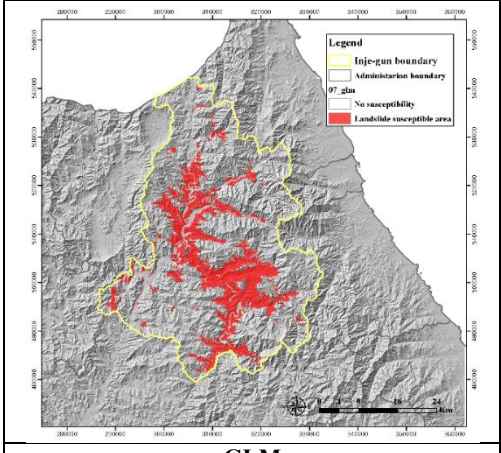

GLM

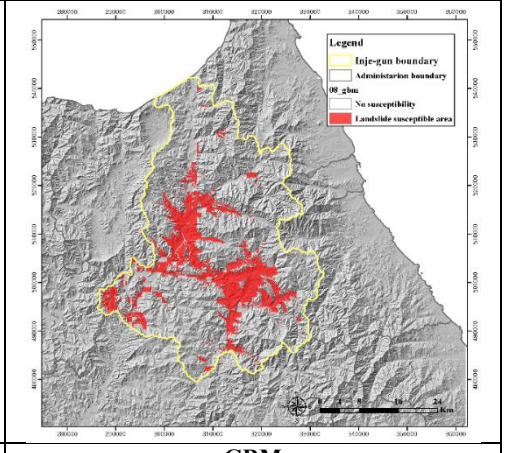

GBM

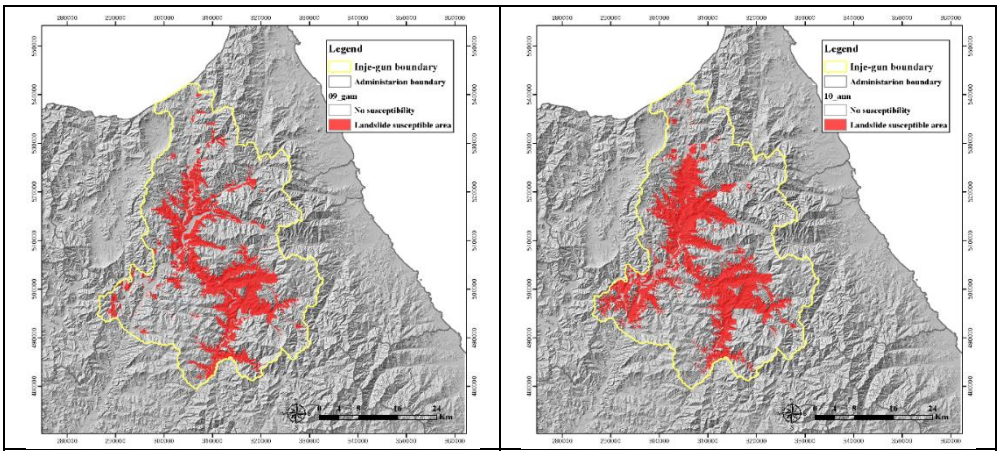

GAM ANN

Figure 22. Landslide projections of the 10 models for present conditions

The average AUC value was calculated for the 10 models (MAXENT, CTA, SRE, MDA, MARS, RF, GLM, GBM, GAM and ANN) to evaluate the reliability of the model (Table 18). The RF model showed the highest AUC value (0.971) among the 10 models. The AUC value of eight models was over 0.9, while the other two models had values over 0.85. Therefore, every model showed good performance according to the criteria used in previous studies [87].

Table 18. Results of the evaluation for the landslide models

Model	AUC value						Rank
	RUN 1	RUN 2	RUN 3	RUN 4	RUN 5	Average	
MAXENT	0.886	0.910	0.875	0.803	0.925	**0.880**	**9**
CTA	0.927	0.946	0.915	0.862	0.965	**0.923**	**8**
SRE	0.866	0.869	0.814	0.871	0.857	**0.855**	**10**
FDA	0.954	0.945	0.923	0.896	0.957	**0.935**	**6**
MARS	0.950	0.965	0.943	0.921	0.966	**0.949**	**3**
RF	0.982	0.976	0.953	0.956	0.987	**0.971**	**1**
GLM	0.962	0.961	0.930	0.909	0.960	**0.944**	**4**

GBM	0.972	0.974	0.950	0.942	0.987	**0.965**	**2**
GAM	0.961	0.960	0.928	0.904	0.953	**0.941**	**5**
ANN	0.882	0.971	0.922	0.925	0.944	**0.929**	**7**

Six ensemble methods were applied to synthesize the results of the 10 SDMs and account for the uncertainty. The ensemble model was also evaluated by using the ROC method (Table 19). The PMW showed the highest AUC value among the six ensemble methods. The PM and PCI (upper model) showed the second highest AUC values. The other methods also had high AUC values, and therefore, every ensemble methods had high reliability.

Table 19. Results of the evaluation for the ensemble models

Abbreviation	Cutoff	Sensitivity	Specificity	AUC	Rank
PM	568.500	93.200	96.149	**0.986**	**2**
PCI (lower model)	463.500	93.600	95.764	**0.985**	**3**
PCI (upper model)	668.000	93.200	96.021	**0.986**	**2**
PME	708.000	92.400	96.277	**0.982**	**4**
CA	470.000	95.600	92.426	**0.985**	**3**
PMW	546.000	94.400	96.149	**0.988**	**1**

Six ensemble maps were derived by projecting the results of each ensemble method (Figure 23). The cutoff value of each ensemble method was used to make binary maps. All maps showed similar susceptible areas (violet color) in the central area of Inje-gun. However, the detailed locations of susceptible areas were different according to the ensemble method.

In particular, CA showed larger susceptible areas than the other ensemble methods. The reason for CA's larger estimates was based on the technique of calculating the average of the binary values for the 10 SDMs. Other ensemble methods calculated the probabilities of 10 SDMs to find the susceptible areas. The

CA could be a good ensemble method for decision makers who want more stable data than the data produced by the other methods. In this study, PMW was selected as the optimal ensemble method to analyze landslide susceptible areas because of our consideration of the results of the evaluation (i.e., AUC values).

The optimal ensemble model (PMW) produced a higher AUC value than any other single model. The extent of landslide susceptible areas with PMW was 30,290 ha. Meanwhile, the extent of susceptible areas with SRE (which had the lowest AUC among the 10 single models) was 48,992 ha, and that of the RF single model (which had the highest AUC among the 10 single models) was 24,359 ha. The single model SRE overestimated susceptible areas and the single model RF underestimated susceptible areas compared to the optimal ensemble model. Thus, the ensemble model was helpful for decreasing the differences among the single models according to the AUC values and extents of susceptible areas.

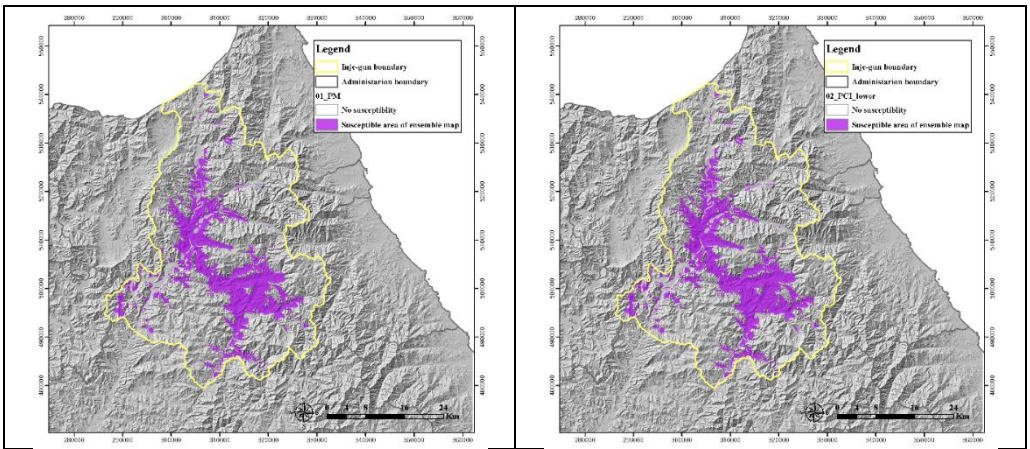

PM	PCI (lower model)

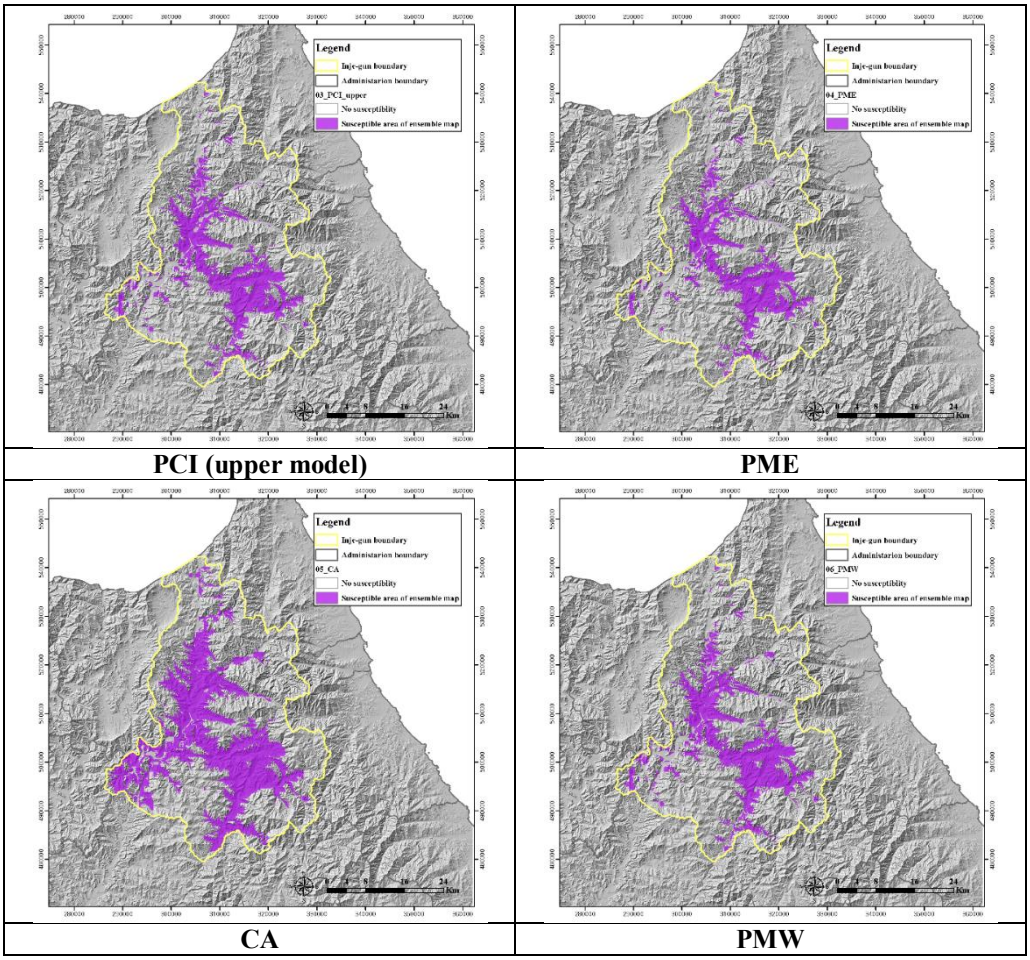

Figure 23. Results of ensemble models for the present conditions

4.3.2. Supporting decision makers: considering the uncertainty in the modeling results

To quantify the uncertainty among SDMs, which was the first research question addressed in this work, the CV value of each cell was calculated. The CV was calculated in each cell by using the probability from the landslide susceptibility maps derived with the 10 SDMs (Figure 24). The CV map was classified by considering the standard deviation values. The northern areas and southern areas of Inje-gun showed high CV values, and conversely, the central areas of Inje-gun

showed low CV values. This pattern was predictable considering the ensemble maps that showed similar susceptible areas in the central areas.

However, there were also areas that had high CV values in the central areas at more detailed scales. Therefore, decision makers could utilize the CV map to view more detailed susceptible areas. In general, the CV map provided a more robust basis to judge the landslide susceptible areas of Inje-gun along with the ensemble map. Meanwhile, the northern areas of the CV map showed no information because of the off-limit military area adjacent to North Korea.

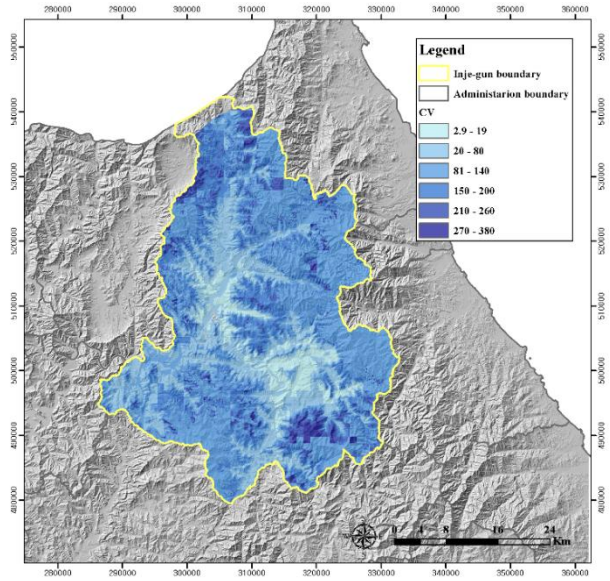

Figure 24. Coefficient of variation (CV) map (uncertainty map)

The second research question involved identifying the effectiveness of the ensemble model for reducing the uncertainty from SDMs. This study used two types of matrixes to analyze the relationship between the PMW ensemble map (optimal ensemble model) and CV map (uncertainty map). The first type of matrix was made

by using the probabilities of landslides (PMW ensemble map) and the CV map (Figure 25). The classification method for both maps was based on the standard deviation.

The objective of this matrix analysis was to identify the effectiveness of the ensemble map in terms of reducing the uncertainty from the various SDMs. The map of Figure 25 shows two key types of areas, namely, areas with high probabilities of landslide and low uncertainties, and areas with low probabilities of landslides and high uncertainties. There are also areas with high probabilities for landslides and high uncertainties, and areas with low probabilities and low uncertainties on the ensemble map. Thus, this can be the basis for using the ensemble method to help evaluate the uncertainty from various SDMs.

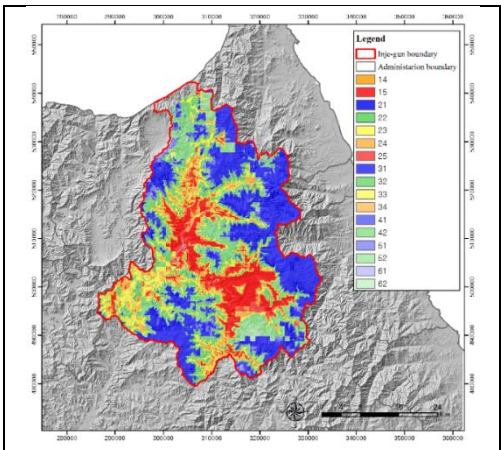

Map

Probability of landslide (Ensemble map)	High	5	15	25	35	45	55	65
	↕	4	14	24	34	44	54	64
		3	13	23	33	43	53	63
	Low	2	12	22	32	42	52	62
		1	11	21	31	41	51	61
Matrix			10	20	30	40	50	60
			Low ↔ High					
			Uncertainty (Coefficient of variation, CV)					

Matrix table

Figure 25. Relationship between the probability of a landslide from the PMW ensemble model and uncertainty

The second type of matrix was made by using the landslide susceptible areas (binary map of the PMW ensemble model) and the CV map (Figure 26). This map shows the low uncertainty regions associated with susceptible areas much more clearly than Figure 25. Figure 26 also shows the low uncertainty regions of

unsusceptibile areas very well. Therefore, this map can provide better information to support decision makers.

Generally, decision makers and policy makers need reliable and detailed information to identify priority areas and allocate resources to those areas. In this respect, the map of the relationship between the susceptible areas and uncertainty could be utilized to find the most urgent areas with credible data. Thus, the ensemble model has benefits for assessing landslide susceptible areas. In summary, an ensemble map can help to minimize uncertainty among SDMs and also support decision makers effectively.

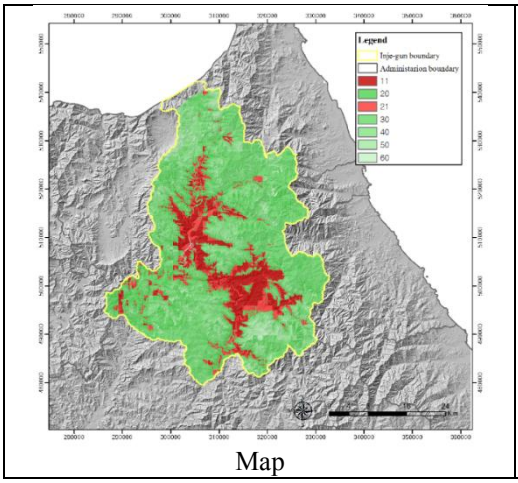

Map

Landslide susceptibility (Ensemble map)	Susceptible area	1	11	21	31	41	51	61
	No susceptibility	0	10	20	30	40	50	60
Matrix			10	20	30	40	50	60
			Low ↔ High					
			Uncertainty (Coefficient of variation, CV)					

Matrix table

Figure 26. Relationship between landslide susceptible areas from the PMW ensemble model and uncertainty

4.4. Conclusion

The objectives of this study were to quantify the uncertainty of SDMs and ensemble models used for landslide susceptibility assessments and to improve the landslide information needed to support decision makers effectively. First, this study

evaluated landslide susceptibility by using 10 important SDMs to consider the uncertainty from the models. Second, six ensemble methods were selected to minimize the average dissimilarity of the SDMs. Third, the effectiveness of the ensemble model was evaluated by analyzing the relationship between the landslide susceptibility data and the uncertainty. These were the most important aspects of this study.

As a result of landslide susceptibility modeling, susceptible areas of each single model were derived as spatial maps. An interesting finding was that the susceptible areas showed similar spatial patterns, but detailed patterns were different according to each SDM. This uncertainty from single SDMs is problematic for decision making (i.e., ideally, data from different models should be consistent, but this is often not the case).

In ensemble modeling, PMW was selected as the optimal ensemble model among six ensemble methods. Meanwhile, the CV was calculated to quantify the uncertainty among the SDMs. The PMW showed better performance than every single model. Especially, the estimations from PMW were of a moderate extent compared to those from RF (the highest AUC among the single models) and SRE (the lowest AUC among the single models). This can be one of the ways to evaluate the reliability of an ensemble model.

The relationship between the landslide susceptibility (ensemble map) and uncertainty (CV map) illustrated the reliability of the ensemble model data. The susceptible areas with low uncertainty represent useful information for protection efforts, and also, unsusceptible areas with low uncertainty can be prioritized for future safe development by policy makers. In this study, the ensemble model showed better performance than any single model.

However, future work is needed to improve considerations of the uncertainty and the reliability of ensemble models. First, time series landslide data are needed to

design better models. This study used only one year's worth data (i.e., from 2006). Second, estimations of future landslide susceptible areas are needed under different climate change scenarios. This study focused only on past landslide susceptibilities; however, the extent of susceptible areas could change in the future.

A total of 91% of the area in Inje-gun consists of forested lands, and therefore, the local authorities of Inje-gun must establish proper adaptation plans for landslides. Reliable data on landslide susceptibilities will be critical for these planning efforts. Furthermore, there are many other areas vulnerable to landslides in the ROK and in other countries, and the framework used here is applicable to these other areas as well. In this context, this study illustrates how to estimate more reliable landslide susceptibility data by using various SDMs and an ensemble model. The results from such an approach can help decision makers to better design adaptation plans to minimize landslide damage.

Acknowledgement

This work was supported by the BK 21 Plus Project in 2015 (Seoul National University Interdisciplinary Program in Landscape Architecture, Global Leadership Program toward Innovative Green Infrastructure) and Korea's Ministry of Environment (Project numbers 2014001310010, 416-111-014).

5. DISCUSSION AND CONCLUSION

In Chapter 1, the study conducted a nation-wide vulnerability test comprising 32 items in seven categories (health, forest, farming, ecosystem, disasters, water management, and fishery), drew a map of most vulnerable regions by combining individual vulnerability maps, and pinpointed regions that most urgently need adaptive measures to be taken. In Chapter 2, the study subjected Gangwon Province to run a spatial distribution model and narrow down to landslide-prone areas of the present and used climate change scenario RCP 4.5 and 8.5 to find out landslide-prone areas of the future. In Chapter 3, the study investigated Inje-gun to device a map of landslide risks based on 10 different spatial distribution models, quantified uncertainties arising from differences in the results between the models, and listed landslide-prone areas that presented low uncertainties.

Although Chapter 1 has limitations in that it is an indicator-based study and the results are qualitative, the results present the highest resolution among the data available at the national level, and the methodology is very effective since it can collect expert opinions. Chapter 2 presents a study that employs a single spatial distribution model and a single climate change model to analyze landslide-prone regions and may have uncertainties. However, it has significance by minimizing uncertainties with repeated runs of the models and applying values from wide ranges based on normal distribution of climate data. Chapter 3 presents limitations in that it did not cover uncertainties in the model's variables and did not find the causes of the uncertainties that could arise over the course of combining the results statistically. However, this study quantified uncertainties that can arise from the differences in the results of the models and listed sensitive regions that presented low uncertainties.

The methodology and results from each would be of great significance in the

future when governments of different sizes central government, municipalities, and counties—can assess the impact of climate change and run vulnerability tests effectively for their own use. Further, the results would be able to set grounds for policymaking to respond to climate change in regions of different sizes.

REFERENCES

1. PROVIA. PROVIA Guidance on assessing vulnerability, impacts and adaptation (VIA). 2012.
2. European Commission. An EU Strategy on adaptation to climate change. 2013.
3. Santini M, Caccamo G, Laurenti A, Noce S, Valentini R. A multi-component GIS framework for desertification risk assessment by an integrated index. Appl Geogr. Elsevier; 2010;30: 394–415.
4. Allison EH, Perry AL, Badjeck M-C, Neil Adger W, Brown K, Conway D, et al. Vulnerability of national economies to the impacts of climate change on fisheries. Fish Fish. Wiley Online Library; 2009;10: 173–196.
5. Camarasa Belmonte AM, López-García MJ, Soriano-García J. Mapping temporally-variable exposure to flooding in small Mediterranean basins using land-use indicators. Appl Geogr. Elsevier; 2011;31: 136–145.
6. Menoni S, Molinari D, Parker D, Ballio F, Tapsell S. Assessing multifaceted vulnerability and resilience in order to design risk-mitigation strategies. Nat hazards. Springer; 2012;64: 2057–2082.
7. Moreno A, Becken S. A climate change vulnerability assessment methodology for coastal tourism. J Sustain Tour. Taylor & Francis; 2009;17: 473–488.
8. European Environment Agency. Climate change, impacts and vulnerability in Europe 2012. 2012.
9. IPCC. Managing the Risks of Extreme Events and Disasters to Advance Climate Change Adaptation. A Special Report of Working Groups I and II of the Intergovernmental Panel on Climate Change. 2012.
10. Arnell N, Tompkins EL, Adger N, Delaney K. Vulnerability to abrupt climate change in Europe. Tyndall Centre for Climate Change Research; 2005;
11. Wang HB, Wu SR, Shi JS, Li B. Qualitative hazard and risk assessment of landslides: a practical framework for a case study in China. Nat hazards. Springer; 2013;69: 1281–1294.
12. Mikami T, Shibayama T, Esteban M, Ohira K, Sasaki J, Suzuki T, et al. Tsunami vulnerability evaluation in the Mentawai islands based on the field

survey of the 2010 tsunami. Nat Hazards. Springer; 2014;71: 851–870.

13. Silva M, Pereira S. Assessment of physical vulnerability and potential losses of buildings due to shallow slides. Nat Hazards. Springer; 2014; 1–22.

14. Füssel H-M, Klein RJT. Climate change vulnerability assessments: an evolution of conceptual thinking. Clim Change. Springer; 2006;75: 301–329.

15. Fekete A. Spatial disaster vulnerability and risk assessments: challenges in their quality and acceptance. Nat hazards. Springer; 2012;61: 1161–1178.

16. Varazanashvili O, Tsereteli N, Amiranashvili A, Tsereteli E, Elizbarashvili E, Dolidze J, et al. Vulnerability, hazards and multiple risk assessment for Georgia. Nat hazards. Springer; 2012;64: 2021–2056.

17. Siagian TH, Purhadi P, Suhartono S, Ritonga H. Social vulnerability to natural hazards in Indonesia: driving factors and policy implications. Nat Hazards. Springer; 2014;70: 1603–1617.

18. Al-Adamat RAN, Foster IDL, Baban SMJ. Groundwater vulnerability and risk mapping for the Basaltic aquifer of the Azraq basin of Jordan using GIS, Remote sensing and DRASTIC. Appl Geogr. Elsevier; 2003;23: 303–324.

19. Antwi-Agyei P, Fraser EDG, Dougill AJ, Stringer LC, Simelton E. Mapping the vulnerability of crop production to drought in Ghana using rainfall, yield and socioeconomic data. Appl Geogr. Elsevier; 2012;32: 324–334.

20. Eckert S, Jelinek R, Zeug G, Krausmann E. Remote sensing-based assessment of tsunami vulnerability and risk in Alexandria, Egypt. Appl Geogr. Elsevier; 2012;32: 714–723.

21. Houghton A, Prudent N, Scott III JE, Wade R, Luber G. Climate change-related vulnerabilities and local environmental public health tracking through GEMSS: A web-based visualization tool. Appl Geogr. Elsevier; 2012;33: 36–44.

22. White GF, Kates RW, Burton I. Knowing better and losing even more: the use of knowledge in hazards management. Glob Environ Chang Part B Environ Hazards. Elsevier; 2001;3: 81–92.

23. Schneider SH, Semenov S, Patwardhan A, Burton I, Magadza CHD, Oppenheimer M, et al. Assessing key vulnerabilities and the risk from climate change. Assessing key vulnerabilities and the risk from climate change. Climate Change 2007: Impacts, Adaptation and Vulnerability. Contribution ofWorking Group II to the Fourth Assessment Report of the Intergovernmental Panel on Climate Change. Cambridge, UK; 2007.

24. McGillivray M, White H. Measuring development? The UNDP's human development index. J Int Dev. Wiley Online Library; 1993;5: 183–192.

25. Noorbakhsh F. The human development index: some technical issues and alternative indices. J Int Dev. Wiley Online Library; 1998;10: 589–605.

26. Turner BL, Kasperson RE, Matson PA, McCarthy JJ, Corell RW, Christensen L, et al. A framework for vulnerability analysis in sustainability science. Proc Natl Acad Sci. National Acad Sciences; 2003;100: 8074–8079.

27. Sullivan CA, Meigh J. Integration of the biophysical and social sciences using an indicator approach: addressing water problems at different scales. Integrated Assessment of Water Resources and Global Change. Springer; 2007. pp. 111–128.

28. Adger WN, Vincent K. Uncertainty in adaptive capacity. Comptes Rendus Geosci. Elsevier; 2005;337: 399–410.

29. o'Brien K, Leichenko R, Kelkar U, Venema H, Aandahl G, Tompkins H, et al. Mapping vulnerability to multiple stressors: climate change and globalization in India. Glob Environ Chang. Elsevier; 2004;14: 303–313.

30. Jeffers JM. Integrating vulnerability analysis and risk assessment in flood loss mitigation: An evaluation of barriers and challenges based on evidence from Ireland. Appl Geogr. Elsevier; 2013;37: 44–51.

31. Tran LT, O'Neill R V, Smith ER. Spatial pattern of environmental vulnerability in the Mid-Atlantic region, USA. Appl Geogr. Elsevier; 2010;30: 191–202.

32. Frazier TG, Thompson CM, Dezzani RJ. A framework for the development of the SERV model: A Spatially Explicit Resilience-Vulnerability model. Appl Geogr. Elsevier; 2014;51: 158–172.

33. Bonachea J, Bruschi VM, Hurtado MA, Forte LM, da Silva M, Etcheverry R, et al. Natural and human forcing in recent geomorphic change; case studies in the Rio de la Plata basin. Sci Total Environ. Elsevier; 2010;408: 2674–2695.

34. Bruschi VM, Bonachea J, Remondo J, Gómez-Arozamena J, Rivas V, Méndez G, et al. Analysis of geomorphic systems' response to natural and human drivers in northern Spain: implications for global geomorphic change. Geomorphology. Elsevier; 2013;196: 267–279.

35. Lee Y, Kim S, Park K. Prediction of Future Land use Using Times Series Landsat Images Based on CA (Cellular Automata)-Markov Technique.

Seoul: The Korean Society of Remote Sensing; 2007. pp. 55–60. Available: http://dlps.nanet.go.kr/SearchDetailView.do?cn=KINX2013091445&sysid=nhn

36. Park J, Lee Y, Kim S, Lee M. The Effect of Future Land Use Change on Hydrology and Water Quality Using SWAT Model. Seoul: Korea Spatial Information Society; 2007. pp. 117–123. Available: http://www.dbpia.co.kr/view/ar_view.asp?arid=1031330

37. Kim Y, Seo C, Ryu J, Chae Y, Baek G, Bae C, et al. Vulnerability assessment on the location of industrial complex considering climate change-Focusing on physical and economic features of province • industrial complex. Korean Soc Environ Impact Assess. Seoul; 2013;22: 627–637. Available: http://dlps.nanet.go.kr/SearchDetailView.do?cn=KINX2014082653&sysid=nhn

38. Ryu J, Han M, Hwang H, Choi J, Kim Y, Im K, et al. Evaluation and Application of CLUE-S Model for Spatio-Temporal Analysis of Future Land use Change in Total Water Pollution Load Management System. Korean Soc Water Envrionment. 2014;30: 418–428.

39. Guzzetti F, Peruccacci S, Rossi M, Stark CP. Rainfall thresholds for the initiation of landslides in central and southern Europe. Meteorol Atmos Phys. Springer; 2007;98: 239–267.

40. Guzzetti F, Peruccacci S, Rossi M, Stark CP. The rainfall intensity--duration control of shallow landslides and debris flows: an update. Landslides. Springer; 2008;5: 3–17.

41. Kim KH, Jung HR, Park JH, Ma HS. Analysis on Rainfall and Geographical Characteristics of Landslides in Gyeongnam Province. J Korean Environ Restor Technol. 2011;14: 33–45. Available: http://kiss.kstudy.com/search/detail_page.asp?key=2931736

42. Knutti R, Sedláček J. Robustness and uncertainties in the new CMIP5 climate model projections. Nat Clim Chang. Nature Publishing Group; 2012;3: 369–373. doi:10.1038/nclimate1716

43. Bathrellos GD, Gaki-Papanastassiou K, Skilodimou HD, Papanastassiou D, Chousianitis KG. Potential suitability for urban planning and industry development using natural hazard maps and geological--geomorphological parameters. Environ Earth Sci. Springer; 2012;66: 537–548.

44. Saha AK, Gupta RP, Sarkar I, Arora MK, Csaplovics E. An approach for

GIS-based statistical landslide susceptibility zonation—with a case study in the Himalayas. Landslides. Springer; 2005;2: 61–69.

45. Ayalew L, Yamagishi H. The application of GIS-based logistic regression for landslide susceptibility mapping in the Kakuda-Yahiko Mountains, Central Japan. Geomorphology. Elsevier; 2005;65: 15–31.

46. Yesilnacar E, Topal T. Landslide susceptibility mapping: a comparison of logistic regression and neural networks methods in a medium scale study, Hendek region (Turkey). Eng Geol. Elsevier; 2005;79: 251–266.

47. Lee S, Sambath T. Landslide susceptibility mapping in the Damrei Romel area, Cambodia using frequency ratio and logistic regression models. Environ Geol. Springer; 2006;50: 847–855.

48. Yilmaz I. Landslide susceptibility mapping using frequency ratio, logistic regression, artificial neural networks and their comparison: a case study from Kat landslides (Tokat—Turkey). Comput Geosci. Elsevier; 2009;35: 1125–1138.

49. Rozos D, Bathrellos GD, Skillodimou HD. Comparison of the implementation of rock engineering system and analytic hierarchy process methods, upon landslide susceptibility mapping, using GIS: a case study from the Eastern Achaia County of Peloponnesus, Greece. Environ Earth Sci. Springer; 2011;63: 49–63.

50. Phillips S, Anderson R, Schapire R. Maximum entropy modeling of species geographic distributions. Ecol Modell. Elsevier; 2006;190: 231–259. doi:10.1016/j.ecolmodel.2005.03.026

51. Felicísimo ÁM, Cuartero A, Remondo J, Quirós E. Mapping landslide susceptibility with logistic regression, multiple adaptive regression splines, classification and regression trees, and maximum entropy methods: A comparative study. Landslides. 2013;10: 175–189. Available: http://www.scopus.com/inward/record.url?eid=2-s2.0-84875731577&partnerID=40&md5=d5a92a0c820742793b108b1446615566

52. Vorpahl P, Elsenbeer H, Märker M, Schröder B. How can statistical models help to determine driving factors of landslides? Ecol Modell. 2012;239: 27–39. Available: http://www.scopus.com/inward/record.url?eid=2-s2.0-84862212238&partnerID=40&md5=2eb6af093fd857358f49d31ea6d7df5b

53. Jyaness ET. Information theory and statistical mechanics. Phys Rev. 1957; 620 – 630.

54. Phillips SJ, Dudík M, Schapire RE. A maximum entropy approach to species

distribution modeling. Brodley CE, editor. Twentyfirst Int Conf Mach Learn ICML 04. ACM Press; 2004;69: 83. doi:10.1145/1015330.1015412

55. Keller EA, Blodgett RH, King HM. Natural hazards: earth's processes as hazards, disasters, and catastrophes. Pearson/Prentice Hall; 2006.

56. Pradhan B, Lee S. Landslide susceptibility assessment and factor effect analysis: backpropagation artificial neural networks and their comparison with frequency ratio and bivariate logistic regression modelling. Environ Model Softw. Elsevier; 2010;25: 747–759.

57. Rozos D, Skilodimou HD, Loupasakis C, Bathrellos GD. Application of the revised universal soil loss equation model on landslide prevention. An example from N. Euboea (Evia) Island, Greece. Environ Earth Sci. Springer; 2013;70: 3255–3266.

58. Choi JH, Oh JY, Kim YS, Kim HT. Analysis of the Controlling Factors of an Urban-type Landslide at Hwangryeong Mountain Based on Tree Growth Patterns and Geomorphology. J Eng Geol. 2011;21: 281–293. Available: http://kiss.kstudy.com/search/detail_page.asp?key=2972909

59. Kim WY, Chae BG. Characteristics of Rainfall, Geology and Failure Geometry of the Landslide Areas on Natural Terrains, Korea. J Eng Geol. 2009;19: 331–344. Available: http://kiss.kstudy.com/search/detail_page.asp?key=2946777

60. Yoo N, Yoon B, Um D, Kim J, Park D. Analysis of Rainfall Characteristics and Landslides at the West Side Area of Gangwon Province. J Korean Geoenvironmental Soc. Korean Geo-Environmental Society; 2012;13: 75–82. Available: http://www.dbpia.co.kr/Article/2931417

61. Ermini L, Catani F, Casagli N. Artificial neural networks applied to landslide susceptibility assessment. Geomorphology. Elsevier; 2005;66: 327–343.

62. Oh HJ. Landslide Detection and Landslide Susceptibility Mapping using Aerial Photos and Artificial Neural Networks. 2010;26: 47–57. Available: http://kiss.kstudy.com/search/detail_page.asp?key=2833837

63. Yeon YK. Evaluation and Analysis of Gwangwon-do Landslide Susceptibility Using Logistic Regression. 2011;14: 116–127. Available: http://kiss.kstudy.com/search/detail_page.asp?key=2963786

64. Pradhan B, Lee S. Delineation of landslide hazard areas on Penang Island, Malaysia, by using frequency ratio, logistic regression, and artificial neural network models. Environ Earth Sci. Springer; 2010;60: 1037–1054.

65. Yao X, Tham LG, Dai FC. Landslide susceptibility mapping based on support vector machine: a case study on natural slopes of Hong Kong, China. Geomorphology. Elsevier; 2008;101: 572–582.

66. Young N, Carter L, Evangelista P. A MaxEnt Model v3.3.3e Tutorial (ArcGIS v10). 2011; 1–30.

67. Al-shalabi M, Billa L, Pradhan B, Mansor S, Al-Sharif AAA. Modelling urban growth evolution and land-use changes using GIS based cellular automata and SLEUTH models: the case of Sana'a metropolitan city, Yemen. Environ Earth Sci. Springer; 2013;70: 425–437.

68. Bathrellos GD, Gaki-Papanastassiou K, Skilodimou HD, Skianis GA, Chousianitis KG. Assessment of rural community and agricultural development using geomorphological--geological factors and GIS in the Trikala prefecture (Central Greece). Stoch Environ Res Risk Assess. Springer; 2013;27: 573–588.

69. Papadopoulou-Vrynioti K, Bathrellos GD, Skilodimou HD, Kaviris G, Makropoulos K. Karst collapse susceptibility mapping considering peak ground acceleration in a rapidly growing urban area. Eng Geol. Elsevier; 2013;158: 77–88.

70. Lee S, Lee M-J. Detecting landslide location using KOMPSAT 1 and its application to landslide-susceptibility mapping at the Gangneung area, Korea. Adv Sp Res. Elsevier; 2006;38: 2261–2271.

71. Oh CY, Choi CU, Kim KT. Analysis of Landslide Characteristics of Inje Area Using SPOT5 Images and GIS Analysis. Korean J Remote Sens. 2009;25: 445–454. Available: http://kiss.kstudy.com/search/detail_page.asp?key=2807632

72. Akgun A, Dag S, Bulut F. Landslide susceptibility mapping for a landslide-prone area (Findikli, NE of Turkey) by likelihood-frequency ratio and weighted linear combination models. Environ Geol. Springer; 2008;54: 1127–1143.

73. Kappes MS, Papathoma-Köhle M, Keiler M. Assessing physical vulnerability for multi-hazards using an indicator-based methodology. Appl Geogr. Elsevier; 2012;32: 577–590.

74. Kim J. The Analysis of planning methode and case study for Model "Climate Change Adaptation City." J KOREA Inst Ecol Archit Environ. 2012;12: 13–19.

75. Catani F, Casagli N, Ermini L, Righini G, Menduni G. Landslide hazard and

risk mapping at catchment scale in the Arno River basin. Landslides. Springer; 2005;2: 329–342.

76. Yilmaz I. Comparison of landslide susceptibility mapping methodologies for Koyulhisar, Turkey: conditional probability, logistic regression, artificial neural networks, and support vector machine. Environ Earth Sci. Springer; 2010;61: 821–836.

77. Akgun A. A comparison of landslide susceptibility maps produced by logistic regression, multi-criteria decision, and likelihood ratio methods: a case study at Izmir, Turkey. Landslides. Springer; 2012;9: 93–106.

78. Claessens L, Schoorl JM, Veldkamp A. Modelling the location of shallow landslides and their effects on landscape dynamics in large watersheds: an application for Northern New Zealand. Geomorphology. Elsevier; 2007;87: 16–27.

79. Ladle R, Hortal J. Mapping species distributions : living with uncertainty. 2013;5: 4–6.

80. Kwon HS. Applying Ensemble Model for Identifying Uncertainty in the Species Distribution Models. 2014;2955: 47–52.

81. Bonachea J, Remondo J, Terán D, Díaz JR, González-Díez A, Cendrero A. Landslide risk models for decision making. Risk Anal. Wiley Online Library; 2009;29: 1629–1643.

82. Sudmeier-Rieux K, Jaquet S, Derron M-H, Jaboyedoff M, Devkota S. A case study of coping strategies and landslides in two villages of Central-Eastern Nepal. Appl Geogr. Elsevier; 2012;32: 680–690.

83. Buisson L, Thuiller W, Casajus N, Lek S, Grenouillet G. Uncertainty in ensemble forecasting of species distribution. Glob Chang Biol. Wiley Online Library; 2010;16: 1145–1157.

84. Thuiller W, Lafourcade B, Engler R, Araújo MB. BIOMOD--a platform for ensemble forecasting of species distributions. Ecography (Cop). Wiley Online Library; 2009;32: 369–373.

85. Kim HG, Lee DK, Park C, Kil S, Son Y, Park JH. Evaluating landslide hazards using RCP 4.5 and 8.5 scenarios. Environ Earth Sci. Springer; 2015;73: 1385–1400.

86. Son JW, Kim KT, Lee CH, Choi CU. Analysis of Ladnslide in Inje Region Using Aerial Photograph and GIS. J Korean Soc geo-spatial Inf Syst. 2009;17: 61–69. doi:10.1017/CBO9781107415324.004

87. Franklin J. Mapping Species Distributions. Cambridge University Press; 2009.

88. Krishnamurti TN, Kishtawal CM, Zhang Z, LaRow T, Bachiochi D, Williford E, et al. Multimodel ensemble forecasts for weather and seasonal climate. J Clim. 2000;13: 4196–4216.

89. Riebau AR, Fox DG. Damage assessment of agrometeorological relevance from natural disasters: economic and social consequences. Natural Disasters and Extreme Events in Agriculture. Springer; 2005. pp. 119–135.

90. Bartlett P, Shawe-Taylor J. Generalization performance of support vector machines and other pattern classifiers. Adv Kernel Methods—Support Vector Learn. 1999; 43–54.

91. Bühlmann P, Yu B. Boosting with the L 2 loss: regression and classification. J Am Stat Assoc. Taylor & Francis; 2003;98: 324–339.

92. Rokach L. Ensemble-based classifiers. Artif Intell Rev. Springer; 2010;33: 1–39.

93. Ghosh J, Acharya A. Cluster ensembles. Wiley Interdiscip Rev Data Min Knowl Discov. Wiley Online Library; 2011;1: 305–315.

94. Lee S, Oh H-J. Ensemble-based landslide susceptibility maps in Jinbu area, Korea. Terrigenous Mass Movements. Springer; 2012. pp. 193–220.

95. Althuwaynee OF, Pradhan B, Park H-J, Lee JH. A novel ensemble bivariate statistical evidential belief function with knowledge-based analytical hierarchy process and multivariate statistical logistic regression for landslide susceptibility mapping. Catena. Elsevier; 2014;114: 21–36.

96. Dimitriadou E, Weingessel A, Hornik K. A cluster ensembles framework. IOS Press; 2003.

97. Thuiller W, Georges D, Engler R. biomod2 package manual. 2015.

98. Kavzoglu T, Sahin EK, Colkesen I. Landslide susceptibility mapping using GIS-based multi-criteria decision analysis, support vector machines, and logistic regression. Landslides. 2013;11: 425–439. doi:10.1007/s10346-013-0391-7

99. Klose M, Damm B, Terhorst B. Landslide cost modeling for transportation infrastructures: a methodological approach. Landslides. Springer; 2014; 1–14.

100. Hansson SL, Röjvall AS, Rastam M, Gillberg C, Gillberg C, Anckarsäter H.

Psychiatric telephone interview with parents for screening of childhood autism--tics, attention-deficit hyperactivity disorder and other comorbidities (A--TAC) Preliminary reliability and validity. Br J Psychiatry. RCP; 2005;187: 262–267.

국문초록

다양한 규모에서의 기후변화에 따른 산사태 영향 및 취약성 평가

김호걸

협동과정 조경학 박사과정,

서울대학교 대학원

지도교수 이동근

최근 우리나라에서는 기후변화로 인해 태풍 및 집중호우와 같은 극한 기상현상이 급속히 증가하고 있다. 극한 기상현상으로 인해 다양한 피해가 발생하고 있는데, 특히 산사태로 인한 피해는 매년 지속적으로 발생하고 있다. 산사태는 재산뿐만 아니라 인명에도 피해를 주는 재해로 적응대책 수립을 통한 피해 예방 및 저감이 시급한 실정이다. 적응대책을 수립하기 위해서는 산사태 위험지역을 파악하고 이를 기반으로 적응대책이 우선적으로 필요한 공간을 파악하는 연구가 중요시 되고 있다.

기후변화 영향은 다양한 규모에서 동시에 발생하고 있으며, 적응대책 수립의 수준 또한 국가, 광역 지방자치단체, 기초 지방자치단체에서 서로 다르게 이루어지고 있다. 기후변화 영향평가 시에 활용이 가능한 자료, 평가의 목적은 규모에 따라서 서로 상이할 수 있다. 따라서 다양한 규모에서 발생하는 기후변화 영향을 서로 다른 특성을 고려하여 평가할 필요가 있다. 이에 본 연구의 목적은 국가, 광역 지방자치단체, 기초 지방자치단체의 서로 다른 규모에서 산사태에 대한 기후변화 영향 및 취약성을

평가하는 방법론을 개발 및 적용하는 것이다.

연구결과, 서로 다른 규모가 요구하는 목적과 해당 규모에서 활용이 가능한 자료에 적합한 평가방법 및 체계를 개발하였으며, 방법론의 적용을 통해 중점 취약지역 또는 위험지역을 도출하였다. 국가 규모에서는 산사태뿐만 아니라 다양한 부문 및 항목을 평가하여, 정부 차원에서 우선적으로 지원해야 할 중점 취약지역을 도출하였다. 광역 지방자치단체 규모에서는 강원도 지역에 대한 산사태 위험지역을 현재와 미래에 걸쳐 분석하여 적응대책 수립이 이루어져야 할 세부지역을 공간적으로 파악하였다. 기초 지방자치단체 규모에서는 강원도 인제군을 대상으로 다양한 모형을 이용하여 불확실성을 고려한 위험지역을 파악하였으며, 불확실성의 정량화를 통해 보다 효과적인 적응대책 수립을 지원하고자 하였다.

본 연구는 서로 다른 규모에서 요구되는 기후변화 영향평가의 목적과, 활용이 가능한 자료를 기반으로 적합한 방법론 및 체계를 개발 및 적용함으로써 기후변화 적응대책 수립 시 의사결정자를 효과적으로 지원할 수 있는 방안을 제시하였다. 향후 산사태를 비롯한 다양한 피해 저감을 위한 기후변화 적응대책 수립 시 서로 다른 규모에서의 기후변화 영향 및 취약성 평가 시에 근거자료로 활용이 가능할 것으로 사료된다.

▣ *주요어: 통계 분포 모델, RCP 기후변화 시나리오, 산사태 민감도, 불확실성*

▣ *학번: 2012-30679*

APPENDIX. Variables and weights for seven fields

1. Health

No	Item	Variables	Sum of weights	First weights	Specific variables	Sum of weights	Second weights
1	Health vulnerability due to floods	Climate exposure	1	0.50	Daily maximum precipitation (mm)	1	0.30
					Number of dates with over 80 mm of precipitation (times)		0.15
					Flooding area (ha)		0.55
		Sensitivity		0.23	Population over 65 years (persons)	1	0.07
					Population under 13 years (persons)		0.07
					Rate of senior citizen who lives alone (%)		0.12
					Rate of basic living security received people (%)		0.11
					Lowland area under 10m (km2)		0.07
					The number of households located in lowland of less than 10m height above sea level (number)		0.14
					The number of flood victims (persons)		0.31
					The number of waterborne disease (persons)		0.11
		Adaptation capacity		0.27	GRDP (million KRW)	1	0.23
					Financial independence (%)		0.30
					Health insurance coverage population ratio (%)		0.11
					Public health labor per ten thousand people (persons)		0.11
					The number of emergency medical institution per million people (place)		0.11
					GRDP of healthcare services and social welfare services sector (million KRW)		0.14
2	Health vulnerability due to typhoons	Climate exposure	1	0.50	Daily maximum precipitation (mm)	1	0.27
					Number of dates with over 80 mm of precipitation (times)		0.25
					Number of dates with over		0.48

					14m/s of daily maximum wind speed (times)		
		Sensitivity		0.23	Population over 65 years (persons)	1	0.10
					Population under 13 years (persons)		0.10
					Rate of senior citizen who lives alone (%)		0.18
					Rate of basic living security received people (%)		0.14
					Lowland area under 10m (km2)		0.14
					The number of households located in lowland of less than 10m height above sea level (number)		0.20
					The number of waterborne disease (persons)		0.14
		Adaptation capacity		0.27	GRDP (million KRW)	1	0.23
					Financial independence (%)		0.28
					Health insurance coverage population ratio (%)		0.11
					Public health labor per ten thousand people (persons)		0.12
					The number of emergency medical institution per million people (place)		0.14
					GRDP of healthcare services and social welfare services sector (million KRW)		0.12
3	Health vulnerability due to heat waves	Climate exposure	1	0.50	Daily maximum precipitation (mm)	1	0.11
					Number of dates with over 33℃ of daily maximum temperature (times)		0.26
					Number of dates with over 25℃ of daily minimum temperature (times)		0.10

					Wind chill(℃)		0.13
					Discomfort index (-)		0.15
					Heatwave index (-)		0.15
					Relative humidity (%)		0.10
		Sensitivity		0.25	Population over 65 years (persons)	1	0.20
					Population under 13 years (persons)		0.10
					Rate of senior citizen who lives alone (%)		0.20
					Rate of basic living security received people (%)		0.10
					Number of death due to cardiovascular disease (persons)		0.16
					Number of death due to heat stroke (persons)		0.24
		Adaptation capacity		0.25	GRDP (million KRW)	1	0.21
					Financial independence (%)		0.21
					Health insurance coverage population ratio (%)		0.10
					Public health labor per ten thousand people (persons)		0.16
					The number of emergency medical institution per million people (place)		0.16
					GRDP of healthcare services and social welfare services sector (million KRW)		0.16
4	Health vulnerability due to cold waves	Climate exposure	1	0.50	Number of dates with daily minimum temperature below zero (times)	1	0.24
					Number of dates with daily average temperature below zero		0.36

					(times)		
					Maximum dates of continuous no rainy day (days)		0.10
					Number of dates with over 14m/s of daily maximum wind speed (times)		0.14
					Snowfall (cm)		0.16
		Sensitivity		0.27	Population over 65 years (persons)	1	0.15
					Population under 13 years (persons)		0.08
					Rate of senior citizen who lives alone (%)		0.24
					Rate of basic living security received people (%)		0.18
					Number of inpatient of a respiratory disease (persons)		0.19
					Number of death due to cerebrovascular disease (persons)		0.20
		Adaptation capacity		0.23	GRDP (million KRW)	1	0.18
					Financial independence (%)		0.26
					Health insurance coverage population ratio (%)		0.09
					Public health labor per ten thousand people (persons)		0.16
					The number of emergency medical institution per million people (place)		0.15
					GRDP of healthcare services and social welfare services sector (million KRW)		0.15
5	Health vulnerability due to ozone enhancement	Climate exposure	1	0.48	Daily maximum precipitation (mm)	1	0.14
					Number of dates with over 100 ppb of the ozone concentration		0.31

					(times)		
					Ozone alert days (days)		0.29
					Number of dates with over 60ppb/8hr of the cumulative ozone concentration (times)		0.26
		Sensitivity		0.27	Population over 65 years (persons)	1	0.16
					Population under 13 years (persons)		0.13
					Rate of senior citizen who lives alone (%)		0.15
					Rate of basic living security received people (%)		0.13
					Number of inpatient of a respiratory disease (persons)		0.25
					Number of death due to cerebrovascular disease (persons)		0.18
		Adaptation capacity		0.25	GRDP (million KRW)	1	0.17
					Financial independence (%)		0.25
					Health insurance coverage population ratio (%)		0.11
					Public health labor per ten thousand people (persons)		0.16
					The number of emergency medical institution per million people (place)		0.16
					GRDP of healthcare services and social welfare services sector (million KRW)		0.15
6	Health vulnerability due to fine dust	Climate exposure	1	0.50	Daily maximum precipitation (mm)	1	0.20
					Concentration of fine dust (ug/㎥)		0.30
					Number of dates with over 100ug/㎥ of the hourly		0.50

					concentration of fine dust (times)		
		Sensitivity		0.28	Population over 65 years (persons)	1	0.14
					Population under 13 years (persons)		0.16
					Rate of senior citizen who lives alone (%)		0.14
					Rate of basic living security received people (%)		0.14
					Number of inpatient of a respiratory disease (persons)		0.26
					Number of death due to cerebrovascular disease (persons)		0.16
		Adaptation capacity		0.22	GRDP (million KRW)	1	0.18
					Financial independence (%)		0.26
					Health insurance coverage population ratio (%)		0.11
					Public health labor per ten thousand people (persons)		0.15
					The number of emergency medical institution per million people (place)		0.15
					GRDP of healthcare services and social welfare services sector (million KRW)		0.10
7	Health vulnerability due to air pollutants	Climate exposure	1	0.50	Daily maximum precipitation (mm)	1	0.10
					CO (except warming in residential sector) (kg)		0.14
					CO (in industrial sector) (kg)		0.16
					Sox (except warming in residential sector) (kg)		0.14
					Sox (in industrial sector) (kg)		0.16
					NOx (except warming in residential sector) (kg)		0.14
							0.16

					NOx (in industrial sector) (kg)		
		Sensitivity		0.23	Population over 65 years (persons)	1	0.14
					Population under 13 years (persons)		0.15
					Rate of senior citizen who lives alone (%)		0.14
					Rate of basic living security received people (%)		0.14
					Number of inpatient of a respiratory disease (persons)		0.25
					Number of death due to cerebrovascular disease (persons)		0.18
		Adaptation capacity		0.27	GRDP (million KRW)	1	0.16
					Financial independence (%)		0.24
					Health insurance coverage population ratio (%)		0.13
					Public health labor per ten thousand people (persons)		0.16
					The number of emergency medical institution per million people (place)		0.15
					GRDP of healthcare services and social welfare services sector (million KRW)		0.16
8	Health vulnerability due to infectious diseases	Climate exposure	1	0.47	Number of dates with over 33℃ of daily maximum temperature (times)	1	0.22
					Number of dates with over 25℃ of daily minimum temperature (times)		0.30
					Daily maximum precipitation (mm)		0.20
					Number of dates with over 80 mm of precipitation (times)		0.28
		Sensitivity		0.30	Population over 65 years (persons)	1	0.13
					Population under 13 years (persons)		0.13
					Rate of senior citizen who lives alone (%)		0.13
					Rate of basic living security received people (%)		0.10
					Annual average number of malaria pathogenesis (persons)		0.26

					Annual average number of Riclieltsia tsuisugamushi pathogenesis (persons)		0.25
		Adaptation capacity		0.23	GRDP (million KRW)	1	0.18
					Financial independence (%)		0.23
					Health insurance coverage population ratio (%)		0.11
					Public health labor per ten thousand people (persons)		0.15
					The number of emergency medical institution per million people (place)		0.18
					GRDP of healthcare services and social welfare services sector (million KRW)		0.15
9	Health vulnerability by waterborne epidemics	Climate exposure	1	0.47	Number of dates with over 33℃ of daily maximum temperature (times)	1	0.25
					Number of dates with over 25℃ of daily minimum temperature (times)		0.25
					Daily maximum precipitation (mm)		0.26
					Number of dates with over 80 mm of precipitation (times)		0.24
		Sensitivity		0.30	Population over 65 years (persons)	1	0.14
					Population under 13 years (persons)		0.19
					Rate of senior citizen who lives alone (%)		0.16
					Rate of basic living security received people (%)		0.13
					The number of waterborne disease (persons)		0.38
		Adaptation capacity		0.23	GRDP (million KRW)	1	0.19
					Financial independence (%)		0.25
					Health insurance coverage population ratio (%)		0.11
					Public health labor per ten thousand people (persons)		0.16
					The number of emergency medical institution per million people (place)		0.14
					GRDP of healthcare services and social welfare services sector (million KRW)		0.15

2. Forest

No	Item	Variables	Sum of weights	First weights	Specific variables	Sum of weights	Second weights
10	Landslides due to heavy rainfall	Climate exposure	1	0.40	Number of dates with over 80 mm of precipitation (times)	1	024
					Daily maximum precipitation (mm)		039
					Summer daily precipitation (mm)		021
					5 days of maximum precipitation (mm)		016
		Sensitivity		0.37	Average slope of regional forest (degrees)	1	035
					Area of coniferous forest (ha)		024
					Average height of regional forest (m)		012
					Dentuded area (ha)		029
		Adaptation capacity		0.23	Government officials per population (persons)	1	020
					Area of preventing forest destruction (ha)		024
					GRDP (million KRW)		018
					Financial independence (%)		038
11	Vulnerability of trails due to landslides	Climate exposure	1	0.38	Number of dates with over 80 mm of precipitation (times)	1	0.26
					Daily maximum precipitation (mm)		0.43
					Precipitation from June to August (㎜)		0.20
					Maximum precipitation per 5 days (㎜)		0.11
		Sensitivity		0.34	Average slope of regional forest (degrees)	1	0.30

					Area of coniferous forest (ha)		0.18
					Average attitude of regional forest (m)		0.10
					Area of unstocked land (ha)		0.25
					Distance of Forest trail (m)		0.17
		Adaptation capacity		0.28	Government officials per population (persons)	1	0.20
					Area of preventing forest destruction (ha)		0.25
					GRDP (million KRW)		0.15
					Financial independence (%)		0.40
12	Vulnerability to forest fire	Climate exposure	1	0.43	Number of dates with over 33℃ of daily maximum temperature (times)	1	0.11
					Number of dates with over 14m/s of daily maximum wind speed (times)		0.19
					Number of dates with under 35% of effective humidity (times)		0.32
					Maximum dates of continuous no rainy day (days)		0.38
		Sensitivity		0.27	Area of coniferous forest (ha)	1	0.19
					Area of broadleaf forest (ha)		0.24
					Area of mixed forest (ha)		0.19
					Soil moisture for 10cm of underground (m^3/m^3)		-0.11
					Average slope of regional forest (degrees)		0.14
					Population (persons)		0.13
		Adaptation capacity		0.30	Government officials per population (persons)	1	0.24
					Area of preventing forest destruction (ha)		0.39
					GRDP (million KRW)		0.16
					Financial independence (%)		0.21

13	Vulnerability of pine trees to disease and pests	Climate exposure	1	0.37	Precipitation from June to August (㎜)	1	0.26
					Daily minimum temperature from June to August (㎜)		0.23
					Daily maximum temperature from June to August (㎜)		0.31
					Number of dates with over 14m/s of daily maximum wind speed (times)		0.20
		Sensitivity		0.38	Area of pine forest (㎡)	1	0.49
					Average slope of regional forest (degrees)		0.12
					Average attitude of regional forest (m)		0.13
					Occurrence area of pest (ha)		0.26
		Adaptation capacity		0.25	Government officials per population (persons)	1	0.21
					Employment for pest control (persons)		0.18
					Area of preventing forest destruction (ha)		0.35
					GRDP (million KRW)		0.11
					Financial independence (%)		0.15
14	Vulnerability of pine trees and pine fungi	Climate exposure	1	0.48	Precipitation from June to August (㎜)	1	-0.30
					Daily average temperature from June to August (℃)		0.23
					Precipitation (㎜/day)		0.17
					Soil moisture for 10cm of underground (m^3/m^3)		-0.15
					Maximum dates of continuous no rainy day (days)		0.15
		Sensitivity		0.30	Area of pine forest (㎡)	1	0.47
					Average attitude of regional forest (m)		0.25
					Amounts of forest products (ton)		0.28
		Adaptation capacity		0.22	Government officials per population (persons)	1	0.20

					Area of preventing forest destruction (ha)		0.45
					GRDP (million KRW)		0.20
					Financial independence (%)		0.15
15	Vulnerability of forest productivity	Climate exposure	1	0.44	Precipitation (㎜/day)	1	0.21
					Daily maximum temperature (℃)		0.19
					Daily minimum temperature (℃)		0.19
					Maximum dates of continuous no rainy day (days)		0.41
		Sensitivity		0.28	Area of coniferous forest (ha)	1	0.40
					Area of broadleaf forest (ha)		0.35
					Area of mixed forest (ha)		0.25
		Adaptation capacity		0.28	Government officials per population (persons)	1	0.15
					Area of preventing forest destruction (ha)		0.30
					Area of forest which is applied nature rest year policy (m^2)		0.16
					Area of conservation for natural forest (ha)		0.15
					Financial independence (%)		0.10
					GRDP (million KRW)		0.14
16	Vulnerability of vegetation due to drought	Climate exposure	1	0.45	Precipitation (㎜/day)	1	0.35
					Maximum dates of continuous no rainy day (days)		0.45
					Number of dates with under 35% of effective humidity (times)		0.20
		Sensitivity		0.30	Area of coniferous forest (ha)	1	0.23
					Area of broadleaf forest (ha)		0.23
					Area of mixed forest (ha)		0.17

					Area of plantation (ha)		0.37
		Adaptation capacity		0.25	Government officials per population (persons)	1	0.20
					Area of preventing forest destruction (ha)		0.35
					GRDP (million KRW)		0.15
					Financial independence (%)		0.15
					Area of conservation for natural forest (ha)		0.15

3. Ecosystem

No	Item	Variables	Sum of weights	First weights	Specific variables	Sum of weights	Second weights
17	Vulnerability of vegetation growth	Climate exposure	1	0.46	Daily average temperature from January to March (℃)	1	0.19
					Temperature (°C)		0.20
					Precipitation (mm/day)		-0.23
					Daily average temperature from June to August (℃)		0.19
					Daily maximum temperature from June to August (℃)		0.19
		Sensitivity		0.31	Area of coniferous forest (ha)	1	0.23
					Timber production of coniferous (㎥)		0.18
					Coniferous forestry by-products (㎥)		0.09
					Number of workers in forest (persons)		0.10
					Cutover area (ha)		0.20
					Number of companies in agriculture and forestry (numbers)		0.10
					Number of workers in agriculture and forestry (persons)		0.10

		Adaptation capacity		0.23	Area of coniferous forest plantation (ha)	1	0.40
					Area of conservation for natural forest (ha)		0.40
					Government officials per population (persons)		0.20
18	Vulnerability of insects	Climate exposure	1	0.48	Daily average temperature from January to March (℃)	1	-0.15
					Number of dates with daily average temperature below zero (times)		0.17
					Daily average temperature in April (℃)		-0.15
					Average relative humidity in April (%)		-0.08
					Maximum dates of continuous no rainy day (days)		0.12
					Evapotranspiration (mm/day)		0.07
					Insolation (W/m2)		-0.10
					Daily average temperature from June to August (℃)		-0.16
		Sensitivity		0.34	Forest insect pests (number of cases)	1	0.19
					Pine pitch canker (number of cases)		0.18
					Number of honeybee farmhouse (numbers)		0.15
					Honeybee breeding size (barrel)		0.15
					Number of arthropod-borne infectious disease (persons)		0.16
					Cutover area by pest damage (ha)		0.08
					Cutting volume by pest damage (㎥)		0.09
		Adaptation capacity		0.18	Time of pest control - Psylla pyricola Foerster (cumulative days)	1	0.23

					Area of preventing forest destruction (ha)		0.22
					Employment for pest control (persons)		0.13
					Number of companies in bioindustry (numbers)		0.13
					Number of farmhouse of environment-friendly fruit (households)		0.16
					Number of farmhouse of environment-friendly special purpose crops (households)		0.13
19	Vulnerability of management of protected areas	Climate exposure	1	0.51	Precipitation (mm/day)	1	0.16
					Maximum dates of continuous no rainy day (days)		0.10
					Number of dates with daily average temperature below zero (times)		0.09
					Number of dates with over 33℃ of daily maximum temperature (times)		0.07
					Precipitation from March to May (㎜)		-0.11
					Precipitation from June to August (㎜)		0.11
					Precipitation from September to November (㎜)		0.09
					Precipitation from December to February (㎜)		-0.09
					Number of dates with over 80 mm of precipitation (times)		0.11
					Number of dates with over 14m/s of daily maximum wind speed (times)		0.07
		Sensitivity		0.28	Number of plant species in National Park (species)	1	0.18
					Number of animal species in National Park (species)		0.18
					Number of visitors (persons)		0.12
					Increase or decrease of visitors compared with the previous year (%)		-0.10

					Number of endangered plant species (species)		0.16
					Number of endangered animal species (species)		0.17
					Number of linked administrative areas for National Park management (numbers)		0.09
		Adaptation capacity		0.21	Number of National Park employees (persons)	1	0.12
					Number of groups in National Park (numbers)		0.10
					Number of National Park offices (numbers)		0.10
					Increase or decrease of National Park Area (㎢)		-0.15
					Operating number of times National Park commentator (times)		0.08
					Area of Buddhist temple in National Park (㎢)		0.08
					Applied area of nature rest system (㎡)		0.20
					Applied length of nature rest system (㎡)		0.17

4. Agriculture

No	Item	Variables	Sum of weights	First weights	Specific variables	Sum of weights	Second weights
20	Vulnerability to erosion of farmlands	Climate exposure	1	0.39	Precipitation (mm/day)	1	0.26
					Number of dates with over 80 mm of precipitation (times)		0.50
					Number of dates with precipitation over 10mm (times)		0.24
		Sensitivity		0.37	Area of rice paddy (ha)	1	0.20
					Area of field (ha)		0.30

					Average slope of regional farmland (degrees)		0.50
		Adaptation capacity		0.24	Ownership in farm mechanization per agricultural land unit (numbers/ha)	1	0.28
					PC advantage farmhouse / total farmhouse		0.12
					Agricultural population per agricultural land unit (persons/ha)		0.10
					Maintenance business employees per cultivation area (persons/ha)		0.10
					GRDP (million KRW)		0.10
					Financial independence (%)		0.24
21	Vulnerability of cultivation facility	Climate exposure	1	0.31	Number of dates with over 14m/s of daily maximum wind speed (times)	1	0.37
					Number of dates with over 20 cm of snowfall (times)		0.28
					Number of dates with over 160 mm of precipitation (times)		0.35
		Sensitivity		0.39	Cultivation area of greenhouse crop (ha)	1	0.15
					Area of breeding facilities (m^2)		0.20
					Damaged area of greenhouse per cultivation area of greenhouse crop		0.40
					Damaged buildings per area of farm (number/ha)		0.25
		Adaptation capacity		0.30	Agricultural population per cultivation/breeding facilities area (persons/ha)	1	0.20
					PC advantage farmhouse / total farmhouse		0.15
					Maintenance business employees per cultivation area (persons/ha)		0.15

					GRDP (million KRW)		0.25
					Financial independence (%)		0.25
22	Vulnerability of productivity of rice crops	Climate exposure	1	0.45	Number of dates with daily minimum temperature below 13℃ from April to June (times)	1	0.10
					Number of dates with daily minimum temperature below 17℃ from July to September (times)		0.15
					Number of dates with daily minimum temperature below 14℃ from September to October (times)		0.10
					Number of dates with daily minimum temperature below 30℃ from April to October (times)		0.10
					Number of dates with over 100 ppb of the ozone concentration from April to October (times)		0.05
					Log(Amount of insolation between April to October) (number)		- 0.25
					Number of dates with over 160 mm of precipitation (times)		0.15
					Number of dates with over 14m/s of daily maximum wind speed (times)		0.10
		Sensitivity		0.26	Area of rice paddy (ha)	1	0.30
					Crop damaged area per area of farm (ha)		0.25
					Possibility of pest damage (%)		0.45
		Adaptation capacity		0.29	Rice production per cultivation area (ton/ha)	1	0.20
					Farmers per cultivation area (persons/ha)		0.25
					Rate of land planning (%)		0.20

					PC advantage farmhouse / total farmhouse		0.05
					Maintenance business employees per cultivation area (persons/ha)		0.05
					GRDP (million KRW)		0.10
					Financial independence (%)		0.15
23	Vulnerability of productivity of apple crops	Climate exposure	1	0.43	Annual average temperature from 8℃ to 11℃	1	0.15
					Daily average temperature in October (℃)		0.10
					Daily average temperature from April to August (℃)		0.15
					Daily average temperature in August (℃)		-0.10
					Daily maximum temperature from April to August (℃)		0.10
					Precipitation from April to October (㎜)		0.15
					Number of dates with over 14m/s of daily maximum wind speed from April to October (times)		0.25
		Sensitivity		0.28	Cultivation area of apple (ha)	1	0.41
					The previous damaged crop areas per unit area (%)		0.59
		Adaptation capacity		0.29	Apple production per cultivation area (kg/10a)	1	0.20
					Farmers per cultivation area (persons/ha)		0.20
					Ownership in farm mechanization per cultivation area of apple (numbers/ha)		0.20
					PC advantage farmhouse / total apple farmhouse		0.05
					Maintenance business employees per cultivation area (persons/ha)		0.10

					GRDP (million KRW)		0.10
					Financial independence (%)		0.15
24	Vulnerability of productivity of livestock	Climate exposure	1	0.34	Number of dates with over 27℃ of daily maximum temperature (times)	1	0.40
					Number of dates with over 72 of temperature humidity index (times)		0.34
					Number of dates with over 20 cm of snowfall (times)		0.14
					Number of dates with over 14m/s of daily maximum wind speed (times)		0.12
		Sensitivity		0.29	Livestock numbers (thousand KRW)	1	0.25
					Damaged buildings per area of farm (number/ha)		0.35
					Potential occurrence probability of livestock disease (%)		0.40
		Adaptation capacity		0.37	Papulation of livestock raiser per unit area of breeding facility (persons/ha)	1	0.30
					Capacity of livestock waste water processing (%)		0.10
					PC advantage farmhouse / total stockbreeding farmhouse		0.10
					Maintenance business employees per cultivation area (persons/ha)		0.10
					GRDP per capita (million KRW)		0.15
					Financial independence (%)		0.25

5. Water management

No	Item	Variables	Sum of weights	First weights	Specific variables	Sum of weights	Second weights
25	Vulnerability of flood	Climate exposure	1	0.37	Daily maximum precipitation (mm)	1	0.13

	regulation				Number of dates with over 80 mm of precipitation (times)		0.31
					5 days of maximum precipitation (mm)		0.23
					runoff(mm/day)		0.19
					Precipitation from June to September (summer season) (mm)		0.16
		Sensitivity		0.30	Lowland area under 10m (km2)	1	0.11
					Buildings in lowland area under 10m (numbers)		0.10
					Rate of bank area in territory (%)		0.10
					Population density (person/km^2)		0.07
					Population (persons)		0.12
					Average slope of region (degrees)		0.10
					Rate of road (%)		0.11
					Flood damage cost during last 3 years (thousands KRW)		0.07
					Flood damage victims during last 3 years (persons)		0.16
		Adaptation capacity		0.33	Financial independence (%)	1	0.15
					Government officials per population (persons/ten thousand people)		0.13
					GRDP (million KRW)		0.07
					Water management government officials per area (person/km2)		0.11
					Rate of river improvement (%)		0.13
					Drainage capability of facilities (m3/min)		0.14
					Flood regulation capacity of reservoir(million m3)		0.21
26	Vulnerability of water utilization	Climate exposure	1	0.31	Maximum dates of continuous no rainy day (days)	1	0.21

					Precipitation from December to February (㎜)		0.22
					Precipitation from March to May (㎜)		0.18
					Evapotranspiration from December to February (mm)		0.21
					Evapotranspiration from March to May (mm)		0.10
					Underground runoff(mm/day)		0.13
		Sensitivity		0.31	Population density (person/km^2)	1	0.15
					Population (persons)		0.11
					Water supply: daily consumption per capita (liter)		0.10
					Grain production per unit area (ton/km^2)		0.07
					Livestock production per unit area (numbers/km^2)		0.07
					Groundwater usage (m^3/year)		0.06
					Stream water usage (m^3/year)		0.08
					Living water usage (thousands m^3/year)		0.09
					Industrial water usage (thousands m^3/year)		0.15
					Agricultural water usage (thousands m^3/year)		0.14
					Financial independence (%)		0.13
		Adaptation capacity		0.38	Government officials per population (persons/ten thousand people)	1	0.12
					GRDP (million KRW)		0.05
					Water management government officials per area (person/km2)		0.09
					Rate of water supply (%)		0.09

					Capacity of underground water (thousands ㎥/year)		0.15
					Reservoir capacity per unit area (thousands m^3)		0.14
					Water reuse per unit area (thousands m^3 /year)		0.21
27	Vulnerability of water quality	Climate exposure	1	0.34	Daily maximum temperature (℃)	1	0.14
					Daily maximum precipitation (mm)		0.13
					Number of dates with over 80 mm of precipitation (times)		0.14
					Maximum dates of continuous no rainy day (days)		0.33
					Number of dates with over 33℃ of daily maximum temperature (times)		0.13
					Number of dates with over 25℃ of daily minimum temperature (times)		0.13
		Sensitivity		0.321	Average slope of region (degrees)	1	0.08
					Rate of river improvement (%)		0.11
					Papulation of livestock raiser(persons/ten thousand people)		0.08
					Livestock products per unit area(number/km2)		0.13
					Fertilizer usage per unit cultivation area(ton/ha)		0.15
					Distribution of major animal species (numbers)		0.09
					Distribution of major plant species (numbers)		0.09
					Rate of forest area (%)		0.14
					Rate of managed land area (%)		0.13

		Adaptation capacity		0.34	Percent of sewered population (%)	1	0.32
					Government officials per population (persons/ten thousand people)		0.11
					Population density (person/km^2)		-0.26
					Rate of road area (%)		-0.18
					Road length per unit area (km)		-0.13

6. Fisheries

No	Item	Variables	Sum of weights	First weights	Specific variables	Sum of weights	Second weights
28	Vulnerability of fisheries due to change in water temperature	Climate exposure	1	0.44	Surface sea temperature (℃)	1	0.22
					Rate of rise of ocean temperature (℃/yr)		0.25
					Number of dates with daily average temperature below zero (times)		0.17
					Number of dates with over 33℃ of daily maximum temperature (times)		0.15
					Number of dates with over 80 mm of precipitation (times)		0.11
					Number of jellyfish damage occurrence (times)		0.09
		Sensitivity		0.34	Farm facilities area(fishery households-cage-aquaculture) (ha)	1	0.25
					Farm facilities area(company-cage-aquaculture) (ha)		0.25
					Farm facilities area(fishery households-cultivating fishery) (ha)		0.16
					Farm facilities area(company-		0.16

					cultivating fishery)(ha)		
					Status of fishery households(cage-aquaculture) (places)		0.09
					Status of fishery households(cultivating fishery) (places)		0.09
		Adaptation capacity		0.22	Financial independence (%)	1	0.28
					Government officials per population (persons/ten thousand people)		0.25
					Farm facilities area(fishery households-land based seawater) (ha)		0.17
					Farm facilities area(company-land based seawater) (ha)		0.15
					Status of fishery households(land based seawater) (places)		0.15

7. Disaster

No	Item	Variables	Sum of weights	First weights	Specific variables	Sum of weights	Second weights
29	Vulnerability of infrastructure to floods	Climate exposure	1	0.45	Number of dates with over 80 mm of precipitation (times)	1	0.41
					Daily maximum precipitation (mm)		0.59
		Sensitivity		0.29	Road area (㎡)	1	0.25
					Water supply facilities area (㎡)		0.09
					Electricity supply facilities area (㎡)		0.09
					Gas supply facilities area (㎡)		0.06
					Heat supply facilities area (㎡)		0.05
					Oil storage and pipeline area (㎡)		0.06

					Sewerage area (㎡)		0.34
					Water pollution prevention facilities area (㎡)		0.06
		Adaptation capacity		0.26	GRDP per capita (million KRW)	1	0.35
					Government officials per population (persons/ten thousand people)		0.15
					Rate of river improvement (%)		0.50
30	Vulnerability of infrastructure to heat waves	Climate exposure	1	0.43	Number of dates with over 33℃ of daily maximum temperature (times)	1	0.65
					Number of dates with over 25℃ of daily minimum temperature (times)		0.35
		Sensitivity		0.21	Road area (㎡)	1	1.00
		Adaptation capacity		0.36	GRDP per capita (million KRW)	1	0.30
					Government officials per population (persons/ten thousand people)		0.14
					Greenspace area per capita (㎡)		0.56
31	Vulnerability of infrastructure to heavy snow	Climate exposure	1	0.45	Snowfall (cm)	1	1.00
		Sensitivity		0.28	Road area (㎡)	1	0.68
					Railroad area (㎡)		0.20
					Airport area (㎡)		0.12
		Adaptation capacity		0.27	GRDP per capita (million KRW)	1	0.65
					Government officials per population (persons/ten thousand people)		0.35

32	Vulnerability of infrastructure to sea level rise	Climate exposure	1	0.50	Annual rate of rising ocean temperature (%)	1	1.00
		Sensitivity		0.20	Road area (㎡)	1	0.30
					Port area(㎡)		0.58
					Water pollution prevention facilities area (㎡)		0.12
		Adaptation capacity		0.30	GRDP per capita (million KRW)	1	0.28
					Government officials per population (persons/ten thousand people)		0.12
					Area of embankment (㎡)		0.60